



UNIVERSITÀ DEGLI STUDI DI PADOVA
DIPARTIMENTO DI CHIMICA BIOLOGICA

SCUOLA DI DOTTORATO DI RICERCA IN
BIOCHIMICA E BIOTECNOLOGIE
INDIRIZZO BIOCHIMICA E BIOFISICA
XXII CICLO

La fosforilazione isoforma-specifica della Ser-20 di p53 da parte di CK1 è determinata sia da un consenso locale che da un sito di interazione remoto

Isoform specific phosphorylation of p53 Ser-20 by CK1 is dictated by both a local consensus and a remote docking site

DIRETTORE: CH.MO PROF. GIUSEPPE ZANOTTI

COORDINATORE: CH.MO PROF. MARIA C. SORGATO

SUPERVISORE: CH.MO PROF. LORENZO A. PINNA

DOTTORANDO: ANDREA VENERANDO

CONTENTS

Summary		III
Riassunto		V
Chapter 1	Posttranslational Modifications: general overview	1
Chapter 2	Protein Kinases	9
Chapter 3	Protein Kinase CK1	23
Chapter 4	Synthetic Peptides: a useful tool to study biomolecules	31
Preface to Chapter 5		37
Chapter 5	Isoform Specific Phosphorylation of p53 by Protein Kinase CK1	41
Preface to Chapter 6		59
Chapter 6	Chemical Dissection of the APC Repeat 3 Multistep Phosphorylation by the Concerted Action of Protein Kinases CK1 and GSK3	61
Preface to Chapter 7		79
Chapter 7	Identification of Novel Protein Kinase CK1 delta (CK1 δ) Inhibitors Through Structure-Based Virtual Screening	83

Preface to Chapter 8		95
Chapter 8		97
Section I	Modulation of Mitochondrial K ⁺ Permeability and Reactive Oxygen Species Production by the p13 Protein of Human T-cell Leukemia Virus Type 1	97
Section II	Possible Role of Phosphorylation in the Regulation of p13 Function	111
Conclusions		119
References		123
Abbreviations		135

SUMMARY

Protein kinase CK1 makes up a small independent group of Ser/Thr protein kinases. So far, seven different CK1 isoforms (α , β , γ_1 , γ_2 , γ_3 , δ , and ϵ) have been characterized in mammals. In addition, alternate splicing generates several variants of their coding genes. While the crystal structure of the δ and γ isoforms have been solved, structural information about CK1 α is not yet available. Members of the CK1 family have been implicated in a variety of biological functions including chromosome segregation, spindle formation, circadian rhythm, nuclear import, Wnt pathway and apoptosis. Deregulation of CK1 has been described in several diseases such as neurodegenerative diseases, including Alzheimer's and Parkinson's disorders, the familial advanced sleep phase syndrome, hepatitis C, leishmaniasis, and cancer. Recently, silencing of CK1 has been associated with disappearance of metastases formation.

Although the list of substrates phosphorylated by CK1 has been growing in the last decade, features underlying substrate specificity by CK1 are still a matter of debate and investigation. Thus, it is difficult to predict residues phosphorylated by CK1 in its potential substrates and evaluate the actual contribution of CK1 to available phosphoproteome data bases. Early studies mostly performed with artificial substrates revealed that CK1 is a "phosphate directed" protein kinase, able to phosphorylate with high efficiency Ser/Thr residues specified by a pre-phosphorylated side chain (either phospho-Ser or phospho-Thr) at position n-3 whose function is not as efficiently replaced by the negatively charged side chains of glutamic and aspartic acids. This means that the requirement of a priming phosphorylation by another kinase restricted CK1 to exert its activity only in the hierarchical phosphorylation of substrates. However, it soon became clear that CK1 not necessarily required a "primed" substrate, since many of its physiological substrates do not contain phosphorylated residues; rather, it often acts as a priming kinase, its intervention being required to generate the consensus sequence for phosphate directed kinases, with special reference to GSK3. Examining the growing list of non-primed CK1 sites it appears that only a few of these are specified by clusters of acidic residues, shown to be able to

effectively replace the individual phosphorylated determinant at position n-3, whereas the majority are to be considered as non-canonical sites whose targeting by CK1 depends on different and somewhat elusive local determinants. Although these atypical local determinants seem to be important for the phosphorylation of full length protein substrates, they are not sufficient alone to confer high affinity to the kinase, as revealed by high K_m values of the derived peptide substrates (close to the millimolar range) as compared to those calculated with whole proteins. In the case of β -catenin, the differences between kinetic parameters observed on whole protein with respect to derived peptide used as substrates in vitro were shown to be accounted for by a remote docking site located in the first Armadillo repeat of β -catenin whose removal caused an increase in the K_m value of three order of magnitude.

The objective of this thesis has been the characterization of substrate specificity of different CK1 isoforms on two different substrates, p53 and adenomatous polyposis coli protein (APC), which play key roles in signal pathways. The use of both recombinant proteins and synthetic peptides reproducing the primary sequence of the phosphoacceptor segments of these two proteins, allowed us to (i) gain deeper insight into the actual ability of different CK1 isoforms to phosphorylate individual residues in the N-terminus of p53 and identify local determinants on p53 and a conserved remote docking site on protein kinase CK1 which is responsible for high affinity binding of p53 with CK1 δ/ϵ and α but not with the γ isoforms; (ii) demonstrate that APC multiple phosphorylation can occur through a cooperative mechanism involving protein kinase CK1 and GSK3.

Furthermore, in collaboration with Giorgio Cozza (Padua), we have identified through virtual-screening and in vitro enzymology approaches, new powerful protein kinase CK1 inhibitors that show high selectivity for the δ isoform of CK1.

The last part of this thesis concerns the study of p13, a small accessory protein of Human T-cell Leukemia Virus type 1. The chemical synthesis of full length p13 allowed us to characterize structurally and functionally this protein. Unpublished data on possible role of phosphorylation in the regulation of p13 function are also reported.

RIASSUNTO

La protein chinasi CK1 rappresenta un piccolo ed indipendente gruppo delle Ser/Thr-protein chinasi. Ad ora, nei mammiferi sono state caratterizzate sette diverse isoforme di CK1 (α , β , γ_1 , γ_2 , γ_3 , δ , and ϵ). Inoltre, lo splicing alternativo dei geni che le codificano genera diverse varianti delle isoforme di CK1. Se da un lato le strutture cristallografiche delle isoforme δ e γ sono state risolte, non sono invece ancora disponibili informazioni strutturali dell'isoforma α . I membri di questa famiglia di chinasi partecipano a diverse funzioni biologiche tra cui si possono annoverare la segregazione cromosomica, la formazione del fuso mitotico, il ritmo circadiano, il trasporto nel nucleo, la via del segnale Wnt e l'apoptosi. Una regolazione alterata di CK1 è stata associata a diverse malattie, quali malattie neurodegenerative, tra cui le sindromi di Alzheimer e di Parkinson, la sindrome ereditaria delle fasi del sonno, l'epatite di tipo C, la leishmaniosi ed infine il cancro. Recentemente, il silenziamento trascrizionale di CK1 è stato associato alla scomparsa della formazione di metastasi.

Sebbene la lista di substrati fosforilati da CK1 sia aumentata nell'ultimo decennio, le caratteristiche che contraddistinguono la specificità di substrato di CK1 sono ancora oggetto di discussione e studio. Di conseguenza, è difficile predire siti bersaglio di CK1 nei suoi potenziali substrati e valutare l'effettivo contributo di CK1 al fosfoproteoma oggi disponibile. I primi studi, per la maggior parte condotti su substrati artificiali, classificarono CK1 come una protein chinasi "fosfato-diretta" data la sua capacità di fosforilare efficacemente residui di serina o treonina caratterizzati da un residuo pre-fosforilato (fosfo-serina o fosfo-treonina) in posizione n-3, la cui funzione non viene efficacemente mimata dalle catene laterali cariche negativamente di un residuo di acido glutammico o aspartico. Questo significa che la necessità di una fosforilazione che faccia da "priming" da parte di un'altra chinasi, relegava CK1 ad esercitare la propria attività solo all'interno di meccanismi gerarchici di fosforilazione di substrati. Tuttavia, presto divenne chiaro che CK1 non necessariamente richiede un substrato pre-fosforilato, dal momento che molti dei suoi substrati fisiologici non contengono residui fosforilati, ma all'opposto svolge la funzione di chinasi "priming", essendo necessario il suo intervento per generare sequenze consenso per altre chinasi fosfato-dirette, in particolare per GSK3. Analizzando la crescente lista

di siti CK1 non pre-fosforilati, appare chiaro che solo alcuni sono caratterizzati da sequenze di residui acidi, che si sono rivelati capaci di sostituire efficacemente il singolo residuo pre-fosforilato in posizione n-3, mentre la maggior parte di essi sono da considerarsi siti non canonici la cui fosforilazione da parte di CK1 dipende da determinanti locali diversi e in alcuni casi sfuggenti. Sebbene questi determinanti locali atipici sembrano essere importanti per la fosforilazione di substrati proteici, non sono tuttavia sufficienti da soli a conferire una alta affinità per la chinasi, come dimostrano alti valori di K_m ottenuti con substrati peptidici che riproducono porzioni della proteina (nell'intervallo del millimolare) se comparati con quelli ottenuti con la proteina intera. Nel caso della β -catenina, le differenze tra i parametri cinetici osservati con la proteina intera e quelli ottenuti con peptidi che riproducono parte di essa usati come substrati in esperimenti in vitro, si sono dimostrate riconducibili a siti di legame remoti situati nel primo Armadillo repeat di β -catenina, la rimozione dei quali causa un aumento di tre ordini di grandezza del valore di K_m .

L'obiettivo di questa tesi è stato quello di caratterizzare la specificità di substrato della diverse isoforme di CK1 prendendo come esempio due substrati di CK1, p53 e la proteina adenomatous polyposis coli (APC), che rivestono un ruolo chiave nelle vie del segnale cellulare. L'utilizzo di proteine ricombinanti e di peptidi sintetici che riproducono la sequenza primaria della porzione fosforilabile di questi due substrati proteici, ci ha permesso di (i) ottenere maggiori informazioni sulla reale capacità delle diverse isoforme di CK1 di fosforilare singoli residui nella porzione N-terminale di p53 e di identificare sia i determinanti locali di fosforilazione su p53 sia un sito di legame remoto conservato sulla protein chinasi CK1 responsabile dell'alta affinità di legame di p53 con CK1 δ/ϵ e α ma non con le isoforme γ ; (ii) dimostrare che la fosforilazione multipla di APC può avvenire attraverso un meccanismo cooperativo che coinvolge le protein chinasi CK1 e GSK3.

Inoltre, in collaborazione con Giorgio Cozza (Padova), attraverso tecniche di virtual-screening e saggi biochimici abbiamo identificato dei nuovi inibitori di CK1 che mostrano una alta selettività per l'isoforma δ di CK1.

L'ultima parte di questa tesi riguarda lo studio di p13, una piccola proteina accessoria del virus HTLV-1. La sintesi chimica di tutta la sequenza aminoacidica di p13 ci ha permesso di caratterizzare questa proteina sia dal punto di vista strutturale che funzionale. Sono inoltre riportati alcuni dati non ancora pubblicati riguardanti il possibile ruolo della fosforilazione nella regolazione della funzione di p13.

CHAPTER 1

Posttranslational Modifications general overview

There are two major mechanisms for expanding the coding capacity of about 30,000 human genes to generate diversity in the corresponding more complex proteome. The first way to increase the diversity of proteins is at the transcriptional level, by mRNA splicing. The second route to proteome expansion is the covalent posttranslational modifications (PTMs) of proteins at one or more sites, made after the messenger RNA code has been translated into the amino acid sequence of nascent proteins [Walsh *et al.*, 2005].

PTMs are enzyme-catalyzed modifications that occur on the side chains or back-bones of proteins after their translational process. Protein PTMs could be divided into two broad categories: enzyme-catalyzed covalent additions of some chemical group to a side chain residue in a protein, and cleavage of peptide back-bones in proteins either by action of proteases or by autocatalytic cleavage. About 5% of the whole genome can be ascribed to enzymes involved in such processes.

Protein covalent modifications can be sorted by different criteria such as the identity of the protein side chain modified, in fact 15 of the 20 natural proteinogenic amino acid side chains undergo such diversification, or by the new function enabled by the covalent addition. However, the most common classification of PTMs is that by the reaction catalyzed by dedicated enzymes. Among the long list (about 200) of posttranslational protein modifications, five types of covalent additions to proteins deserve special attention due to their high frequency in the cell and also to the key role in expanding the proteome structurally and functionally. They are phosphorylation, acylation, alkylation, glycosylation, and oxidation. The protein products obtained by these reactions account for the complexity of the proteome. Furthermore, a variety of very complicated modifications have been observed in one protein and these modifications, alone or in various combinations, at multiple sites or in tandem cascades, occurring time- and signal-dependent manner [Seo and Lee, 2004].

Protein posttranslational modifications are a highly dynamic and cell-status responsive process. Such modifications *in vivo* occur only on a (small) fraction of total proteins, although they are crucial for their functions. Thus, at any moment, sampling of the proteome in an organism or cell provides only a snapshot of the PTMs pattern at that given time.

Posttranslational modifications of proteins determine their tertiary and quaternary structure and regulate their functions by causing changes in protein activity, their cellular locations, and interactions with other proteins. Thus, posttranslational modifications have a great impact on almost all cellular processes where these proteins are involved. At a more global cellular level, PTMs have been shown to influence cellular processes ranging from metabolism to gene expression, from cell cycle progression to programmed cell death [Knippschild *et al.*, 2005].

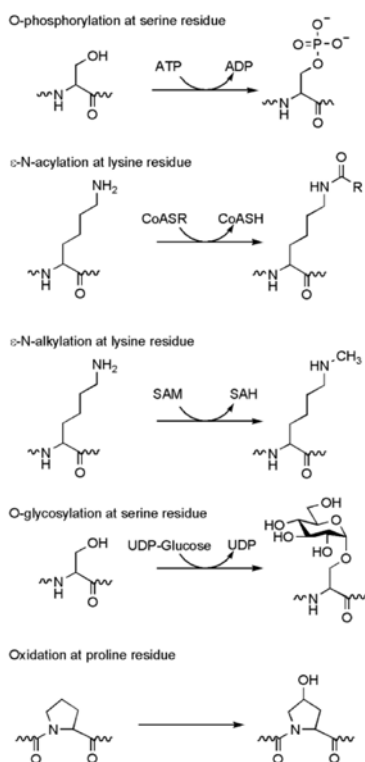


Figure 1. Five major types of covalent additions to protein side chains: phosphorylation, acylation, alkylation, glycosylation, oxidation [Walsh *et al.*, 2005].

Additionally, there is evidence that sometimes posttranslational modifications are in competition with each other resulting in opposing functional consequences for the target protein (e.g. in the C-terminus of the transcription factor p53, five lysine residues can be acetylated or ubiquitylated promoting or not the lifetime of the protein in cells [Li *et al.*, 2002]). In other instances the opposite may apply, whenever the modification of a given residue is a prerequisite for the modification of another one.

Because PTMs are central to all aspects of cell, a series of protein modifications are involved in the signaling pathways from membrane to nucleus in response to external stimuli. In addition,

signaling proteins, modified by PTMs, serve as scaffold proteins for the assembly of multi-protein signaling complexes, such as adaptors, transcription factors, and regulators.

Depending on the biological purpose of a particular covalent modification of a protein, reversibility may or may not be an important parameter to control [Walsh *et al.*, 2005]. The most important and the best known reversible modification is protein phosphorylation, consistent with its dominant role in protein-based signaling in eukaryotes.

The enzymes dedicated to reversible protein phosphorylation are the largest class of PTM enzymes. To date, there are something like 10,844 non-redundant phosphorylation sites identified from Human embryonic stem cells and there are likely more than 500,000 potential phosphorylation sites in a cellular proteome [Lemeer and Heck, 2009].

Phosphorylation of proteins on serine, threonine and tyrosine residues is recognized as a key mode of signal transduction and amplification in eukaryotic cells. Approximately one-third of all eukaryotic proteins are modified by phosphorylation during their lifetime in the cell [Zolnierowicz and Bollen, 2000].

Protein phosphorylation is a specific enzymatic reaction in which one protein serves as substrate for a protein kinase. Introduction of the charged, dianionic, and tetrahedral phosphate group induces altered conformations in local protein microenvironments providing a mechanism for the cell to switch on or switch off many diverse processes and exerting a tight regulation on signal transduction pathways, therefore protein phosphorylation plays a major role in biological systems [Johnson and Lewis, 2001].

Because of the stability of the generated phosphate esters, other enzymes, protein phosphatases, are required for their removal. The concerted and highly regulated action of both protein kinases and protein phosphatases is used by the cell to create a temporally and spatially restricted signal influencing the activity state of proteins in a highly specific way [Krauss, 2003].

The simplicity, flexibility, and reversibility of this posttranslational modification, coupled with the ready availability of ATP (or GTP) as phosphate source, explains its selection as the most general regulatory device adopted by eukaryotic cells [Cohen, 2002].

Human genome encodes more than 500 protein kinases and a third that number of protein phosphatases. It has been calculated that 30% of whole human proteome contains covalently bound phosphate [Manning *et al.*, 2002]. It has also been well known that abnormal phosphorylation and mutations in particular protein kinases and phosphatases are cause or

consequence of many disorders and diseases such as neoplasias, cardiovascular diseases, neurodegenerative diseases, immunodeficiency, rheumatoid arthritis and endocrine disorders. Moreover, naturally occurring toxins and pathogens exert their pathogenic effects by altering the normal phosphorylation pattern of intracellular proteins [Cohen, 2001]. Therefore, it does not come as surprise if the interest in elucidating protein phosphorylation machinery is growing up, and more and more protein kinases and phosphatases are becoming targets for drug development.

In the work presented below, different context of protein phosphorylation will be considered.

The tumor suppressor protein p53 induces or represses the expression of a variety of target genes involved in cell cycle control, senescence, and apoptosis in response to oncogenic or other cellular stress signals. The tight control of this protein, named “the guardian of the genome”, is fundamental and it can be obtained by a series of posttranslational modifications. Among them, protein phosphorylation represents a central tool for maintaining the proper level of p53 in the cell.

Not less than 17 phosphorylated residues have been detected in human p53, whose phosphorylation is promoted by a variety of protein kinases each of which in turn may impinge on more than one residue. In particular, we focused our attention on protein kinase CK1 in order to gain deeper insight into the actual ability of different CK1 isoforms to phosphorylate individual residues in the N-terminus of p53.

In the Wnt signaling pathway, reversible phosphorylation occurs all along the signaling cascade, modulating the activity of almost all the proteins which participate in this signal transduction. This complex signaling network allows the cell to exert a tight control on the cytoplasmic level and activity of β -catenin, a crucial regulator of cell development and proliferation. In particular, we dissected adenomatous polyposis coli (APC) phosphorylation mechanism that occurs as a result of GSK3 and CK1 protein kinases concerted action, a crucial event in the context of protein recruitment within the Wnt/ β -catenin signaling pathway.

Members of the CK1 family have been implicated in a variety of biological functions including chromosome segregation, spindle formation, circadian rhythm, nuclear import, Wnt pathway, and apoptosis. Deregulation of CK1 has been described in several diseases such as neurodegenerative diseases, including Alzheimer’s and Parkinson’s disorders, the familial

advanced sleep phase syndrome, hepatitis C, leishmaniasis, and cancer. Recently, silencing of CK1 has been associated with disappearance of metastases formation. So far, very few potent and selective CK1 inhibitors have been described. We performed an intensive screening campaign combining *in silico* and *in vitro* approaches in particular on the CK1 δ isoform due to its key role in the possible pathogenesis of several neurodegenerative diseases and cancer.

The chemical synthesis of the full length p13, an accessory protein of Human T-cell Leukemia Virus type 1, the causative agent of both an aggressive neoplasia refractory to current therapies, and a neurodegenerative disease, allowed us to characterize structurally and functionally this small (87-mer) protein. *In vitro* studies carried out using synthetic p13 and isolated mitochondria showed that p13 induces a potential-dependent K⁺ influx into the mitochondrial matrix, accompanied by a dose-dependent depolarization, and reduces the threshold for permeability transition pore opening. Preliminary data on the possible role of phosphorylation in the regulation of p13 function are also reported.

CHAPTER 2

Protein Kinases

Reversible phosphorylation of amino acid side chains is an ubiquitous mechanism in both eukaryotes and prokaryotes for regulation of many diverse processes including metabolic pathways, kinase cascades activation, membrane transport, gene transcription, and motor mechanisms. Protein kinases are members of a large and evolutionarily conserved family of molecules sharing with protein phosphatases the responsibility of regulating, in a concerted manner, virtually every kind of cellular functions [Pinna and Ruzzene, 1996]. Protein kinases are phosphotransferases. These enzymes use the γ -phosphate of ATP (or GTP) to generate phosphate monoesters using protein alcohol groups (on Ser and Thr) and/or protein phenolic groups (on Tyr) as phosphate acceptors [Hanks and Hunter, 1995]. In eukaryotes, the protein kinase domain responsible for phosphorylation on serine, threonine, or tyrosine residues is the first, second, and third most common domain in the genome sequences of yeast, the worm, and the fly, respectively, indicating the importance of phospho-signaling in these organisms [Johnson and Lewis, 2001]. In humans the protein kinase domain represent the third most populous domain of the total human genome. Almost all intracellular signaling pathways use protein phosphorylation to create signals and conduct them further.

The completion of the human genome sequence project allowed the identification of the whole human kinome. The Hanks and Hunter [Hanks and Hunter, 1995] human kinase classification of five broad groups, 44 families, and 51 subfamilies, was extended by adding four new groups, 90 families, and 145 subfamilies [Manning *et al.*, 2002]. Kinases classification was made by sequence comparison of their catalytic domains aided by knowledge of sequence similarity and domain structure outside this region, known biological functions, and a similar classification of the yeast, worm, and fly kinomes [Manning *et al.*, 2002*]. The total (518) predicted by Manning *et al.* in 2002 were further subdivided into 478 eukaryotic protein kinases (ePKs) and 40 atypical protein kinases (aPKs). The aPKs lack sequence similarity to the ePK catalytic domain but are known to have catalytic functional activity. We now believe the number of human ePKs to be 480 and, since the publication of the original list by Manning *et al.*, several more aPKs have been identified [Braconi Quintaje and Orchard, 2008]. In any case, the total amount of kinases calculated is about half than predicted 15 years ago, but is still a strikingly large number, corresponding to 1.7% of all human genes.

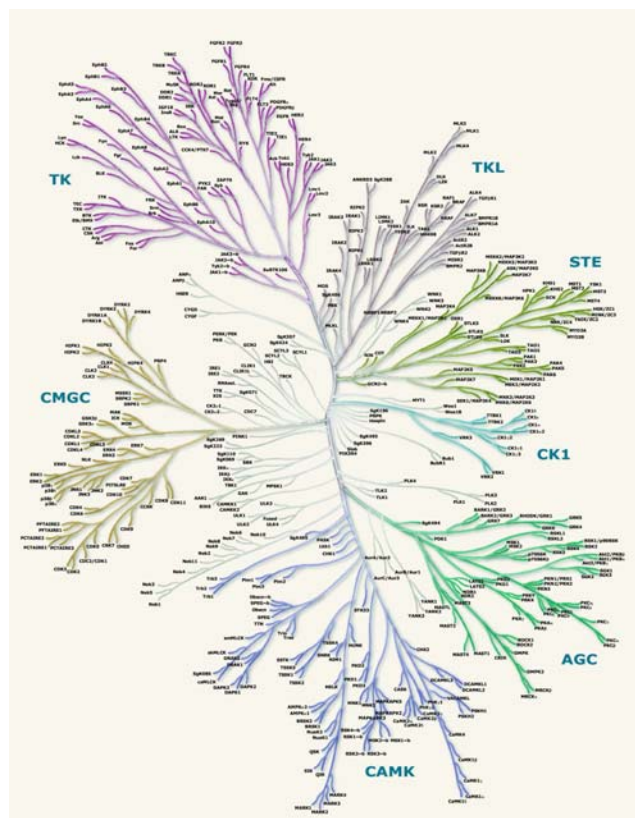


Figure 1. The Manning's kinome. The ePKs could be assigned to seven major groups on the basis of characteristic sequence identification: AGC, cAMP-dependent protein kinase/protein kinase G/protein kinase C extended family; CAMK, Calcium/calmodulin-dependent protein kinase; CMGC, cyclin-dependent kinase, mitogen-activated protein kinase, glycogen synthase kinase 3, and CK2; CK1, casein kinase 1; STE, Homologs of yeast Sterile 7, Sterile 11, Sterile 20 kinases; TK, tyrosine kinase; TKL, tyrosine kinase-like (from Cell Signaling Technology).

Structure and function of protein kinases

Protein kinases can be said to share a single function: the transfer of a phosphate group from nucleotide (ATP or GTP) to a protein substrate molecule. Addition of a phosphoryl group confers properties that can have profound effects on protein substrates conformation and function. At physiological pH, the dianionic, double-negative charged phosphoryl group (phosphate group pK_a is ~ 6.7) and its capacity to form extensive hydrogen-bond networks with the four phosphoryl oxygens, confers special characteristics. By note, the property of a double-negative charge is not carried by any of naturally occurring amino acids [Johnson and Lewis, 2001]. The most common effects of protein phosphorylation are induction of conformational changes by allosteric mechanisms, direct interference with binding of substrate or other binding partners, and creation of binding sites for effector molecules in the protein sequence [Kraus, 2003]. Stoichiometry of phosphorylation is generally relatively low: in general, only a small

fraction of the available intracellular pool of proteins is phosphorylated at any given time as a result of a stimulus [Mann *et al.*, 2002].

The stability of phosphate esters formed by protein phosphorylation on Ser/Thr and Tyr residues and the required intervention of protein phosphatases for their removal, give to the cell a magnificent tool to create a temporally and spatially restricted regulatory signal that functions as a switch in signaling pathways, influencing the activity state of proteins in a highly specific way.

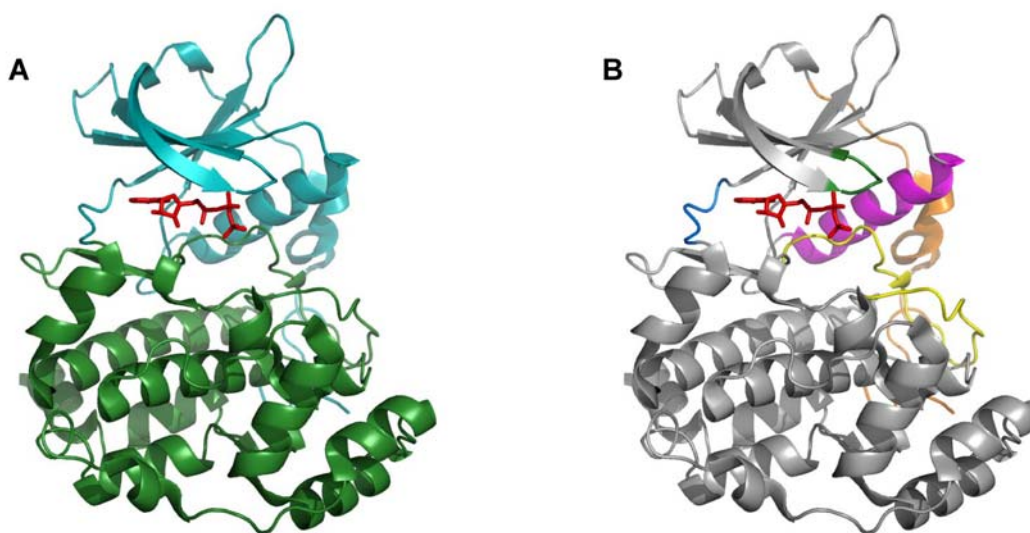


Figure 2. Crystallographic structure of the α -subunit of CK2 from *Zea Mays* (PDB code: 1DAW). (A) The common bilobal structure with the N-terminal (cyan) and the C-terminal (green) domains. In the cleft between the two lobes a pseudo-substrate (red) is shown. (B) Structural elements of catalytic domain: hinge region (blue); C-helix (magenta); Glycine-rich loop (green); activation loop (yellow); N-terminal segment (orange).

The Ser/Thr- and Tyr-specific protein kinases share many common features. The catalytic mechanism, structural properties, and mechanisms of kinase control are very similar for the two kinase classes [Kraus, 2003]. The highly conserved catalytic domain of ca. 300 amino acids of all eukaryotic protein kinases shows a very similar fold, as anticipated by sequence analysis, reflecting a common phosphotransferase mechanism. The fold comprises an N-terminal lobe mostly composed of β -sheets with one α -helix, termed C-helix, and a C-terminal domain that is mostly α -helical with a small amount of sheet. These two lobes are linked by a flexible hinge. The catalytic site for the ATP moiety of the substrate is located into the deep cleft at the two lobes interface [Johnson and Lewis, 2001].

The kinase domain of ePKs fulfil three separate roles: binding and orientation of the ATP (or seldom GTP) phosphate donor as a complex with divalent cation (usually Mg^{2+} or Mn^{2+});

binding and orientation of the protein (or peptide) substrate; and transfer of the γ -phosphate from ATP (or GTP) to the acceptor hydroxyl residue (Ser, Thr, or Tyr) of the protein substrate [Hanks and Hunter, 1995].

Some structural elements (or subdomains, in the Hanks and Hunter review) have been found to be critical for catalysis and for protein kinase control:

- Glycine-rich loop in the N-terminal lobe (subdomain I): this structure acts as a flexible flap that covers and anchors the non-transferable phosphate residues of ATP;
- The C-helix of the N-terminal lobe (subdomain II–III) forms a salt-bridge between nearly invariant Glu to an invariant Lys within the N-terminal lobe, which has been recognized as being essential for maximal enzyme activity, allowing optimal positioning of the ATP phosphate;
- The catalytic loop (subdomain VIa/b) folds into a large hydrophobic portion. A conserved Asp, presumed to be the catalytic base during the phosphotransfer mechanism, is involved in Mg^{2+} -ATP-binding;
- The activation segment (subdomain VII) is one of the most important control elements of protein kinase activity. It contains a highly conserved DFG triplet. The Asp of this motif chelates the primary activating metal ion(s) that bridges the β - and γ -phosphates of the ATP, and thereby helps to orient the γ -phosphate for transfer;
- Autoinhibitory sequence elements (subdomain VIII): these elements occupy the substrate peptide-binding groove in a mode like the real substrate but, lacking the phosphorylatable residues, they act as pseudo-substrates.

Additionally, most protein kinases act in a network of kinases and other signaling effectors, and are modulated by autophosphorylation and/or phosphorylation by other kinases. Other domains within these proteins regulate its kinase activity, link to other signaling modules, or its subcellular localization [Manning *et al.*, 2002].

Site specificity in the substrate binding and recognition

As protein kinases are implicated in a wide variety of cellular processes and as they should affect only one or few of the many potential phosphoacceptor residues in their targets, they must be endowed with terrific selectivity [Pinna and Ruzzene, 1996]. The pleiotropicity of protein kinases is extremely variable: some of them are dedicated enzymes, impinging on just one or few substrates (i.e. phosphorylase kinase), while others are very pleiotropic with hundreds protein

targets subjected to their control [Salvi *et al.*, 2009]. Obviously, the sequence in the neighbourhood of a Ser/Thr or Tyr residue is an important determinant of specificity (site and sequence specificity). Different protein kinases show different “consensus sequences” with respect to the neighbouring sequence of the residues to be phosphorylated. However, it is quite clear that consensus specificity is not the only tool ensuring the selectivity of protein kinases. The co-localization of protein kinases and their substrates at distinct subcellular compartments and specific association mediated by targeting elements outside the catalytic domain, greatly enhance the specificity of the kinase reaction [Pinna and Ruzzene, 1996]. Noteworthy, the recognition elements are not entirely located in the primary structure of the phosphoacceptor site but either constitute structural parts of the substrate protein distinct from the phosphorylation site or belong to it in the tertiary structure. As a matter of fact, peptides reproducing the primary structure around the phosphoacceptor residue generally are poor substrates compared to the intact protein [Bustos *et al.*, 2006].

Negative determinants, whose presence can compromise the phosphorylation of otherwise suitable sites, should also be taken into account. While this deleterious effect is well documented in some cases, little is known about the negative determinants of most protein kinases [Pinna and Ruzzene, 1996].

The majority of the phosphorylated proteins in a eukaryotic cell contain multiple sites of phosphorylation and activities of many proteins are regulated by phosphorylation at more than one site. Phosphorylations by multiple kinases can be additive, hierarchical, or mutually exclusive [Roach, 1991; Cohen, 2000; Holmberg *et al.*, 2002]. However, there are situations in which a protein is modified at multiple sites by a single protein kinase. This type of multisite phosphorylation can be carried out by processive mechanism, in which kinase binds substrate and catalyzes all the possible phosphorylation events before dissociating, or non-processive mechanism, in which each phosphorylation requires a separate binding event between the kinase and substrate [Patwardhan and Miller, 2007]. Recently, Selenko and co-workers have shown that processive reaction behaviour, in the case of protein kinase CK2, is nearly unlikely [Selenko *et al.*, 2008].

Structural information shows that the peptide substrate is bound via multiple interactions. There is a marked complementarity between the binding pocket on the kinase and the peptide substrate in regard to shape, hydrophathy and electrostatic potential [Kraus, 2003].

Control of protein kinases

Protein kinases can exist in active and inactive conformations that are dependent on various different regulatory mechanisms [Johnson, 2009]. The duration and extent of activation depends on the nature of the signal that induces the transition from the inhibited "off" state to the activated "on" state. The cell uses a multitude of mechanisms to control the activity of different protein kinases that include control by phosphorylation, regulation by additional domains that may target other molecules, binding and regulation by additional subunits, and control by protein–protein association. These controls operate mainly at two levels: via allosteric regulation of kinase activity and via co-localization of kinase and substrate protein.

In addition to phosphorylating other proteins, many protein kinases are able to catalyse autophosphorylation reactions. The phosphate may be incorporated either in the enzyme catalytic domain or in the regulatory domain(s). One of the most dynamic regions of the protein kinase core, the activation loop, typically contains one or more critical phosphorylation sites. The activation loop phosphorylation represents a common tool regulating the activity of most, albeit not all protein kinases [Smith *et al.*, 1993].

General classification

Protein kinases are certainly one of the largest families of genes in eukaryotes. Based on the nature of the phosphoacceptor residue, two classes of protein kinases can be distinguished. In addition to already mentioned Ser/Thr- and Tyr-specific protein kinases, there are protein kinases belonging to the same family that phosphorylate histidine residues, forming a phosphorous amide with position 1 or 3 of His.

Several hundreds different protein kinases are known in mammals, most of which are Ser/Thr- or Tyr-specific. In humans, phosphorylation on serine, threonine and tyrosine is approximately 86.4, 11.8, and 1.8%, respectively [Olsen *et al.*, 2006]. Ser/Thr-specific protein kinases constitute the majority of kinases within the human kinome. However, tyrosine phosphorylation and, consequently, Tyr-specific protein kinases are crucially important in health and disease.

Ser/Thr-specific protein kinases

Ser/Thr-specific protein kinases represent the majority of the kinome in eukaryotes comprising many different subfamilies. Among them, are included: protein kinases regulated by

cyclic nucleotide (i.e. protein kinase A, PKA), diacylglycerol-regulated protein kinases (i.e. protein kinase C, PKC), Ca^{2+} /calmodulin-regulated protein kinases, G-protein-coupled receptor protein kinases, protein kinase CK1 and CK2, Glycogen synthase kinase (GSK3), CDC2 kinases, and mitogen-activated kinases (MAP kinases). There are many other protein kinases that do not show any close relationship to these subfamilies. These include protein kinases with dual specificity, in that they can phosphorylate Ser/Thr and also Tyr residues. The only physiologically relevant example of dual specificity protein kinase is given by MAP kinase kinase (MEK) family [Pinna and Ruzzene, 1996]. There are also Ser/Thr-specific protein kinases that are an integral part of transmembrane receptor or of ion channels [Krauss, 2003]. Examples of such members are TGF β -receptor and transient receptor potential channels (TRP channels), that carry protein kinase activities on their cytoplasmic portion.

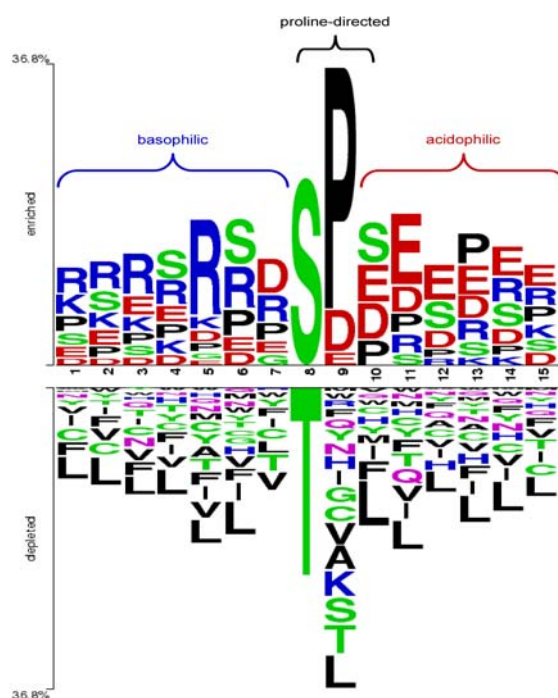


Figure 3. Two-sample logo based on 10,899 phosphosites in humans (from Pinna LA, 2009, Screening, MedChem and ADMET Europe, Berlin, Germany). Upper, the most representative residues found in the neighbourhood of phosphorylated Ser/Thr in phosphopeptides; Bottom, the most depleted.

Within the class of Ser/Thr-specific protein kinases, features underlying the preference for either seryl or threonyl residues remain unclear. As a general rule, Ser/Thr-specific protein kinases tend to prefer seryl over threonyl residues. Both from target sequences analysis and from studies with synthetic peptide substrates, it has emerged that Ser/Thr protein kinases are, with few exceptions,

markedly sequence-specific. Indeed, they recognize specific consensus determinants in the substrate primary sequence that allow to divide Ser/Thr protein kinases class into three distinct groups: (1) basophilic protein kinases use basic and, often, also hydrophobic residues as specificity determinants, usually located in the N-terminal side of the target residue (including the whole of the large ACG group, e.g. PKA, PKC, and all the members of CaMK group); (2) proline-directed protein kinases share the absolute requirement of the S/T-P motif (comprising members of the CMGC group that belong to the families of both cyclin-dependent kinases and MAP kinases, including JNK); (3) acidophilic and phosphate-directed Ser/Thr protein kinases use carboxylic and/or phosphorylated side chains as specificity determinants (among them CK2, GSK3, CK1 and the Golgi apparatus casein kinase G-CK) [Pinna and Ruzzene, 1996]. It should be noted, on the basis of this classification, that a recent study [Salvi *et al.*, 2009] on the more up-to-date phosphopeptides databases has shown that the majority of phosphopeptides appear to be not generated by basophilic protein kinase (the largest branch of Ser/Thr-specific protein kinases) but by proline-directed and by acidophilic protein kinases. This latter represents a tiny minority of the kinome and, among them, CK2 might be responsible alone for the generation of a substantial proportion of the eukaryotic phosphoproteome.

Protein kinases belonging to the acidophilic and phosphate-directed group are able to generate multiple phosphorylation cascades also termed "primed" phosphorylations. The introduction of a primary phosphate, by either the same or another kinase, generates a phosphoacceptor site suitable for a secondary phosphorylation [Marin *et al.*, 2003]. The term "hierarchical phosphorylation" has been coined to indicate this multiple phosphorylation taking place at contiguous sites and involving phosphorylatable residues with definite spacing between each other [Roach, 1991].

Although some Ser/Thr-specific protein kinases are constitutively active in the cell, most of them are tightly regulated. The low basal activities of several regulatable protein kinases are often due to interactions of an "autoinhibitory" domain, located within the enzyme, with its catalytic site, thereby blocking binding of substrates (e.g. protein kinase CK1 displays an autoinhibitory autophosphorylation site that *in vivo* is maintained in the dephosphorylated, active state by cellular protein phosphatases [Rivers *et al.*, 1998]). The hypothesis is that binding of allosteric activators induces conformational changes in the autoinhibitory domain that disrupt its interaction with the catalytic domain, hence activating the kinase to phosphorylate exogenous substrates [Soderling, 1990].

Tyr-specific protein kinases

In the past thirty years, tyrosine phosphorylation has been required as a fundamentally important mechanism of signal transduction and regulation in all eukaryotic cells [Hunter, 2009]. The conventional protein tyrosine kinases (PTKs) group includes a large number of enzymes (90 in humans) with quite closely related kinase domains that specifically phosphorylate Tyr residues. Tyrosine phosphorylation proved to be involved not only in growth factor receptor signaling but also in many other processes from cell adhesion to cell cycle control, from transcriptional activation to even aging. Perturbations in tyrosine phosphorylation underlie many human disease and cancer [Hunter, 2009].

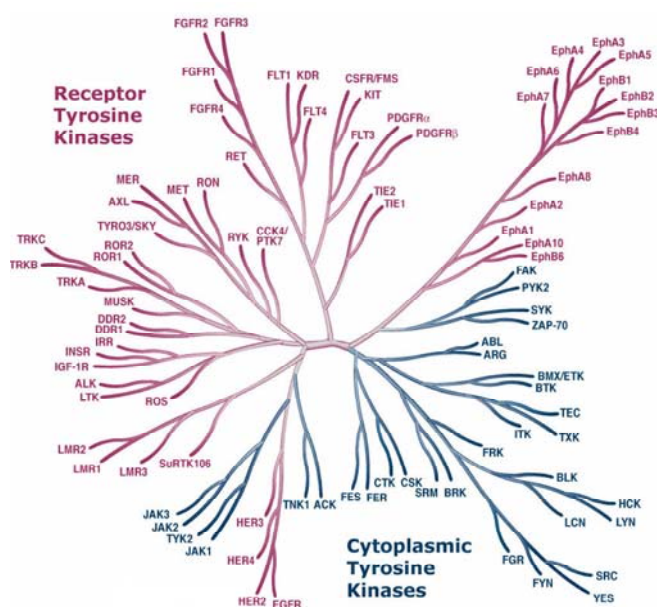


Figure 4. Human tyrosine kinases. Two groups corresponding to cytoplasmic and receptor tyrosine kinases are reported (from Cell Signaling Technology).

Tyrosine kinase family can be further divided into two broad classes: receptor Tyr kinases (RTKs) are type I transmembrane proteins characterized by an extracellular ligand-binding domain, a transmembrane region, and a C-terminal cytoplasmic domain which includes the catalytic domain; non-receptor Tyr kinases (nRTKs) are intracellular molecules that lack the transmembrane domain but other are able to bind transmembrane receptors through their molecular interaction regions, such as SH2 (Src Homology 2) and SH3 (Src Homology 3) domains, thus participate in signal transduction cascades originating from extracellular signals. Most RTKs are activated upon binding to their extracellular domain of specific ligands, such as growth factors and cytokines. Ligand binding induces RTK oligomerization and subsequent

activation of the cytoplasmic catalytic domain. This results in trans-phosphorylation, initially in the activation loop (which turns on catalytic activity) and, then, in regions lying outside the catalytic domain whose phosphorylation is crucial for further recruitment and activation of a variety of signaling proteins [Schlessinger, 2000]. In general, tyrosine autophosphorylation both stimulates the intrinsic receptor catalytic activity and generates recruitment sites for downstream signaling proteins containing phospho-tyrosine recognition domains, thereby transducing extracellular signals across the plasma membrane.

The definition of the specificity determinants of PTKs has not been as clear-cut as that of Ser/Thr-specific protein kinases [Pinna and Ruzzene, 1996], although a predilection for acidic residues at consistently not fixed positions either downstream or upstream the target Tyr has been shown. However, other factors, primarily second site interaction between the kinase and the potential substrate (such as that mediated by SH2, SH3, and protein tyrosine-binding domains), and shared subcellular localization dictate target specificity of Tyr-specific protein kinases.

The crystal structures of the cytoplasmic domain of several receptor tyrosine kinases have been solved, disclosing the mechanisms of activation of tyrosine kinases, through dimerization, and auto/trans-phosphorylation-induced conformational changes [Hunter, 2009]. The catalytic domain of PTK, like that of any protein kinase, consists of an upper lobe, a lower lobe, and a cleft between the two lobes [Hubbard *et al.*, 1994]. The cleft is the active site and contains two loops: the activation loop and the catalytic loop. The activation loop controls kinase activity by adopting different phosphorylation-dependent conformations [Smith *et al.*, 1993].

As protein tyrosine kinases are important modulators of intracellular signal transduction pathways, their activity must be tightly controlled and regulated. Perturbations of PTKs signaling by mutations and other genetic alterations result in deregulated kinase activity, usually constitutive kinase activation, leading to malignant transformation [Blume-Jensen and Hunter, 2001].

A druggable kinome in health and disease

Protein kinases are a large and evolutionarily conserved family of molecules that play a key role in both inter- and intracellular signaling. At least 30% of the human proteome has been phosphorylated by protein kinases. In any processes governed by protein phosphorylation, a fine

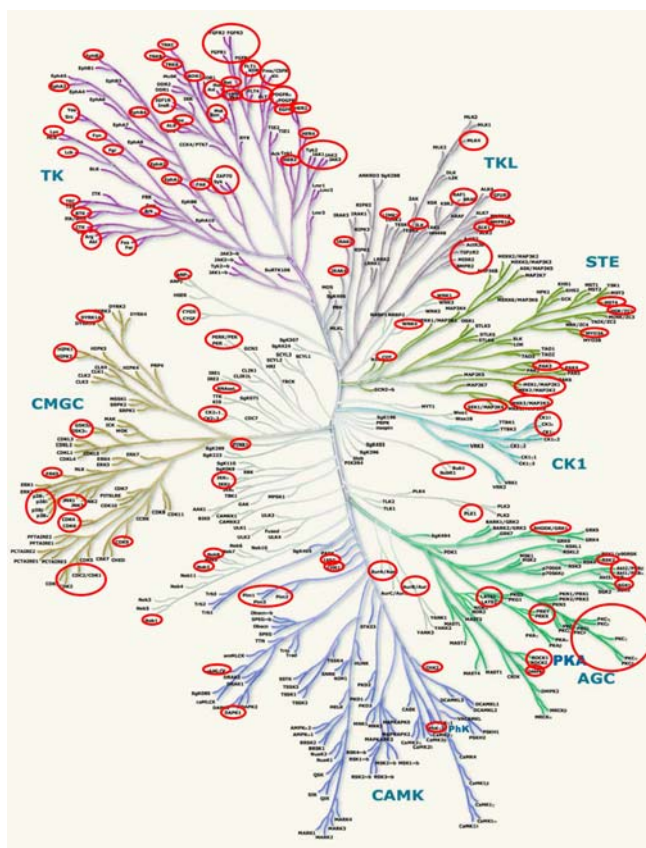


Figure 5. The druggable kinome. Red circles denote kinases associated with disease (based on www.cellsignaling.com).

balance between the activities of protein kinases and protein phosphatases is crucial for cellular physiologic function [Braconi Quintaje and Orchard, 2008]. Abnormal phosphorylation of proteins or mutations in particular protein kinases and phosphatases are cause or consequence of many diseases and the thin regulation of protein phosphorylation is frequently disrupted in pathological conditions, especially in cancer. Approximately 50 of the 100 known genes that have been directly linked to the induction of cancer, encode protein kinases. The remainder of the oncogenes specify proteins that either activate kinases or are phosphorylated by kinases [Giamas *et al.*, 2007]. Therefore, the kinome has been prime target for drug discovery and development, representing as much as 30% of all protein targets under investigation by pharmaceutical companies [Giamas *et al.*, 2007].

CHAPTER 3

Protein Kinase CK1

The CK1 family represents a small independent group within the superfamily of Ser/Thr-specific protein kinases and is found in all eukaryotic organisms from yeast to human. For instance, there are ~ 70 CK1 family members in the *C. elegans* kinome. So far, at least seven CK1 isoforms (α , β , γ_1 , γ_2 , γ_3 , δ , and ϵ) have been characterized in mammals. In addition, alternate splicing generates several variants of their coding genes. The family members have the highest homology in their kinase domains (53–98% identical) [Price, 2006] and differ from most other protein kinases by the presence of the sequence SIN instead of APE in kinase subdomain VIII [Hanks and Hunter, 1995]. Outside of the kinase domain, CK1 family members show little homology to each other and differ in length and amino acid sequence of their N- and C-terminal extensions.

The sequence homology within the CK1 catalytic domains allows an estimation of the evolutionary relationship between isoforms [Longenecker *et al.*, 1996]. CK1 δ appears to be very similar to CK1 ϵ , with which it forms the so-called δ/ϵ subfamily. Both isoforms have a long C-terminal tail (ca. 120–200 residues), responsible for regulating enzyme activity through inhibitory autophosphorylation [Gietzen and Virshup, 1999; Graves and Roach, 1995].

Although the kinase domain sequences of CK1 α and CK1 β are closely related to δ/ϵ subfamily, they have much shorter C-terminal domains (ca. 13–25 residues). Another group is formed by the CK1 γ isoforms (γ_1 , γ_2 , γ_3), which are the most remote of the subfamily, showing only 51–59% identity to the other isoforms within the protein kinase domain [Zhai *et al.*, 1995].

The molecular weight of mammalian CK1 isoforms varies from 37 kD to 51 kD. They have been described to act as monomeric, constitutively active enzymes. CK1 isoforms exclusively exploit ATP as phosphate donor and are generally co-factor independent [Flotow *et al.*, 1990].

So far, several splice variants have been described for different CK1 isoforms. CK1 α mRNA processing can generate the insertion of a long (L, 28 aa) or a short (S, 12 aa) segment into the catalytic or C-terminal domain, producing the variants CK1 α , CK1 α S, CK1 α L, and CK1 α LS, all of which have been identified in many species [Fu *et al.*, 2001; Burzio *et al.*, 2002]. These splice variants of CK1 α differ in their kinase activity, functions, subcellular localization, and biochemical properties [Budini *et al.*, 2008]. Similarly, three CK1 ϵ splice variants (CK1 ϵ_1 ,

CK1 ϵ_2 , CK1 ϵ_3) have been described in rat differing in their kinase activity and tissue expression [Takano *et al.*, 2004].

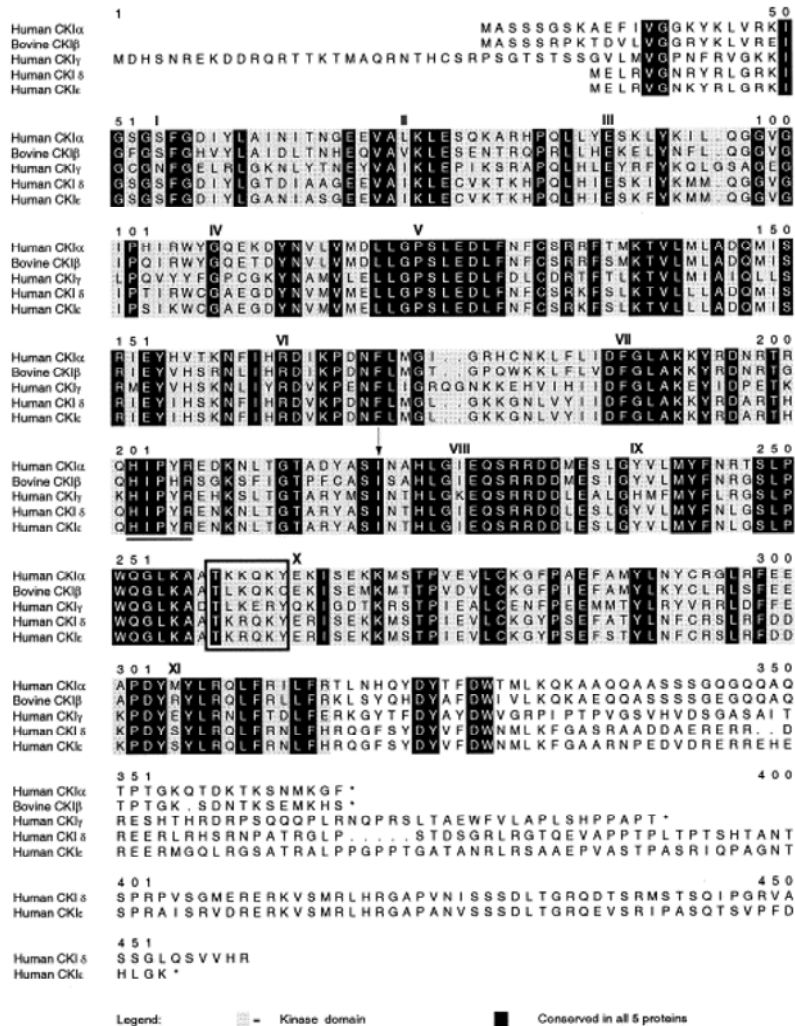


Figure 1. Sequence alignment of the human CKI isoforms (with the exception of the β isoform, which is currently known to exist only in bovine brain). Grey indicates kinase catalytic domain and black indicates amino acid residues conserved in all isoforms. An arrow marks the position at which the Asp-Pro-Glu motif of domain VIII, which is common to most Ser/Thr kinases, should reside but instead has been replaced with Ser-Ile-Asn [Gross and Anderson, 1998].

Substrate specificity

Despite the similar names (derived from the misnomer, casein kinase) and the common propensity to phosphorylate casein *in vitro*, CK1 is totally unrelated to CK2 in the protein kinase phylogenetic tree [Pinna and Ruzzene, 1996]. Although the list of substrates phosphorylated by CK1 has been growing in the last decade, features underlying substrate specificity by CK1 are

still a matter of debate and investigation. Thus, it is difficult to predict residues phosphorylated by CK1 in its potential substrates and evaluate the actual contribution of CK1 to available phosphoproteome data bases.

The CK1 family members appear to have similar substrate specificity *in vitro* [Pulgar *et al.*, 1999] and substrate selection is thought to be regulated *in vivo* via subcellular localization and docking sites in specific substrates [Price, 2006].

Early studies mostly performed with artificial substrates revealed that CK1 is a “phosphate directed” protein kinase, able to phosphorylate with high efficiency Ser/Thr residues specified by a pre-phosphorylated side chain (either phospho-Ser or phospho-Thr) at position n-3. This means that the requirement of a priming phosphorylation by another kinase restricted CK1 to exert its activity only in the hierarchical phosphorylation of substrates [Roach, 1991]. However, it soon became clear that CK1 not necessarily required a “primed” substrate, since many of its physiological substrates do not contain phosphorylated residues; rather, it often acts as a priming kinase, its intervention being required to generate the consensus sequence for phosphate directed kinases, with special reference to GSK3. Furthermore, it was demonstrated that the phosphorylated amino acid could be replaced by an aspartic acid at position n-3 and, even more efficiently, by a stretch of acidic amino acids [Marin *et al.*, 1994; Songyang *et al.*, 1996]. However, an individual Asp or Glu residue proved unable to effectively replace the crucial phospho-serine/threonine acting as specificity determinant [Pulgar *et al.*, 1999]. In addition, a non-canonical motif consisting of the sequence S*LS, in which (S*) is the target serine, in combination with a cluster of acidic amino acid residues C-terminally the phosphoacceptor site, has been shown to be recognized by CK1 [Marin *et al.*, 2002; Marin *et al.*, 2003]. In this respect, evidence have been accumulated that CK1 is implicated in the multi-phosphorylation of proteins, notably the transcription factors family NF-AT, β -catenin and adenomatous polyposis coli (APC), that do not display the canonical consensus for this kinase, either primed by previous phosphorylation or specified by acidic residues upstream, rather show non-canonical motif in their amino acid sequences. As well, it has also been postulated that some of this proteins (e.g. NF-AT and Per), possess a FXXXF box (where X represent any amino acid residues) which signals their tight binding of CK1, presumably favouring their phosphorylation [Okamura *et al.*, 2004].

The recognition of canonical sites, defined either by a phosphorylated residue or by an acidic cluster upstream the target amino acid, appears to rely on a structural element conserved in CK1 isoforms, that is a basic stretch K²²⁹KQK²³² in the CK1 α isoform. Mutation to alanines of the

whole basic stretch or even of K232 alone, which is one of the strongest conserved residues within this stretch in all CK1 isoforms, has a detrimental effect on CK1 activity, leading to a protein mutant defective in the ability to recognize pre-phosphorylated substrates, especially if the priming phosphate is at position n-4 [Bustos *et al.*, 2005].

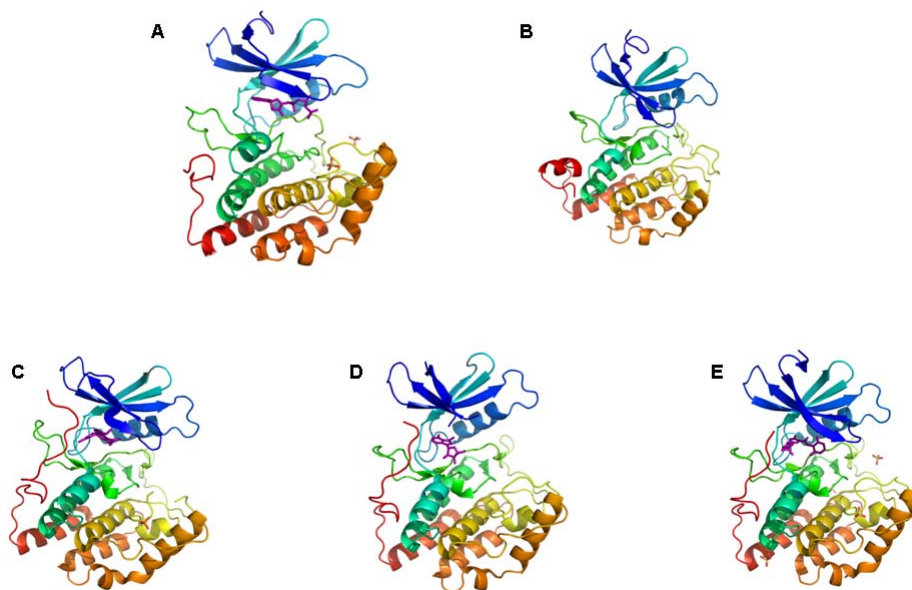


Figure 2. Crystal structures of CK1. (A) CK1 from *S. pombe* (PDB: 1CSN); (B) CK1 δ from rat (PDB: 1CKI); (C) human CK1 γ_1 (PDB: 2CMW); (D) human CK1 γ_2 (PDB: 2C47); (E) human CK1 γ_3 (PDB: 2CHL).

Examining the growing list of non-primed CK1 sites it appears that only a few are specified by clusters of acidic residues, shown to be able to effectively replace the individual phosphorylated determinant at position n-3, whereas the majority are to be considered as non-canonical sites whose targeting by CK1 depends on different and somewhat variable local determinants. Although these atypical local determinants seem to be important for the phosphorylation of full length protein substrates, they are not sufficient alone to confer high affinity to the kinase, as revealed by high K_m values of the derived peptide substrates (close to the millimolar range) as compared to those calculated with whole proteins. In the case of β -catenin, the difference in values of kinetic parameters observed on full-length protein with respect to derived peptide used as substrates in vitro has been shown to be account for by a remote docking site located in the first Armadillo repeat of β -catenin whose removal caused an increase in the K_m value of three orders of magnitude [Bustos *et al.*, 2006]. Thus, the phosphorylation of a protein substrate by

CK1 seems depend on the consensus sequence, but also on the tertiary structure of the substrate [Cegielska *et al.*, 1998].

Structural features

While the crystal structure of enzymes belonging to the δ (PDB code: 1CKI; 1CSN) and γ (PDB code: 2CMW; 2C47; 2CHL) isoforms have been solved [Xu *et al.*, 1995; Longenecker *et al.*, 1996], structural information of CK1 α is not yet available.

All CK1 family members contain a catalytic domain of about 300 amino acids, while differ for the highly variable C-terminal extensions that have been implicated in both subcellular targeting and regulation of the activity. In respect of this latter, it has been shown that the C-terminal regions, particularly of CK1 α , δ and ϵ , are autophosphorylated and this phosphorylation inhibits the activity of the kinase domain, although, *in vivo*, phosphatases keep it constitutively active in many cases [Rivers *et al.*, 1998; Budini *et al.*, 2009].

CK1 display the common three-dimensional bilobal structure: the smaller N-terminal lobe primarily consist of β -strands in a barrel configuration; the larger C-terminal lobe is largely made up of α -helices providing the structural framework necessary to support loops which may participate in substrate recognition. The nucleotide binding site is located in the cleft between the two lobes [Longenecker *et al.*, 1996]. In addition, a putative nuclear localization sequence situated in the C-terminal lobe, offers abundant access to any factor(s) involved in CK1 nuclear uptake.

Noteworthy, the derivative structures of CK1 isoforms identify a potential primary point of phosphorylated substrate recognition within the interacting region with ions [Xu *et al.*, 1995; Longenecker *et al.*, 1996].

Regulation and functions

CK1 isoforms can be isolated from all cellular compartments in all tissues or cell lines tested as active enzymes. Nevertheless, a number of effectors are able to modulate CK1 expression and activity. Stimulation of cells by insulin or by viral transformation, as well as treatment with topoisomerase inhibitors or γ -irradiation, leads to elevated CK1 activity and/or protein levels. On the contrary, increased membrane concentration of phosphatidylinositol-4,5-biphosphate reduces CK1 α activity in erythrocytes and neuronal cells [Knippschild *et al.*, 2005]. The subcellular

localization and compartmentalization is essential for CK1 function, bringing constitutively active kinase and substrate into close proximity. Another mechanism affecting CK1 activity is its inhibitory autophosphorylation, which occurs especially in the C-terminal domain and in some cases additionally in the kinase domain [Gietzen and Virshup, 1999]. C-terminal domains of at least CK1 α , δ , ϵ , and γ_3 have been suggested to function as pseudo-substrates thereby inhibiting their own kinase activity.

Collectively taken, CK1 enzymes have been implicated in a variety of biological functions, including chromosome segregation, spindle formation, circadian rhythm, nuclear import, Wnt pathway, and apoptosis [Gross and Anderson, 1998; Knippschild *et al.*, 2005]. Deregulation of CK1 isoforms has been described in neurodegenerative and sleeping disorders, and in cancer. Recently, silencing of CK1 has been associated with the disappearance of metastases formation [Adorno *et al.*, 2009].

CHAPTER 4

Synthetic Peptides a useful tool to study biomolecules

Understanding the control, at the molecular level, of the mechanisms and principles governing structural and functional properties of bioactive proteins is an important objective in biological and medical research [Kimmerlin and Seebach, 2005]. The first requirement for the study of proteins is to obtain a useful and pure amount of them. There are three main routes to consider, each of which has its advantages and disadvantages: native protein isolation, recombinant techniques for the expression of proteins in microorganisms, and chemical synthesis.

Chemical synthesis of peptides and small proteins has become one of the most useful and powerful techniques in the biochemical and biomedical studies. Since the first synthesis of a dipeptide by Emil Fisher in 1901, peptide science has made tremendous progress and, with recent innovations, it is currently possible to routinely synthesize proteins.

Peptides represent one of the most important class of molecules in biochemistry, biomedicine and physiology. Many biologically active molecules are peptide, thus, biochemical, physiological, structural, functional, and pharmacological studies can be easily performed thanks to the possibility to synthesize this biomolecules. Moreover, peptide substrates can be used to study kinetics, mechanisms of action, consensus sequences, proteins interactions, and structure–function relationships. Pharmaceutical applications of these molecules are drug design, for instance to discover enzymes inhibitors, production of polyclonal or monoclonal antibodies functioning as synthetic antigens, and finally development of synthetic vaccines determining and miming biologically active regions of proteins.

It is for these reasons that the peptide synthesis has become more and more important.

The historical landmark that opened the way to the enormous success of peptides in chemistry, biochemistry and biomedicine was the paper published by Bruce Merrifield [Merrifield, 1963], the first describing the development of solid-phase peptide synthesis (SPPS).

The concept of SPPS is to link the nascent peptide chain to an insoluble polymeric support by a covalent attachment of the first amino acid, usually through its acidic group, via esterification reaction. The reactive side chains of the amino acids must be permanently protected until the synthesis is complete, while the amino group must be temporary protected. The synthesis proceeds from the C- to the N-terminal residues following these steps:

- Deprotection of the α -amino amine of the amino acid anchored to the resin (or of the last amino acid in the growing peptide chain);
- Activation of the carboxyl group of the new α -amino amine protected amino acid;
- Coupling reaction with formation of the amidic bond.

These steps are then repeated until the sequence is complete.

A polymeric support with specific functional groups which allow the anchor of the peptide, represents a system macroscopically insoluble. On the other hand, it is possible to obtain strong solvation of the resin with specific solvents. Cleavage and deprotection of amino acid side chains constitute the final steps of the synthetic phase followed by purification procedures.

Fmoc Chemistry

The choice of the α -amino protecting group determines the type of chemistry which is used for the synthesis. There are two major used forms of solid-phase peptide synthesis: Fmoc (base-labile α -amino protecting group) and t-Boc (acid-labile protecting group). Each method involves different resins and amino acid side chain protections and subsequent cleavage/deprotection steps. Fmoc chemistry is known for generating peptides of higher quality and in greater yield than t-Boc chemistry.

The 9-fluorenylmethoxycarbonyl (Fmoc) group is completely stable in acidic conditions while it can be removed in basic conditions [Carpino and Han, 1972]. The Fmoc deprotection reaction is catalyzed by primary, secondary, and, very slowly, tertiary amines but, usually, piperidine 20–50% in DMF or NMP is used [Fields and Fields, 1991]. Piperidine, in fact, reacts with a highly reactive dibenzofulvene intermediate (derived by the removal of the Fmoc) and gives a stable adduct that can be spectrophotometrically monitored.

The possibility to select as protecting groups of the side chains a series of chemical groups which are stable in basic conditions, allows one to apply an orthogonal synthetic strategy in which the polypeptide chain can grow step by step just removing the Fmoc, consequently freeing the N-terminal function, while the reactive functions on the side chains result stable during the whole synthetic process. At the end of the synthesis, the use of specific organic or inorganic acids is necessary in order to eliminate all the protecting groups and to obtain the final peptide.

SPPS workflow

The most part of the solid-phase synthetic strategy are carried out in the C- to N-term direction. The first step consists therefore in the anchoring of the first amino acid by its carboxyl group to a polymeric solid support. A wide series of polymeric supports have been developed in order to obtain the best result under different conditions. Generally, the resin used in SPPS is a polystyrene suspension polymer cross-linked with 1% of 1,3-divinylbenzene that can easily swell with organic solvents.

The attachment of the first α -amino-protected amino acid to the linker functionality of the resin is usually carried out with an esterification reaction between the amino acid carboxyl group and the functional group (commonly a benzyl group) of the resin. The activation of the acidic function of the amino acid usually requires the generation of a symmetric anhydride by using N,N'-dicyclohexylcarbodiimide.

To allow the peptide chain growth, the Fmoc protecting group have to be removed. This reaction is catalyzed by amines, commonly piperidine 20–55% in DMF or NMP, which permit to remove the Fmoc leaving intact amide bonds, esteric bond between the peptide and the solid support, and bonds between amino acids and side chain protecting group.

The next step requires the activation of the carboxylic group of the new amino acid that will react with the α -amino group generating the peptide bond. Relatively recent protocols use activating substances as phosphonium and uronium salts (e.g. HBTU/HOBt or HATU) in presence of tertiary amines (e.g. diisopropylethylamine). These new activating reagents give a much more efficient coupling and, at same time, suppress the racemization and other side reactions that occurred with the activating substances previously used in the SPPS.

Fmoc removal, activation of new amino acid and coupling steps are repeated until the polypeptide chain reaches the desired length and sequence.

At the end of the synthetic process, it is necessary to remove the peptide from the polymeric support and eliminate all the side chain protecting groups. Cleavage mixtures composed of trifluoroacetic acid (TFA) and other scavenger substances represent the first choice for this operation. Actually, TFA breaks not only the bonds between peptide chain and side chain protecting groups but also the bond between the polymeric support and the polypeptide chain.

The final step of the peptide synthesis consists obviously in the purification of the crude product. A normal, not too complicated purification procedure is usually made by reversed-phase HPLC with C18 resin. Based on the hydrophobic content of the peptide, it is always possible to select a less functionalized resin for the best chromatographic resolution. Moreover, the purification of

some special synthetic peptides requires several steps that can involve other chromatographic methods such as ion exchange, metal affinity, or molecular exclusion chromatography in order to obtain the complete purification of the SPPS product.

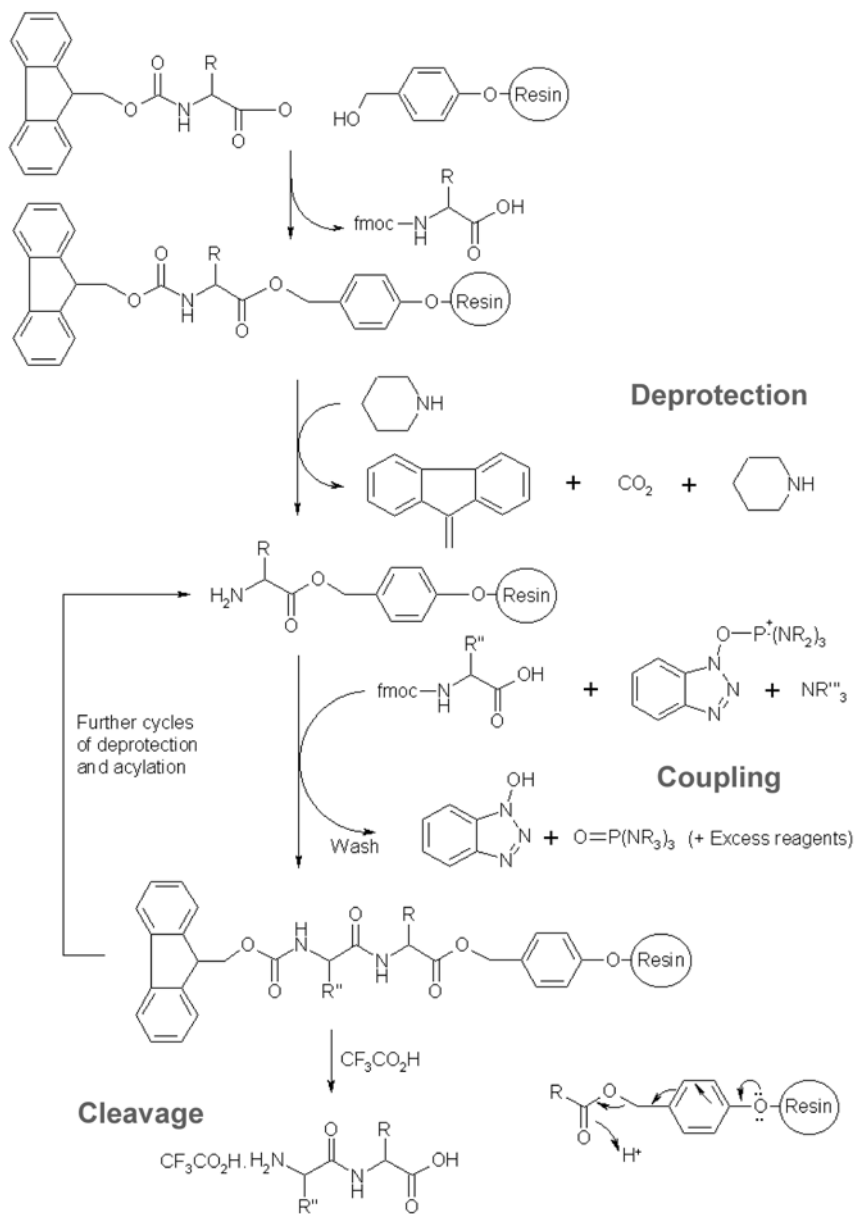


Figure 1. Fmoc solid-phase peptide synthesis.

Preface to CHAPTER 5

The response of cells to DNA damage involves recognition and repair of the lesions in DNA to minimize the risk of genetic instability [Lavin and Gueven, 2006]. There are multiple DNA damage detection and repair systems in the cell but every type of DNA damage is ultimately related to the p53 protein and its pathway [Levine *et al.*, 2006]. The short-lived p53 transcription factor is essential for the prevention of cancer development. Indeed, p53 has been called the “genome guard” due to its capacity to mediate innate tumour suppression preventing the malignant progression of tumour cells [Meek, 2009]. Oncogenic studies have revealed that either missense mutations of the p53 gene or alterations in genes encoding crucial regulators of p53 are among the most common genetic alterations in human cancers [Matsumoto *et al.*, 2006].

The p53 tumour suppressor is a modular protein that belongs to a small family of related proteins including p63 and p73, both of which can interact with the p53 pathway in addition to their own functions. The N-terminal region of p53 consists of an intrinsically disordered acidic transactivation domain (TAD), required for transcriptional activation of target genes, and a proline-rich region (PRR), involved in multiple protein–protein interactions. The central region of p53 contains a large DNA-binding domain (p53C), that accounts for most mutations in a wide variety of cancers. This region is followed by a tetramerization domain that regulates the oligomerization state of p53, promoting the formation of the active tetrameric form of p53, with four identical chains. Finally, the C-terminal region contains the so-called regulatory domain. This naturally unfolded region rich in basic residues is able to bind non-specifically to damaged DNA and harbours three nuclear localization signals.

The most extensively studied function of p53 is its transcriptional activity that both positively and negatively regulates the expression of a large and disparate group of responsive genes (more than 100) [Laptenko and Prives, 2006; Wei *et al.*, 2006]. Clear evidence for a role of p53 in the regulation of glycolysis and autophagy, the repair of genotoxic damage, cell survival and regulation of oxidative, invasion and motility, cellular senescence, angiogenesis, differentiation, and bone remodelling outline an overall model of p53 activity that might be at the base not only of the regulation of cancer progression, but also of the control of other aspects of health and disease [Vousden and Lane, 2007]. Although the ability of p53 to regulate gene expression is a key mechanism for the activation of the broad number of cellular responses, transcriptionally-independent activities of p53, that can potentiate the apoptotic response, have also been described. Actually, p53 has been reported to translocate to the outer mitochondrial membrane where it interacts with pro- and antiapoptotic members of the Bcl-2 protein family [Chipuk and Green, 2003].

Noteworthy, key factors that determine the outcome of p53 induction, at least in cultured cells, are the type and intensity of stress, the cell type and the genetic background [Meek, 2009].

The propensity of p53 to interact and form complexes with a multitude of other proteins [Braithwaite *et al.*, 2006] characterizes also the tight control of cellular concentrations of the p53 protein. The levels of the p53 protein are predominantly regulated by its proteolytic turn-over. In fact, p53 has a short half-life dictated, mainly, by its interaction with the ubiquitin ligase MDM2. The negative regulator Mouse double minute 2 (MDM2), in concert with its homolog MDM4, maintains p53 at low levels within the cell under normal conditions, by adding ubiquitin chains to p53 protein, thus targeting p53 to proteasomal degradation [Brooks and Gu, 2003]. Noteworthy, p53 stimulates the expression of MDM2 and thus operates in a negative feedback loop with its principal inhibitor [Meek, 2009]. In response to oncogenic or other cellular stress, p53 is activated, such an activation being defined as an increase in the concentration of the p53 protein, and accumulates in the cell inducing up- or downregulation of a variety of downstream target genes involved in cell cycle arrest, DNA repair, senescence, or apoptosis.

The crucial event in the induction of the p53 pathway is, indeed, the uncoupling of p53 from its regulators MDM2 and MDM4. Although after some types of DNA damage, i.e. gamma radiation, the MDM2 protein is auto-polyubiquitinated resulting in its degradation and consequent increase in p53 levels and activity [Stommel and Wahl, 2004], this mechanism is not observed in all types of DNA damage or stress signals [Levine *et al.*, 2006]. A common outline is that once different stimuli, acting at different levels of cellular physiology, stabilize and

activate p53, a series of posttranslational modifications influence the interaction between p53 and MDM2 [Harris and Levine, 2005]. Both p53 and its negative regulator MDM2 are extensively modified after a stress signal [Appella and Anderson, 2001]. Interestingly, the extent and nature of these protein alterations differ with different types of inputs. Therefore, posttranslational modifications to p53 and MDM2, subcellular redistribution, inhibition of MDM2 activity and direct repression of MDM2 transcription are all mechanisms exploited by the cell to promote the rapid accumulation of p53 in response to stress signals [Ryan *et al.*, 2001].

p53 is subjected to a complex and diverse array of covalent posttranslational modifications, which markedly influence the expression of p53 target genes. The primary amino acid sequence of p53 contains many conserved serine, threonine, and lysine residues that are of potential regulatory significance. Posttranslational modifications at these conserved residues have a crucial role in p53 stabilization and activation [Toledo and Wahl, 2006]. The most commonly reported PTMs of p53 include phosphorylation of serines and/or threonines and acetylation, ubiquitylation and sumoylation of lysine residues. Other reported modifications of p53 include glycosylation and ribosylation. The consequent cellular response is dependent on the particular posttranslational modifications conferred on the p53 protein [Bode and Dong, 2004], which form a chemical code that could inform the p53 protein and the cell about the type of stress that is occurring.

Phosphorylation, as well as acetylation, has been proposed to be an important mechanism by which stabilization and function of p53 are regulated [Meek, 1994; Prives, 1998]. Most sites are phosphorylated in response to different stress signals, in addition there are also a few sites in p53, which are constitutively phosphorylated (e.g. Ser378) and certain sites are actually dephosphorylated in response to stress signals, such as Ser376 and Thr55 [Olsson *et al.*, 2007].

Not less than 17 phosphorylated residues have been detected in human p53 [Bode and Dong, 2004], whose phosphorylation is promoted by a variety of protein kinases each of which in turn may impinge on more than one residue. Many of these residues are clustered in the N-terminal region, within the transactivation domain, whose phosphorylation is generally believed to increase the stability and level of p53 by reducing the interaction with the main negative regulator MDM2 while promoting the binding of the acetyltransferase p300 [Lacroix *et al.*, 2006]. These are seryl residues 6, 9, 15, 20, 33, 37, and 46 and the threonyl residue 18 [Appella and Anderson, 2001]. They share the property of being phosphorylated in response to ionizing

radiations or UV light, but a complex panel of partially unidentified protein kinases are responsible for their individual phosphorylation. In particular, CK1 has been implicated in the phosphorylation of Ser6 and Ser9 (in a hierarchical fashion) [Higashimoto *et al.*, 2000; Knippschild *et al.*, 1997; Cordenonsi *et al.*, 2007] and of T18 [Dumaz *et al.*, 1999; Sakaguchi *et al.*, 2000], an event primed by previous phosphorylation of Ser15 by a variety of kinases, including DNA-PK [Shieh *et al.*, 1997], ATM [Saito *et al.*, 2002], ATR [Tibbetts *et al.*, 1999], ERKs, and p38 [She *et al.*, 2000]. Recently, however, the characterization of a kinase responsible for the phosphorylation of p53 at Ser20 in response to DNA viral infections led to its identification as CK1 α [MacLaine *et al.*, 2008]. This came as a surprise, since Ser20 was previously reported to be a target of kinases other than CK1, notably CHK1/CHK2 [Chehab *et al.*, 1999; Unger *et al.*, 1999], JNK, and MAPKAPK2 [She *et al.*, 2002]. Of note in this respect, several studies have suggested that phosphorylation of human p53 at serine 20, which is located within the α -helix involved in MDM2 interaction, plays an important role in p53 stabilization after DNA damage by disrupting MDM2–p53 interaction [Shieh *et al.*, 1999; Unger *et al.*, 1999; Chehab *et al.*, 1999].

CHAPTER 5

Isoform Specific Phosphorylation of p53 by Protein Kinase CK1

The ability of three isoforms of protein kinase CK1 (α , γ_1 , and δ) to phosphorylate the N-terminal region of p53 has been assessed using either recombinant p53 or a synthetic peptide reproducing its 1–28 sequence. Both substrates are readily phosphorylated by CK1 δ and CK1 α , but not by the γ isoform. Affinity of full size p53 for CK1 is 3 orders of magnitude higher than that of its N-terminal peptide (K_m 0.82 μ M vs 1.51 mM). The preferred target is S20, whose phosphorylation critically relies on E17, while S6 is unaffected despite displaying the same consensus (E-x-x-S). Our data support the concept that non-primed phosphorylation of p53 by CK1 is an isoform-specific reaction preferentially affecting S20 by a mechanism which is grounded both on a local consensus and on a remote docking site mapped to the K²²¹RQK²²⁴ loop according to modeling and mutational analysis.

This chapter was published in:

Andrea Venerando, Oriano Marin, Giorgio Cozza, Victor H. Bustos, Stefania Sarno, and Lorenzo A. Pinna (2009) Isoform specific phosphorylation of p53 by protein kinase CK1. *Cellular and Molecular Life Sciences* doi:10.1007/s00018-009-0236-7

Materials and methods

Solvents and coupling reagents for peptide synthesis were from Applied Biosystems (Foster City, CA). Protected amino acids were from Novabiochem (brand of Merck, Darmstadt, Germany). All other analytical grade reagents were from Sigma–Aldrich (St. Louis, MO). Monoclonal antibody against p53 and phospho-p53 (Ser6), (Ser9), (Ser15), (Thr18), (Ser20), (Ser37), (Ser46), (Ser392) antibodies were from Cell Signaling Technology (Beverly, MA). [γ - ^{33}P]ATP (3,000 Ci/mmol) was purchased from Perkin Elmer (Waltham, MA). Plasmid pGEX-4T1 for GST-hp53 was kindly supplied by Dr. Michelangelo Cordenonsi (Padua).

Synthetic peptides

The p53-derived synthetic peptides on display in Table 1 were synthesized by solid-phase peptide synthesis method using a multiple peptide synthesizer SyroII (MultiSynTech, Witten, Germany) on 4-Hydroxymethylphenoxyacetyl PEGA resin (Novabiochem) solid support. The 9-fluorenylmethoxycarbonyl (Fmoc) strategy [Fields and Noble, 1990] was applied throughout the peptide chain assembly, using 2-(1H-benzotriazol-1-yl)-1,1,3,3-tetramethyluronium hexafluorophosphate (HBTU) and 1-hydroxybenzotriazole (HOBT) as coupling reagents. The side-chain protected amino acid building blocks were as follows: Fmoc-Glu(tert-butyl), Fmoc-Asp(tert-butyl), Fmoc-Ser(tert-butyl), Fmoc-Ser(PO(Bzl)OH), Fmoc-Thr(tert-butyl), Fmoc-Lys(tert-butyloxycarbonyl), Fmoc-His(trityl), Fmoc-Gln(trityl), and Fmoc-Trp(tert-butyl oxycarbonyl). Cleavage of the peptides was performed by reacting the peptidyl-resins with a mixture containing trifluoroacetic acid/water/thioanisole/ethanedithiol/phenol (10 ml/0.5 ml/0.5 ml/0.25 ml/750 mg) for 2.5 h. Crude peptides were purified by a preparative reverse phase HPLC. Molecular masses of the peptides were confirmed by mass spectroscopy on a model 4800 MALDI TOF-TOF mass spectrometer (Applied Biosystems). The purity of the peptides was in the range 95–98% as evaluated by analytical reverse phase HPLC. Additionally, two lysine residues were introduced at C-terminal side of each peptide. Such a basic motif was essential for the protein kinase assay based on phosphocellulose paper substrate absorption.

Protein cloning, expression, and purification

The clones of CK1 α (gene code Q8JGT0) and CK1 δ (isoform B, gene code Q6P3K7) from zebrafish (*Danio rerio*), and the clone of CK1 γ_1 (gene code Q5PRD4) from rat were obtained as

described previously [Ferrarese *et al.*, 2007; Burzio *et al.*, 2002]. All the isoforms of CK1 contained six histidines in the N-terminus to facilitate the purification. The delta isoform was obtained either full length or with a C-terminal truncation ($\Delta 317$). This latter, which is nearly indistinguishable from the corresponding sequence of the ϵ isoform (95% identity), was used throughout the paper, unless indicated differently. Two mutants of CK1 $\delta^{\Delta 317}$ (K221L and K224A) were generated with the QuikChange Site-Directed Mutagenesis Kit (Stratagene, La Jolla, CA) using the forward and reverse primer oligonucleotides as follows: for K221L, 5'-GAAAGCCGCCACCTTGAGACAGAAGTATGAGCG-3' and 5'-CGCTCATACTTCTGTCTC AAGGTGGCGGCTTTC-3', respectively; for K224A, 5'-GCCGCCACCAAGAGACAGGC GTATGAGCGTATC-3' and 5'-GATACGCTCATAACGCCTGTCTCTTGGTGGCGGC-3', respectively. The E17A p53 mutant was generated with the QuikChange Site-Directed Mutagenesis Kit using pGEX-4T1-hp53 as template and forward and reverse primer oligonucleotides as follows: 5'-CCTCTGAGTCAGGCAACATTTTCAGACC-3' and 5'-GGTCTGAAAATGTTGCCTGACTCAGAGG-3', respectively. The mutations were confirmed by DNA sequencing.

Conventional name	Amino acids sequence
WT	MEEPQSDPSVEPPLSQETFSDLWKLPEKK
S6A	MEEPQADPSVEPPLSQETFSDLWKLPEKK
S9A	MEEPQSDPAVEPPLSQETFSDLWKLPEKK
S15A	MEEPQSDPSVEPPLAQETFSDLWKLPEKK
E17A	MEEPQSDPSVEPPLSQATFSDLWKLPEKK
S20A	MEEPQSDPSVEPPLSQETFADLWKLPEKK
S6S9AA	MEEPQADPAVEPPLSQETFSDLWKLPEKK
S15S20AA	MEEPQSDPSVEPPLAQETFADLWKLPEKK
S6S9S15AAA	MEEPQADPAVEPPLAQETFSDLWKLPEKK
S6S9S20AAA	MEEPQADPAVEPPLSQETFADLWKLPEKK
S6S9S15E17AAAA	MEEPQADPAVEPPLAQATFSDLWKLPEKK
pS6S15S20AA	MEEPQpSDPSVEPPLAQETFADLWKLPEKK
pS15	MEEPQSDPSVEPPLpSQETFSDLWKLPEKK
pS20	MEEPQSDPSVEPPLSQETfpSDLWKLPEKK
pS6pS9	MEEPQpSDPpSVEPPLSQETFSDLWKLPEKK
pS6pS9pS15	MEEPQpSDPpSVEPPLpSQETFSDLWKLPEKK

Table 1. N-terminal p53 peptides used in the present study. The wild-type peptide reproduces the 1–28 sequence of human p53 with the addition of two C-terminal lysine residues (in italics) required for protein kinase assay by phosphocellulose p81 paper absorption method. Residues substituted relative to wild-type are in bold. For details, see “Materials and methods”. pS Phosphoserine.

Protein expression and purification

CK1 α and CK1 γ were expressed in *Escherichia coli* BL21(DE3) cells. The plasmids of CK1 δ (full length, $\Delta 317$ and its mutants) were used to transform *E. coli* strain B834. Cells were grown

at 37°C to an OD₆₀₀ of 0.5–0.6. At this point, protein expression was induced by adding isopropyl β-D-thiogalactoside (IPTG) to a final concentration of 0.3, 0.8, and 1 mM for CK1α, CK1γ, and CK1δ, respectively. Induction was carried out overnight at 20°C in the case of CK1α and CK1δ, while for CK1γ, the temperature was 25°C. Afterwards, the cells were harvested by centrifugation at 3,000g for 20 min at 4°C, and resuspended in lysis buffer (50 mM Tris/HCl, pH 8.0, 20% v/v glycerol, and 0.5 M NaCl, supplemented with protease inhibitor cocktail from Sigma). Cells were lysed by French press. The soluble fraction, obtained after 30 min of centrifugation at 10,000g, was applied onto Ni–NTA–agarose columns (Sigma) equilibrated with the lysis buffer. The columns were extensively washed and the proteins were subsequently eluted with a buffer containing 50 mM Tris/HCl, pH 6.8, 5% v/v glycerol, 50 mM NaCl, and 300 mM imidazole. CK1γ and CK1δ were further purified by gel filtration with Superdex 75 10/300GL column (Amersham Pharmacia Biotech) equilibrated in a buffer containing 25 mM Tris/HCl, pH 7.0, 0.1 M NaCl, and 1 mM dithiothreitol (DTT).

GST-fusion protein of human recombinant p53 and its E17A mutant were expressed in *E. coli* BL21(DE3) cells. Cells were grown at 37°C to an OD₆₀₀ of 0.7. Protein expression was induced by adding 1 mM IPTG and it was allowed to proceed for 4 h at 30°C. Afterward, cells were pelleted at 3,000g for 20 min at 4°C, and cell pellets were resuspended in PBS, added with protease inhibitors, and lysed using a French press. After centrifugation at 10,000g for 30 min, the supernatant was loaded onto Glutathione–Sepharose 4 Fast Flow columns (GE-Healthcare, UK), equilibrated with binding buffer (PBS, pH 7.3, and 1 mM DTT). Proteins were eluted with a buffer containing 50 mM Tris/HCl, 0.1 M NaCl, 1 mM DTT, and 10 mM glutathione, and the most pure fractions were pooled, concentrated, and applied onto a gel filtration Superdex 200 HiLoad 26/60 column (Amersham Pharmacia Biotech), equilibrated in a buffer containing 25 mM Tris/HCl, pH 8, 0.1 M NaCl, 10% v/v glycerol, and 1 mM DTT. Untagged recombinant p53 was obtained by cleaving GST-p53 bound to the Glutathione–Sepharose 4 Fast Flow resin (GE-Healthcare) in the presence of 40 U of thrombin at 4°C over night. The column was washed with 50 mM Tris/HCl, 0.1 M NaCl, 10% v/v glycerol, and 1 mM DTT; the fractions containing untagged p53 were collected, concentrated, and applied onto a gel filtration Superdex 200 HiLoad 26/60 column (Amersham Pharmacia Biotech) for a further purification. Its apparent MW, as assessed by gel filtration experiments, was consistent with a tetrameric form of p53.

Phosphorylation assays

Reaction conditions for peptide phosphorylation experiments were the following: a range of concentration of synthetic peptides derived from human p53 N-terminal region were phosphorylated by incubation in a 20- μ l volume containing 50 mM Tris/HCl, pH 7.5, 10 mM MgCl₂, 100 mM NaCl, and 50 μ M [γ -³³P]ATP (specific radioactivity 1,500–2,000 cpm/pmol). The reaction was started by the addition of protein kinases CK1 α , CK1 γ , and CK1 δ (either full length or Δ 317) normalized against a common peptide substrate, derived from Inhibitor-2 of protein phosphatase-1 (the ‘‘I-2’’ peptide RRKHAAIGDDDDAYSITA) [Marin *et al.*, 1994], as previously described [Ferrarese *et al.*, 2007]. More precisely, each amount of CK1 isoform displayed with I-2 peptide an activity of 12 pmol of phosphate transferred per minute. The reaction mixtures were incubated for the indicated time at 37°C and stopped by ice cooling and absorption on phospho-cellulose p81 paper. Papers were washed three times with 75 mM phosphoric acid, dried, and counted in a scintillation counter. Reaction conditions for full-length p53 phosphorylation were identical to those used for peptide phosphorylation except for the replacement of the peptide with full-length p53, either GST-tagged or deprived of the tag at concentrations ranging between 30 nM and 2.5 μ M. The reaction was stopped by the addition of 5 x concentrated Laemmli buffer and boiling followed by SDS-polyacrylamide gel electrophoresis (SDS-PAGE), Coomassie staining, and autoradiography (PerkinElmer’s Cyclone Plus Storage Phosphor System). Results are representative of at least three independent experiments. ³³P incorporation was evaluated by excision of protein bands from the gel followed by counting in a scintillation counter.

Initial rate data were fitted to the Michaelis–Menten equation with the program Prism (GraphPad Software, La Jolla, CA) to obtain K_m and V_{max} values.

Phospho-aminoacids analysis

After phosphoradiolabeling, peptides were separated from reaction mixture by filtration on Strata C18-E columns (Phenomenex, Torrance, CA), lyophilized, and digested with 6 N HCl for 4 h at 110°C. Each sample was subjected to high-voltage paper electrophoresis at pH 1.9 for 2.5 h, in the presence of non-radioactive phospho-amino acids, as migration reference, followed by autoradiography [Perich *et al.*, 1992].

Western blotting

GST-p53 proteins after *in vitro* kinase reaction were resolved by 11% SDS-PAGE, and transferred onto Immobilon-P membranes (Millipore, Billerica, MA). Membranes were probed with the indicated antibody, and detected by ECL (enhanced chemiluminescence; Amersham Biosciences). Quantitation of the signal was obtained by chemiluminescence detection on Kodak Image Station 440cf (Eastman Kodak, New Haven, CT) and by analysis with the Kodak 1D image software.

Protein–protein docking

For the computer-aided protein–protein docking stages, rat CK1 δ isoform and the mouse p53 were retrieved from the PDB (PDB code: 1CKJ and 2IOI, respectively). Hydrogen atoms were added to the protein structure using standard geometries with the MOE program [MOE, 2008]. To minimize contacts between hydrogens, the structures were subjected to Amber99 force field minimization until the rms of conjugate gradient was $<0.1 \text{ kcal mol}^{-1} \text{ \AA}^{-1}$, keeping the heavy atoms fixed at their crystallographic positions [MOE, 2008]. After this initial *in silico* approach, a set of protein–protein docking experiments was performed. Protein–protein docking is a computational tool useful for predicting the 3D structure of protein complexes from the coordinates of its subunits. We have adopted a two-stage approach, which recently proved quite successful [Cozza *et al.*, 2008; Poletto *et al.*, 2008]; in the first stage, the two monomers were treated as rigid bodies and all the rotational and translational degrees of freedom were fully explored, using a cluster of protein–protein docking algorithms (Zdock, Gramm and Echer); in the second stage, a small number of structures deriving from the initial stage was refined in the docking zone using side-chain rotamers and energy-minimization strategy.

Results

Several phosphorylated residues, generated by the concerted action of a variety of protein kinases, are clustered in the N-terminal segment of p53 [Bode and Dong, 2004]. These include the amino acids phosphorylated by CK1, whose precise identification is still a matter of debate. *A priori*, the only residues displaying a canonical sequence (E/D-x-x-S) for non-primed phosphorylation by CK1 appear to be S6, (which, once phosphorylated, could prime subsequent phosphorylation of S9) and S20. In turn, S15, believed to be a substrate of kinases other than CK1 (DNA-PK [Shieh *et al.*, 1997], ATM [Saito *et al.*, 2002], ATR [Tibbetts *et al.*, 1999],

ERKs, and p38 [She *et al.*, 2000]), once phosphorylated is in the right position to prime phosphorylation of T18 by CK1 [Dumaz *et al.*, 1999; Sakaguchi *et al.*, 2000]. Given these premises, peptides encompassing the N-terminal segment of p53 have been widely employed in mechanistic studies dealing with the implication of CK1 (and also of other kinases) in p53 phosphorylation [Appella and Anderson, 2001; Knippschild *et al.*, 1997; Dumaz *et al.*, 1999].

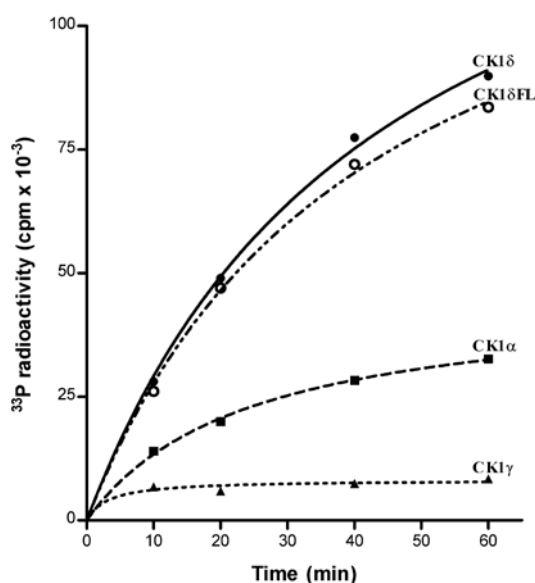


Figure 1. Time-courses of phosphorylation of p53_[1-28] peptide by CK1 isoforms. Phosphorylation was performed in the presence of equiactive amounts of the indicated CK1 isoforms, as detailed in “Materials and methods”. The peptide concentration was 1 mM.

We therefore started our investigation by assaying a peptide encompassing residues 1–28 of p53 for its ability to undergo phosphorylation by different isoforms of CK1, namely the α , γ_1 , and δ isoforms. The peptide concentration was 1 mM and equi-active amounts of the CK1 isoforms were used, normalized for displaying identical activity toward a common peptide substrate (see “Materials and methods”). Under these comparable conditions, the time courses of phosphorylation reported in Fig. 1 were obtained: they show that, while the peptide is readily phosphorylated by CK1 δ , phosphorylation by CK1 α was much less pronounced, and that by the γ isoform was hardly detectable. Note that phosphorylation by C-terminally deleted CK1 δ isoform, which is substantially identical to CK1 ϵ (see “Materials and methods”) is superimposable on that of full-length CK1 δ . Phospho-amino acid analysis revealed only phosphoserine, ruling out any appreciable phosphorylation of T18 (Fig. 2, lane 1).

To gain information about the seryl residues phosphorylated in the p53 peptide, these were individually or multiply replaced by the non-phosphorylatable residue alanine (see Table 1). The

phosphorylation rates of the substituted peptides relative to the parent peptide (wild-type) are shown in Fig. 3a. While substitution of S6 and S9 (either single or double) reduces phosphorylation by less than 30%, a much more dramatic drop in phosphorylation rate was observed upon substitution of both seryl residues 15 and 20, consistent with the view that S15 and/or S20 are the main target(s) of CK1 δ . The actual implication of S20 rather than S15 is supported by the additional finding that replacement of S20 with alanine is detrimental both in the wild-type peptide and in the S6S9-substituted one. By sharp contrast, the individual replacement of S15 did not decrease but slightly increases the phosphorylation rate of the wild-type peptide. The same phosphorylation patterns were obtained by replacing truncated CK1 δ with either full-length CK1 δ or CK1 α (data not shown).

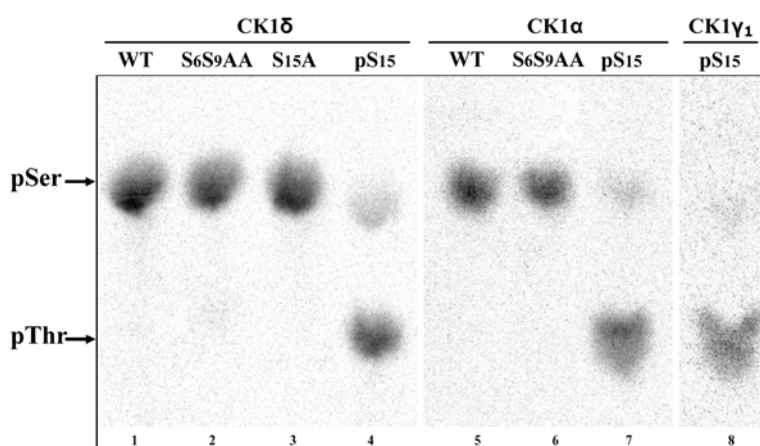


Figure 2. Phosphoaminoacid analysis of high-voltage paper electrophoresis. Peptides (0.5 mM) were incubated with indicated CK1 isoforms for 60 min in the presence of radioactive phosphorylation mixture. ^{33}P -radiolabeled peptides (as indicated) were hydrolyzed in 6 N HCl at 110°C for 4 h, and subjected to high-voltage paper electrophoresis followed by autoradiography for the identification of the phospho-amino acid (see “Materials and methods”). The position of phospho-amino acids (pSer and pThr), determined by cold standard migration, is indicated by the arrows.

These data are consistent with the conclusion that the main CK1 δ and CK1 α target in the N-terminal segment of p53 is S20 whose replacement with alanine is invariably causative of a dramatic drop in phosphorylation rate whether it is performed in the wild-type or in the S15A or in the S6S9AA peptides (85, 80, and 94%, respectively). Interestingly, S20 phosphorylation by CK1 is clearly relying on the weak consensus generated by a glutamic acid at position n-3 (E-t-f-S20), as the replacement of this residue (E17) with alanine, either in the wild-type peptide or in the triply substituted one (S6S9S15AAA) has a detrimental effect, comparable to that of the replacement of S20 itself (see Fig. 3a). Minor phosphorylation of S6 and/or S9, on the other hand, is consistent with residual (around 20%) phosphorylation of the S15S20-substituted

peptide and with decreased phosphorylation observed by replacing serines 6 and 9 in the wild-type peptide (about 25%) and, even more in the S15A-substituted peptide. Of note in this respect is the significant drop in phosphorylation rate promoted by the S9 substitution as opposed to the almost negligible effect of the S6 substitution. These data suggest that a significant albeit weak non-primed phosphorylation of S9, but not of S6, is catalyzed by CK1 δ and CK1 α . Non-primed phosphorylation of T18 has to be ruled out in any case since no detectable phospho-threonine could be isolated from the wild-type or S15A or S6S9AA peptides ^{33}P -radiolabeled by either CK1 δ or CK1 α (see Fig. 2, lanes 1–3 and 5–6, respectively).

It is worth noting in this respect that if S15 instead of being replaced by alanine is substituted by a phosphoserine, thus mimicking a reaction occurring *in vivo* by the intervention of various protein kinases, notably DNA-PK [Shieh *et al.*, 1997], the radioactivity incorporated by CK1 δ is dramatically increased (see Fig. 3b) being now almost entirely accounted for by phospho-threonine (Fig. 2, lane 4). This leads to the conclusion that, while S20 is the main non-primed target of CK1 δ , preferentially affected when the p53 peptide is not phosphorylated, once S15 is phosphorylated, primed phosphorylation of T18 becomes predominant over non-primed phosphorylation of S20. It is also worth noting in this respect that, while non-primed phosphorylation of S20 is catalyzed by the δ and to a lesser extent by the α isoform but not by the γ_1 isoform (see Fig. 1), primed phosphorylation of T18 in the pS15 peptide can also be performed by all three isoforms of CK1 (Fig. 3b–d), though in the case of CK1 γ_1 , it is still much less pronounced than that mediated by CK1 δ . The possibility that variable phosphorylation of the pS15 peptide by CK1 isoforms could be due to the targeting of different residues was ruled out by showing that T18 was the main phospho-acceptor residue, regardless to the isoform used (see Fig. 2, lanes 4, 7, 8). The priming potential of S6 appears to be weaker than that of S15 since its chemical phosphorylation within a peptide, in which S15 and S20 have been replaced by alanine, promotes a moderate phosphorylation of S9 by CK1 δ and α , having no effect at all with CK1 γ_1 (see Fig. 3, compare panels b, c, d). We have also examined the behavior of additional phosphopeptides, singly phosphorylated on S20, or doubly phosphorylated on S6 and S9, or triply phosphorylated on S6, S9, and S15. Their phosphorylation by CK1 δ is shown in Fig. 3b. Previous phosphorylation of S20 has a detrimental effect comparable to its replacement with alanine, reinforcing the conclusion that S20 is the main target of CK1 which becomes nearly inactive whenever S20 is no longer available as a phosphoacceptor residue. Quite unexpectedly, the doubly phosphorylated peptide pS6pS9 has lost any susceptibility to CK1 catalyzed phosphorylation. This is probably an artefact due to cyclization of the phosphopeptide through electrostatic interaction between the phosphates and the two C-terminal lysines added for

rendering possible the phosphorylation assay with phosphocellulose paper (see Table 1). This point of view, supported by dynamic modelization (not shown), is also corroborated by the triply phosphorylated peptide (pS6, pS9, pS15) where primed phosphorylation of T18 becomes eightfold slower than that of its congener singly phosphorylated at S15 (Fig. 3b).

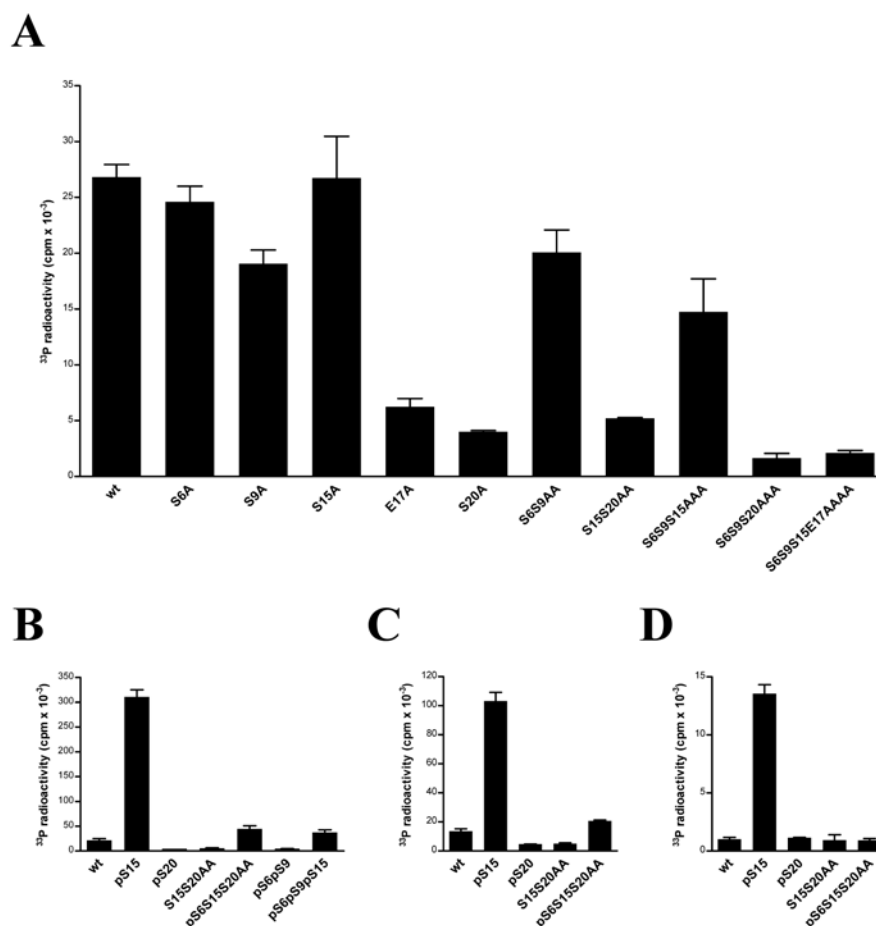


Figure 3. Phosphorylation of substituted p53 N-terminal peptides by CK1. (A) The effect due to replacing serines and E17 with alanine is analyzed. Phosphorylation was performed by incubation with CK1 δ for 10 min at 37°C. A superimposable histogram was obtained by replacing CK1 δ with CK1 α . (B–D) p53 phosphopeptides (as indicated) underwent phosphorylation assays in the presence of CK1 δ , CK1 α , and CK1 γ_1 , respectively. Phosphorylation rates of the unprimed peptides, WT and S15S20AA, is also reported for comparison. For peptide nomenclature, see Table 1. The concentration of the peptides was 1 mM.

From the kinetic constants presented in Fig. 4, it appears that the p53 N-terminal peptides display with either the δ or the α isoforms K_m values around 1 mM, denoting low affinity for CK1. This also seems to be a common feature of peptides reproducing phosphoacceptor sites for CK1 in other physiological substrates, notably NF-AT4, β -catenin and APC [Marin *et al.*, 2002; Bustos *et al.*, 2006; Ferrarese *et al.*, 2007]. Interestingly, it has been shown that such a weakness of the

local determinants may be compensated for by remote docking sites which in the case of β -catenin cause a drop in K_m value from over 1 mM to 0.19 μ M [Bustos *et al.*, 2006].

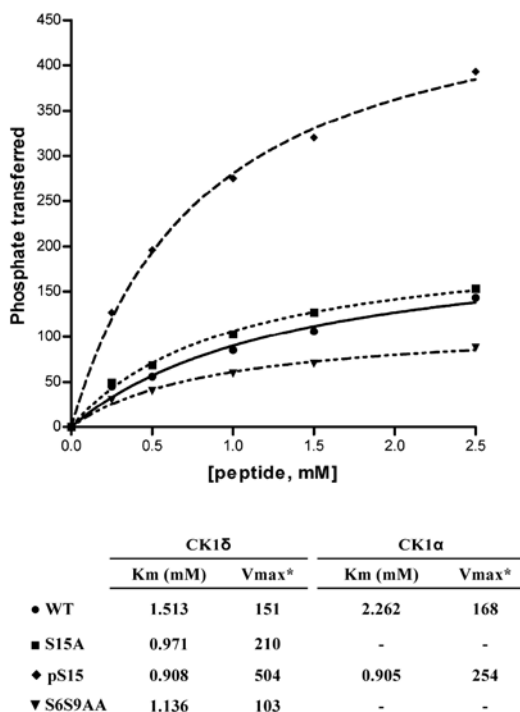


Figure 4. Kinetics of p53 peptides phosphorylation by CK1 α and δ . The indicated peptides were subjected to phosphorylation with CK1 α (not shown on graph) and δ as described in “Materials and methods”. Initial rate data were fitted to the Michaelis–Menten equation to obtain V_{max} and K_m values reported in the inset. * V_{max} is expressed as picomoles of phosphate transferred per minute per unit of enzyme (one unit being defined as the amount of enzyme that transfers 1 nmol of phosphate per minute on the I–2 reference peptide). Therefore, they are not representative of specific activity. See “Materials and methods” for details.

We therefore suspected that a similar situation may also apply to p53, and to assess this point we have run kinetics with full length p53 replaced for the p53_[1–28] peptide. The phosphorylating enzyme was CK1, either α , or γ_1 , or δ isoforms. As in the case of the p53 peptide, the γ isoform proved unable to catalyze any significant phosphorylation of full-length p53; the α isoform, however, albeit less active than δ on the peptide (see Fig. 1), was able to phosphorylate full-size p53 with kinetics comparable to those of the δ isoform (Fig. 5a). Note that with both isoforms the K_m is in the submicromolar range, highlighting a 3 orders of magnitude higher affinity of CK1 δ and CK1 α for the full size protein as compared to the derived peptide. By sharp contrast the V_{max} with the peptide is about 50-fold higher than with the full-size protein as also observed with other CK1 substrates [Marin *et al.*, 2003; Bustos *et al.*, 2006]. We can conclude therefore that unprimed full-length p53 can be efficiently phosphorylated by both the α and δ but not by

the γ isoform of CK1. Also noteworthy are the identical kinetic constants calculated using either full length or truncated CK1 δ . This latter displays a nearly 100% identity with the corresponding sequence of the ϵ isoform, consistent with the knowledge that p53 is also readily phosphorylated by CK1 ϵ [Knippschild *et al.*, 1997; Behrend *et al.*, 2000].

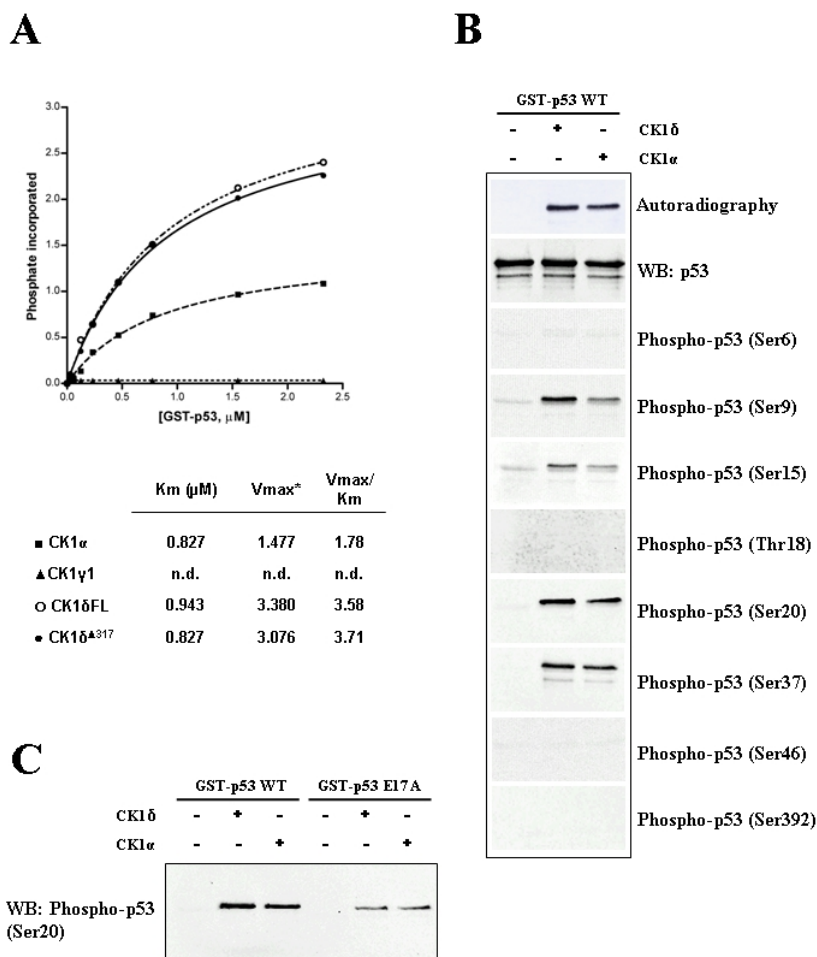


Figure 5. Phosphorylation of p53 proteins by CK1 isoforms. (A) The kinetics of phosphorylation by CK1 isoforms of increasing concentrations of full-length GST-p53 wild-type are illustrated. p53 was subjected to phosphorylation with the indicated CK1 isoforms as described in “Materials and methods”. Of note are the identical kinetics of full-length and truncated (Δ 317) CK1 δ , this latter sharing 95% identity with the ϵ isoform. *V_{max} is expressed as picomoles of phosphate transferred per minute per unit of enzyme; n.d. not determined due to undetectable phosphorylation. (B) Full-length human GST-p53 (1.2 μ g) produced in *E. coli* was phosphorylated by 10 min incubation with either CK1 δ or α isoforms and subjected to western immunoblotting analysis with the antibodies indicated on the right. Superimposable kinetics and phosphorylation pattern were obtained replacing GST-p53 with untagged p53 obtained by proteolytically removing of the tag (see “Materials and methods”). (C) Effect of the Glu17 to Ala mutation on p53 S20 phosphorylation by CK1. Equal amounts (1.2 μ g) of full-length p53, either wild-type or E17A mutant, were incubated under the same conditions (see “Materials and methods”) with CK1 δ or CK1 α . Western immunoblot with the specific phospho-p53 (Ser20) antibody is shown. Densitometric analysis of the anti-phospho-S20 signal shows a remarkable decrease in phosphorylation of the E17A mutant by CK1 α (70%) and δ (90%).

To localize the residues affected by CK1 in full-length p53, advantage has been taken of commercially available phosphospecific antibodies raised against individual p53 phosphoresidues. These were probed by western blot analysis on p53 phosphorylated by CK1 α

and δ at a concentration close to its K_m value (750 nM). As shown in Fig. 5b, p53 immunoreacts with specific antibodies raised against phospho-S9, phospho-S15, phospho-S20, and phospho-S37, but not with the phospho-S6, phospho-T18, phospho-S46, and phospho-S392 antibodies. Lack of immunoreaction with phospho-p53 (T18) antibody reinforces the view that T18 phosphorylation is a primed event detectable only if previous substantial phosphorylation of S15 by protein kinases other than CK1 takes place. Although the data shown in Fig. 5 were obtained using GST-p53 as phosphorylatable substrate, no significant differences could be observed if this was replaced by untagged p53 (see caption of Fig. 5).

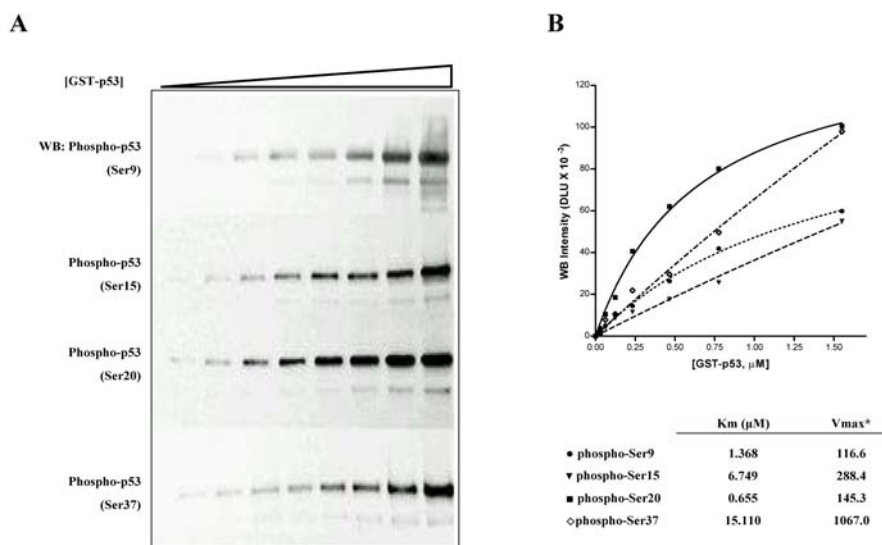


Figure 6. Kinetic analysis of individual phosphoacceptor residues upon phosphorylation of full length p53 by CK1 δ . (A) The effect due to increasing concentration of p53 on the phosphorylation rate of S9, S15, S20, and S37 was monitored by western blotting with specific phospho-serine antibodies. (B) The specific phospho-serine bands detected in (A) were quantified by densitometric analysis using the Kodak 1D image analysis software and normalized to total p53 amount. Data were plotted against GST-p53 concentration using the Graphpad Prism software to calculate K_m and V_{max} values. V_{max} evaluated with the phospho-p53 (S15) antibody may represent an overestimate, since the intensity of this band unlike those of the other bands was not linear with incubation time, as it already reached a maximum intensity after 5 min. * V_{max} is expressed as densitometry light units (DLU).

In an attempt to evaluate differences in phosphorylation efficiency among the p53 sites affected by CK1 δ kinetics were performed in which the phosphorylation of individual residues was detected and quantified by western blotting with the phosphospecific antibodies. The experimental curves are shown in Fig. 6 and the calculated K_m values, which are independent of the sensitivity of the different antibodies, are reported in the inset. It appears that the highest affinity (K_m value even lower than that of the p53 protein as a whole) is displayed by S20, followed by S9 (with twofold higher K_m), while the K_m values of S15 and S37 are 10- and >20-fold higher than that of S20, respectively. In the inset of Fig. 6, the V_{max} values are also reported;

it should be warned, however, that these are not suitable for a comparative analysis since they were calculated from data with different antibodies, whose sensitivity can be quite variable. Also of interesting in the case of full-size p53 (as already observed with the peptide) the phosphorylation of S20 is critically dependent on E17 whose replacement with alanine in the E17A mutant causes a dramatic drop in S20 phosphorylation (Fig. 5c).

Taken collectively, these data are consistent with a phosphorylation pattern of full-length p53 by CK1 δ similar to that observed with the peptide, with a marked preference for S20, as compared to S9, not to say S15 and S37 (this latter not included in the peptide anyway), whose K_m for CK1 δ is one order of magnitude higher. S6 despite its consensus sequence is not significantly phosphorylated either in the peptide (Fig. 3a) or in the protein (Fig. 5b). Likewise, non-primed phosphorylation of T18 by CK1 could not be detected in full-size p53, consistent with the view that its phosphorylation needs to be primed by stoichiometric amounts of phospho-S15 which cannot be generated under our conditions.

Thus, the only remarkable difference between full-length p53 and the peptide is the much lower affinity of the latter, strongly suggesting that a remote docking site is present in p53 which ensures high affinity binding to CK1 δ and α isoforms. In an attempt to identify such a putative docking site, we have concentrated our attention on a region which is conserved in the δ , ϵ , and α isoforms of CK1 but not in the γ isoforms. A sequence fulfilling such criteria is the K²²¹RQK²²⁴ quartet belonging to the loop next to the G helix in CK1 δ (see Fig. 7a). Indeed, the analysis of the possible interactions between CK1 δ and p53 through our protein–protein docking strategy suggests, for this quartet, one particular binding pose (see Fig. 7b). According to this model, the basic side chains of K221 and R222 interact with two acidic residues of p53, E224 and E228, respectively; note that these residues of p53 contribute to the most negatively charged stretch of the protein, where three acidic residues are clustered together (E221, E224, and E228). K224 of CK1 δ is not involved in this kind of interaction because of its implication in a tungstate ion bridge which connects the loop to the kinase core [Longenecker *et al.*, 1996]. From the analysis of CK1 δ and γ sequences and crystal structures from the protein data bank, it is possible to note that the conserved K224 (an arginine in the γ isoforms) maintains its interactions with ions or water molecules in the same position. By sharp contrast, the substitution of K221 with a leucine residue in all γ isoforms is responsible for an alteration of the loop secondary structure, with an extension of the adjacent α -helix G. In this situation, the CK1 γ lysine residue, corresponding to CK1 δ R222, is moved back by about 4.7 Å, breaking the interaction with p53 E228. Consequently, in the case of all CK1 γ isoforms, both the interactions with p53 E224 and E228

are missing, which may account for weaker affinity of CK1 γ_1 for p53, as compared to the α , δ , and ϵ isoforms.

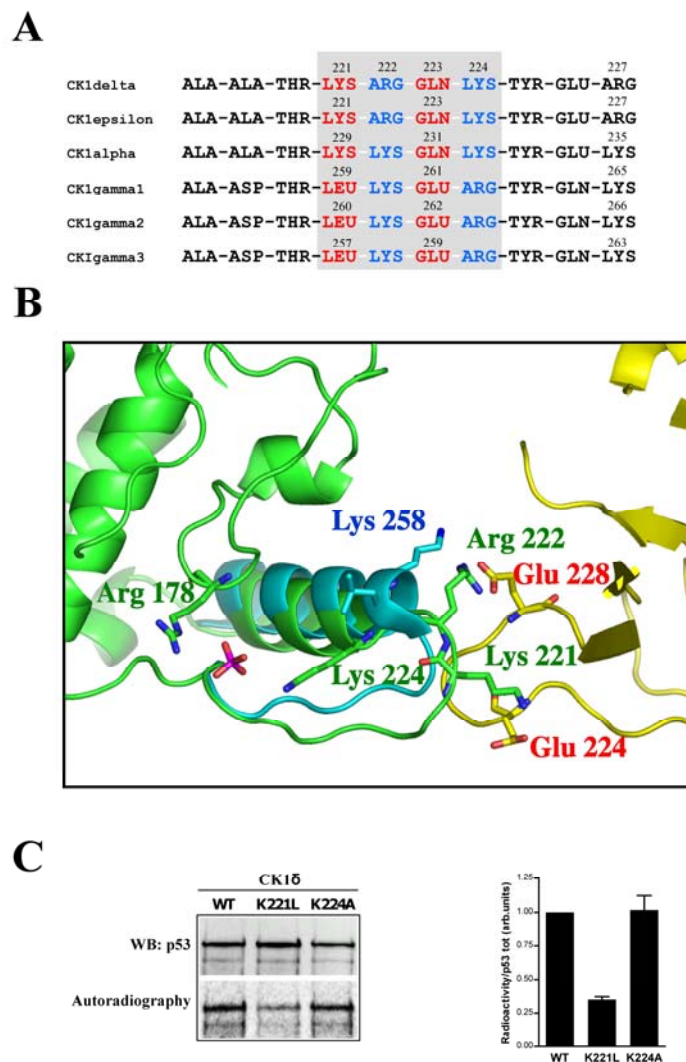


Figure 7. Mapping the putative CK1 δ docking site responsible for high affinity binding of p53. (A) Multiple alignment of the α -helix G region in different CK1 isoforms. The four residues located in the basic loop adjacent to α -helix G are displayed in the gray box. This quartet is conserved between the δ/ϵ and α isoforms (with conservative substitution of R222 with lysine) while it is deeply altered in the γ isoforms. Mutation within the loop are in red, conserved basic residues are in blue. (B) Computer-aided protein-protein docking analysis of interaction motifs between CK1 δ isoform (green) and p53 (yellow). CK1 γ (blue) is unable to bind p53 due to the substitution of K221 with leucine which causes an extension of α -helix G, thus breaking the interaction between K258 (R222 in CK1 δ) and p53 E228. For additional explanation, see text. (C) Lys221 to Leu mutation drastically reduces the ability of CK1 δ to phosphorylate p53. GST-p53 was incubated for 10 min with equi-active amounts of either CK1 δ wild-type, or its K221L or K224A mutants under the conditions for protein phosphorylation, as detailed in “Materials and methods”. Western immunoblot with p53 antibody and autoradiography are shown. Densitometric analysis of western blot and of autoradiography was performed with Kodak 1D and with Optiquant (PerkinElmer) image analysis software, respectively. The results are also shown as a bar graph where p53 radioactivity has been normalized to total p53 amount.

This model has been validated by mutational data showing that replacement of K221 with leucine in CK1 δ has a detrimental effect on its ability to phosphorylate p53 (Fig. 7c). In contrast, the mutation of K224 which, according to the model is not implicated in the interactions with p53, has no appreciable effect on p53 phosphorylation.

Discussion

Plenty of data in the literature support the implication of CK1 in the regulation of the tumour suppressor gene product p53, as amply documented in all recent reviews listing CK1 among the numerous kinases participating in the complicated mechanism of p53 modulation [Bode and Dong, 2004; Lacroix *et al.*, 2006; Appella and Anderson, 2001]. However, the identification of the CK1 isoforms implicated, as well as of the individual p53 residues affected, and of the mechanism underlying their targeting by CK1, is still poorly understood. In tables and cartoons summarizing p53 multi-phosphorylation, CK1 (with special reference to its δ and ϵ isoforms, nearly identical with each other) is invariably represented as an “N-terminal” p53 kinase impinging on S6 and S9, the latter presumably through a hierarchical mechanism, after S6 has been phosphorylated. Of note is that S6 displays the consensus for unprimed phosphorylation by CK1 owing to two acidic residues at positions n-3 and n-4 (E-E-p-q-S6). Its phosphorylation by CK1, however, is not supported by incontrovertible evidence, while it has been reported to be a target for another kinase, JNK2 [Oleinik *et al.*, 2007]. On the other hand, primed phosphorylation of T18 by CK1 isoforms has been independently reported by two groups as relying on previous phosphorylation of S15 [Dumaz *et al.*, 1999; Sakaguchi *et al.*, 2000]. This latter appears to be a target for many kinases, notably DNA-PK, ATM, ATR, ERK, and p38 [Shieh *et al.*, 1997; Saito *et al.*, 2002; Tibbetts *et al.*, 1999; She *et al.*, 2000], but not for CK1. Recently, a work aimed at the identification of kinase(s) responsible for the phosphorylation of p53 at S20 in response to HHV-6B viral infection has led to the isolation of CK1 as the most likely cellular virus-induced S20 kinase [MacLaine *et al.*, 2008]. Although S20 displays the minimum consensus for unprimed phosphorylation by CK1 (E-t-f-S²⁰), its phosphorylation was previously ascribed to kinases other than CK1, namely CHK1, CHK2 [Chehab *et al.*, 1999; Unger *et al.*, 1999], JNK, and MAPKAPK2 [She *et al.*, 2002].

The results of our mechanistic study—the first systematically performed with different isoforms of CK1 tested on full-length p53 and on a set of variably substituted N-terminal p53 segments—strongly corroborates the concept that indeed S20 displays the features for being the preferred target for the δ and ϵ and, to a lesser extent, for the α isoforms of CK1 in unprimed p53, either

full length or its N-terminal peptide. S20 is in fact the only seryl residue whose replacement with alanine in the peptide alone causes a >80% drop in phosphorylation rate (see Fig. 3), and whose phosphorylation in full-size p53 occurs with a K_m in the sub-micromolar range, comparable to that displayed by p53 as such (see Figs. 5a and 6b).

Unlike the δ and α isoforms of CK1, CK1 γ_1 proved unable to catalyze any appreciable phosphorylation of p53 or of the p53 unprimed peptide. In contrast, primed phosphorylation of T18, specified by previous phosphorylation of S15, is readily performed by all the three isoforms of CK1, albeit with variable efficiencies (see Fig. 3).

Phosphorylation of S20 in the p53 peptide clearly relies on the minimum consensus generated by E17, since the substitution of this residue with alanine has a detrimental effect comparable to that of substituting S20 itself (see Fig. 3a). Interestingly, although a similar (and even “stronger”) consensus is present upstream from S6, this residue does not appear to be susceptible to phosphorylation by CK1, either in the peptide, where its substitution has no significant effect, or in full size p53 where its phosphorylation was flatly undetectable (Fig. 5b). Incidentally, this sheds doubt on the commonly held concept that phospho-S6 is required to prime S9 phosphorylation by CK1; it is quite clear from our experiments with recombinant GST-p53 that S9 is robustly phosphorylated by CK1 δ (Figs. 5b and 6) in the absence of any appreciable phosphorylation of S6. Additionally data with phosphopeptides show that the priming efficacy of phospho-S6 on S9 phosphorylation is not as pronounced as that of phospho-S15 on T18, which is not to say that it is entirely lacking with the γ isoform (see Fig. 3).

Somewhat unexpected was the finding that p53 undergoes significant phosphorylation by CK1 δ at S15, albeit with a K_m value denoting an affinity tenfold below that of S20 (K_m 6.74 vs 0.65 μ M; see Fig. 6b). The actual intensity of S15 phosphorylation within full-size p53 may be also questionable considering that time course analysis with phospho-p53 (S15) antibody does not display time dependency as in the case of the other phosphosites (data not shown), suggesting that they might at least partially reflect an artefact due to the antibody. As a matter of fact, S15 phosphorylation is not taking place within the peptide as judged from the observation that the individual substitution of S15 with alanine has no detrimental effect whatsoever (Fig. 3a).

It should be underscored in this respect, however, that high affinity targeting of full size p53 is critically relying on remote docking site(s) which are lost in the peptide, whose phosphorylation pattern therefore could incompletely reflect that of the full-size protein. This is unambiguously demonstrated by strikingly different kinetic constants calculated for CK1 δ and α phosphorylation of either the peptide or the protein at the same residues (with the marginal exception of S37). Although in fact the phosphorylation rate with the peptide is higher (V_{max} 151 vs 3.07 pmol per

minute per unit of enzyme), its affinity is >3 orders of magnitude lower (K_m 1.51 mM as compared to 0.82 μ M), consistent with the view that physiological targeting of p53 by CK1 requires high affinity interactions between a remote complementary domain, which is lost in passing from full-size p53 to its N-terminal segment. A similar situation has been described in the case of p53 serine 20 phosphorylation after HHV-6B viral infection, whose occurrence depends on interaction of CK1 with Box IV and Box V domains of p53 [MacLaine *et al.*, 2008]. It is likely that these elements are also responsible for the high affinity phosphorylation of full-size p53 as compared to its N-terminal peptide reported here. Our additional observation that such a phosphorylation is catalyzed by the α and δ/ϵ , but not by the γ , isoforms of CK1 would map the complementary docking site to a region which is not conserved in the γ isoforms. From the alignment of the CK1 isoforms, it appears that such a putative docking site might correspond to the K²²¹RQK²²⁴ sequence set on the loop next to the G-helix in CK1 δ . This basic sequence is conserved both in α (KKQK) and in ϵ (KRQK) isoforms but is lacking in all the γ isoforms where the first lysine is replaced by leucine and glutamine by glutamic acid (see Fig. 7a). The role of this motif as a remote docking site responsible for high affinity binding of p53 has been corroborated by computer-aided protein–protein docking strategy highlighting the special relevance of K221 which in the γ isoforms is replaced by a leucine. Such a model has been further validated by mutational analysis showing that replacement of K221 with leucine drastically impairs phosphorylation efficiency.

Interestingly, however, as in the case of β -catenin S45 phosphorylation by CK1 [Bustos *et al.*, 2006], phosphorylation of p53 S20 appears to depend not only on remote but also on local recognizing elements since replacement of E17 with alanine is equally detrimental in the N-terminal peptide and in full-size p53 despite the ability of this latter to interact with the remote docking site present in both CK1 δ and CK1 α (see Fig. 5c).

Preface to CHAPTER 6

Development and homeostasis in all multicellular organisms depend on a complex interplay between processes involved in cellular proliferation, migration, differentiation, adhesion, and death. This diverse array of cellular responses is largely coordinated by a relatively small number of intracellular signals, including the TCF, Notch, Hedgehog and Wnt pathways. Recent studies indicate that the signaling pathways triggered by these factors are very often deregulated in pathological conditions [Gregorieff and Clevers, 2005].

Signaling of the Wnt family of secreted lipoproteins has central roles in embryogenesis and in adult tissue homeostasis. Moreover, Wnt signaling has been implicated in the initiation and maintenance of many types of tumors [Clevers, 2006; Price, 2006].

The transduction of Wnt signals between cells proceeds in a series of events including posttranslational modification, secretion of Wnt signaling molecules, binding to transmembrane receptors, activation of cytoplasmic effectors, and finally, transcriptional regulation of target genes.

Genetic and biochemical data allowed to identify more than 50 proteins directly involved in Wnt signals. Three different pathways are believed to be activated upon Wnt receptor activation: the canonical Wnt/ β -catenin cascade, the non-canonical planar cell polarity (PCP) pathway, and the Wnt/ Ca^{2+} pathway [Clevers, 2006].

A key feature of the highly conserved canonical Wnt/ β -catenin signaling is the regulation of the stability of the cytoplasmic transcriptional coactivator β -catenin. Binding of a secreted Wnt protein to the Frizzled/LRP coreceptor complex results in stabilization and increase in steady-state level of β -catenin, thus leading to the LEF-1/ β -catenin-dependent downstream expression

of Wnt target genes [Kikuchi *et al.*, 2006]. In the absence of Wnt signal, protein levels of β -catenin in the cytoplasmic pool are kept low by a degradation complex made up by several proteins. Among them, central players are the scaffolding protein Axin, the adenomatous polyposis coli tumour suppressor protein (APC), Dishevelles (Dvl), protein phosphatase 2A, and the two protein kinases CK1 and glycogen synthase kinase 3 (GSK3) [Polakis, 2002]. This “destruction complex” promotes the phosphorylation and ubiquitination of β -catenin, thus targeting β -catenin for rapid destruction by the proteasome. Noteworthy, CK1 and GSK3 perform paradoxical roles in the Wnt pathway: at the level of the LRP coreceptor they act as agonists, whereas in the destruction complex they act as antagonists [Clevers, 2006]. Particularly, CK1 holds a role both in negative and in positive regulation of Wnt signaling. Different isoforms of CK1 has been described to phosphorylate β -catenin at S45, thereby priming GSK3 β -mediated phosphorylation of β -catenin at T41, S37, and S33 and downregulating β -catenin. Interestingly, point mutations at these phosphorylation sites are frequently found in cancers, consistent with the importance of this phosphorylation event in the downregulation of the Wnt signaling pathway [Knippschild *et al.*, 2005*]. Furthermore, a second level of negative regulation of Wnt signaling is the phosphorylation by CK1 of both LEF-1 and β -catenin disrupting the transcriptional activity of the LEF-1/ β -catenin complex [Hammerlein *et al.*, 2005].

CK1 isoforms have been shown to phosphorylate other members of the Wnt pathways, notably axin, Dvl, and APC, contributing to positive regulation of this important pathway [Peters *et al.*, 1999; McKay *et al.*, 2001; Gao *et al.*, 2002].

APC, a multi-functional protein involved in central biological processes, appears to be critical for the rapid turnover of β -catenin, promoting β -catenin degradation via the ubiquitin ligase–proteasome pathway, through a mechanism that is still poorly understood [Choi *et al.*, 2004]. Loss of APC function leads to uncontrolled activation of the Wnt/ β -catenin pathway and provides a proliferative advantage to the mutated cell [Moon *et al.*, 2002]. More recent works [Ha *et al.*, 2004; Xing *et al.*, 2004] demonstrated that the β -catenin binding repeats in APC can be multiply phosphorylated by the combined intervention of CK1 and GSK3 β . These authors also demonstrated the relevance of these phosphorylations to potentiate the binding of APC to β -catenin, an event that competes against axin binding, thus leading to the release of phosphorylated β -catenin from the destruction complex [Xing *et al.*, 2003].

CHAPTER 6

Chemical Dissection of the APC Repeat 3 Multistep Phosphorylation by the Concerted Action of Protein Kinases CK1 and GSK3

A crucial event in machinery controlled by Wnt signaling is the association of β -catenin with the adenomatous polyposis coli (APC) protein, which is essential for the degradation of β -catenin and requires the multiple phosphorylation of APC at six serines (1501, 1503, 1504, 1505, 1507, and 1510) within its repeat three (R3) region. Such a phosphorylation is believed to occur by the concerted action of two protein kinases, CK1 and GSK3, but its mechanistic aspects are a matter of conjecture. Here, by combining the usage of variably phosphorylated peptides reproducing the APC R3 region and Edman degradation assisted localization of residues phosphorylated by individual kinases, we show that the process is initiated by CK1, able to phosphorylate S1510 and S1505, both specified by non-canonical determinants. Phosphorylation of S1505 primes subsequent phosphorylation of S1501 by GSK3. In turn, phospho-S1501 triggers the hierarchical phosphorylation of S1504 and S1507 by CK1. Once phosphorylated, S1507 primes the phosphorylation of both S1510 and S1503 by CK1 and GSK3, respectively, thus completing all six phosphorylation steps. Our data also rule out the intervention of CK2 despite the presence of a potential CK2 phosphoacceptor site, S¹⁵¹⁰LDE, in the R3 repeat. S1510 is entirely unaffected by CK2, while it is readily phosphorylated even in the unprimed peptide by CK1 δ but not by CK1 γ . This discloses a novel motif significantly different from non-canonical sequences phosphorylated by CK1 in other proteins, which appears to be specifically recognized by the δ isoform of CK1.

This chapter was published in:

Anna Ferrarese, Oriano Marin, Victor H. Bustos, Andrea Venerando, Marcelo Antonelli, Jorge E. Allende, and Lorenzo A Pinna (2007) Chemical dissection of the APC Repeat 3 multistep phosphorylation by the concerted action of protein kinases CK1 and GSK3. *Biochemistry*, 46, 11902-11910

Materials and methods

Solvents and coupling reagents for peptide synthesis and protein sequencing were from Applied Biosystems (Foster City, CA). Building blocks for solid-phase peptide synthesis were purchased from Novabiochem (Laufelfingen, Switzerland). All other analytical grade reagents were from Sigma–Aldrich (St. Louis, MO). [γ - ^{33}P]ATP (3,000 Ci/mmol) was purchased from Amersham Pharmacia Biotech (Cleveland, OH).

CK1 isoforms cloning, expression, and purification

The cDNA clone of CK1 γ_1 from rat was provided for Dr. Peter Roach (Indiana University, Bloomington, IN). It was subcloned in the vector pQE80L using the primers 5'-TATATAGTCGACTTATGTGGGTGCTGGTGGGTGGGA-3' and 5'-TATATAGGATCCGAC CATTCTAATAGAGAAAAGG-3'. CK1 δ_1 full-length, the zebrafish homologue to human CK1 δ_2 , was cloned between the sites Bgl II and Not I of the plasmid pT7HX, using the primers 5'-TATATAAGATCTATGGAGCTACGAGTTGGAAAC-3' and 5'-ATATAGCGGCCGCCTA CTTGCCGTGGTGATCG-3'. The clone of CK1 δ from zebrafish, deleted in residue 317 to prevent autophosphorylation, was subcloned into the plasmid pQE80L using the primers 5'-TATATAGTCGACGAATTAAGAGTAGGAAACC-3' and 5'-TATATAGGATCCTCACCT TGCCGTATCCTTTCC-3'. The clone of CK1 α was obtained as described previously [Burzio *et al.*, 2002]. All the isoforms of CK1 contained six histidines in the N-terminus to facilitate the purification.

Protein expression and purification

The plasmids of CK1 α and CK1 γ were used to transform *Escherichia coli* BL21(DE3) cells. The plasmid of CK1 δ was used to transform *E. coli* B-834. Cells were grown at 37°C to an OD₆₀₀ of

0.4–0.6. At this point, protein expression was induced by adding IPTG (isopropyl β -D-thiogalactoside) to a final concentration of 100 μ M. In the case of CK1 α , induction was carried out overnight at 22°C, while for CK1 δ and CK1 γ , the temperature was maintained at 37°C for 3 h. Afterward, the cells were pelleted at 3,000g for 20 min at 4°C, and cell pellets were resuspended in lysis buffer (50mM Tris/HCl, pH 8.0, 500 mM NaCl, 1% Triton X-100, protein inhibitors from Sigma). Cells were lysed using a French press. After centrifugation at 10,000g for 30 min, the supernatant was applied to Ni-NTA-agarose columns that were washed and subsequently eluted with a buffer containing 50 mM Tris/HCl, pH 7.5, 0.2 M NaCl, and 1% Triton X-100 with 250 mM imidazole.

Human recombinant α and β subunits of CK2 were expressed in *E. coli*, and the holoenzyme was reconstituted and purified as described previously [Sarno *et al.*, 1996]. Purified GSK3 β was purchased from Upstate (Lake Placid, NY). For the sake of comparison, the activities of CK2 and GSK3 were normalized to those of CK1 isoforms using the specific peptide substrates RRRADDSDDDDD and YRRVPPSPSLSRHSSPHQpSEDEEE, respectively.

	Immobilized peptides
R3	DGFSASSLSALSLEPFIQ
R3 DE/AA	DGFSASSLSALSLE <u>AA</u> PFIQ
R3 pS1505	DGFSASS <u>p</u> SLSALSLEPFIQ
R3 pS1510	DGFSASSLSAL <u>p</u> SLEPFIQ
R3 pS1501-1505	DGF <u>p</u> SASS <u>p</u> SLSALSLEPFIQ
R3 pS1501-1504-1505	DGF <u>p</u> S <u>A</u> <u>p</u> S <u>p</u> SLSALSLEPFIQ
R3 pS1507	DGFSASSLS <u>p</u> SALSLEPFIQ
	Soluble peptides
RRR-R3	<u>RRR</u> DGFSASSLSALSLEPFIQ
RRR-R3 S1505/A	<u>RRR</u> DGFSASS <u>A</u> SALSLEPFIQ

Table 1. Peptides derived from APC R3 repeat used in the present study. Parent peptide R3 APC encompasses the R3 motif with a four residue extension on the C-terminal side. Underlining denotes substituted residues. Phosphoserine replaced for serine is indicated in bold as pS.

Peptide synthesis. anchored peptides

The peptide substrate DGFSASSLSLEPFIQ corresponding to APC repeat three (R3) and its phosphorylated derivatives were synthesized by solid-phase peptide synthesis as permanently resin-anchored peptides on the solid support amino-PEGA resin (Novabiochem, Bad Soden, Germany). The syntheses were performed using an automatized peptide synthesizer (model 431-A, Applied Biosystems). The 9-fluorenylmethoxycarbonyl (Fmoc) strategy was used throughout the peptide chain assembly [Fields and Noble, 1990]. The building blocks were as follows: Fmoc-Ala-OH, Fmoc-Asp(t-butyl)-OH, Fmoc-Gln(trityl)-OH, Fmoc-Glu(t-butyl)-OH, Fmoc-

Phe-OH, Fmoc-Gly-OH, Fmoc-Ile-OH, Fmoc-Leu-OH, Fmoc-Pro-OH, Fmoc-Ser(t-butyl)-OH, and Fmoc-Ser-[PO(O-benzyl)OH]-OH. Coupling was performed with a single reaction for 40–50 min by a 0.45 M solution in N,N-dimethylformamide (DMF) of 2-(1-benzotriazol-1-yl)-1,1,3,3-tetramethyluronium hexafluorophosphate (HBTU) and N-hydroxybenzotriazole (HOBt) in the presence of N-ethyl-diisopropylamine (DIEA) following the manufacturer's protocols. The correct amino acid incorporation into nascent peptide chains was evaluated by monitoring the absorbance at 301 nm of Fmoc removal at every synthesis cycle. At the end of the synthesis, the side chain protecting groups were cleaved by reacting the peptidyl resins with TFA/H₂O/thioanisole/1,2-ethanedithiol/phenol (10 mL/0.5 mL/0.5 mL/0.250 mL/750 mg) for 2–2.5 h [King *et al.*, 1990]. Then, the peptidyl resin was filtered and extensively washed with water, 10% aqueous TFA, DMF, diethyl ether, and methanol and dried.

Soluble peptides

The synthesis of the peptides RRRDGFSASSLSLDEPFIQ and RRRDGFSASSALSLEPFIQ was performed using the same Fmoc strategy previously described for anchored peptides except for the solid support that was the HMPA-PEGA resin (Novabiochem, Bad Soden, Germany). Additionally, Fmoc-Arg(2,2,4,6,7-pentamethyl-dihydrobenzofuran-5-sulfonyl) was used as a building block amino acid to assemble the arginyl triplet at its N-terminal side. Such a basic motif was essential for the protein kinase assay based on phosphocellulose paper substrate absorption. Cleavage of the peptides was performed by reacting the peptidyl resins with a mixture containing TFA/H₂O/thioanisole/1,2-ethanedithiol/phenol (10 mL/0.5 mL/0.5 mL/0.25 mL/750 mg) for 2.5 h. Crude peptides were purified by preparative reversed-phase HPLC. Molecular masses of the peptides were confirmed by mass spectroscopy with direct infusion on a Micromass ZMD-4000 mass spectrometer (Waters–Micromass, Manchester, U.K.). The purity of the peptides was about 95% as evaluated by analytical reversed-phase HPLC.

Peptide phosphorylation assay

Synthetic peptide substrates derived from the APC R3 sequence and covalently bound to the resin beads (0.5 mg, ~200 nmol) were phosphorylated by incubation in a medium (50 µL final volume) containing 50 mM Tris/HCl buffer (pH 7.5), 10 mM MgCl₂, 100 mM NaCl, and 100 µM [γ -³³P]ATP (specific radioactivity 1,500–2,000 cpm/pmol). The reaction was started with the addition of protein kinases CK1 α , CK1 δ , and CK1 γ ₁ normalized against a common peptide

substrate, namely, the one derived from inhibitor-2 of protein phosphatase-1 (I-2) RRKHAAI GDDDDAYSITA [Marin *et al.*, 1994]. More precisely, each amount of CK1 isoform displayed on peptide I-2 a specific activity of 2.5 pmol of phosphate transferred per minute. The reactions were incubated for the indicated time at 37°C and stopped by ice cooling and the addition of 50 µL of TFA (5% final concentration). The phosphorylated peptidyl-resin was separated from the reaction mixture by filtration and washed exhaustively with 3% phosphoric acid solution, water, 1 M NaCl, and methanol. To evaluate the radioactivity incorporated, each sample was mixed with 2 mL of scintillation cocktail and counted for 1 min in a liquid scintillation counter. Results are representative of at least three independent experiments.

Phosphorylation of soluble peptides was performed in solution in the same incubation medium used for immobilized peptides. The concentration of the peptides was 1 mM. The radioactivity incorporated was quantified by the phosphocellulose paper procedure as previously described [Marin *et al.*, 2003], taking advantage of the arginyl triplet added on the N-terminal side of the peptides.

Solid-phase Edman sequencing

Aliquots (0.5 mg) of synthetic peptide substrates covalently bound to the beads employed for solid-phase synthesis were phosphorylated in the presence of [γ - ^{33}P]ATP as described previously and exhaustively washed. Subsequently radiolabeled peptidyl resin was resuspended in methanol, and a few beads, corresponding to 1,000–10,000 cpm, were spotted onto a micro-TFA filter (Applied Biosystems, Foster City, CA) placed inside the cartridge of a Procise HT 491 protein sequencer (Applied Biosystems). After solvent evaporation, the samples were subjected to N-terminal sequencing analysis utilizing a modified Cartridge chemistry cycle [Campbell and Morrice, 2002] to isolate ATZ amino acids accordingly to the manufacturer. No flask cycle or HPLC gradient cycles were loaded. At every cycle, the removed ATZ amino acids were quantitatively transferred to an external fraction collector connected to the ATZ port, using 90% methanol/10% water as the solvent (S1). The collected fractions (600 µL) were mixed with 2 mL of scintillation cocktail and counted for 1 min in a liquid scintillation counter. The recovered ^{33}P radioactivity at every cycle was plotted against the primary sequence of the peptide substrate. All reported data are representative of multiple experiments.

Results

A 20 amino acid peptide reproducing the R3 region of APC (residues 1498–1517, see Table 1) with C1502 substituted by alanine to avoid side reactions such as the oxidation of the thiol group and the formation of disulfide bridges, and with a triplet of arginines added to its N-terminus to make applicable the phosphocellulose paper kinase assay (see Materials and methods), was synthesized and assayed for its susceptibility to phosphorylation by a number of kinases implicated in the Wnt signaling, namely, three isoforms: CK1, GSK3, and CK2. The R3 region was chosen for this study first because it is the tightest binding site of APC to β -catenin [Rubinfeld *et al.*, 1997] and second because the crystal structure of its complex with β -catenin has been solved, revealing the importance of individual phosphorylated residues [Ha *et al.*, 2004; Xing *et al.*, 2004]. This peptide (RRR-R3) as well as its resin immobilized congener deprived of the arginyl triplet (R3), on display in Table 1 together with a number of (phospho)derivatives used in this study, contains six seryl residues at positions 1501, 1503, 1504, 1505, 1507, and 1510 whose phosphorylation is required for high affinity association with β -catenin. The phosphorylation assays were performed in the presence of equivalent amounts of the kinases, in terms of units, defined using the specific peptide substrate of each kinase (see the Materials and methods). As can be seen in Figure 2A, where the results of a time course experiments are reported, the peptide is readily phosphorylated by CK1 γ 1 and CK1 δ and more slowly by CK1 α ; in contrast, it was entirely unaffected by GSK3 β and CK2.

```

R1 [1265-1284] EDTPICFSRCSSLSSLSSAE
R2 [1378-1397] QETPLMFSRCTSVSSLDSE
R3 [1494-1513] ESTPDGFSCSSSLALSSLDE
R4 [1645-1664] EGTPINFSTATSLSDLTIES
R5 [1850-1869] EGTPYCFSRNDSLSLDFDD
R6 [1957-1976] ENTPVCFSHNSSLSDID
R7 [2015-2034] EDTPVCFSRNSSLSDIDS

```

Figure 1. Sequence alignment of the seven 20-amino acid repeats [R1–R7] of human APC (accession no. REFSEQ NP_000029). Seryl residues that were found phosphorylated in the APC R3 repeat/ β -catenin complex [Ha *et al.*, 2004; Xing *et al.*, 2004], denoted by an asterisk (*), are S1501, S1503, S1504, S1505, S1507, and S1510. Conserved residues are underlined.

To check if phosphorylation by CK1 could prime subsequent phosphorylation by GSK3, the experimental conditions were modified to increase the stoichiometry of phosphorylation by CK1, which in the experiment of Figure 2A was negligible (0.2% or less). By prolonging incubation

up to 2 h and increasing the amount of CK1 γ 1, we could approach a phosphorylation stoichiometry around 0.05 mol of phosphate per mol of peptide. Under these conditions, a clear indication that CK1 primes further phosphorylation by GSK3 was obtained, as illustrated in Figure 2B, showing a cooperative effect of adding GSK3 together with CK1 on the R3 peptide phosphorylation. Interestingly, as also shown in Figure 2B, substitution of S1505 by alanine abolishes such a synergistic effect, while also significantly decreasing the extent of phosphorylation by CK1 alone. These data would indicate that although S1505 is not the only target of CK1, it is nevertheless essential for priming subsequent phosphorylation by GSK3.

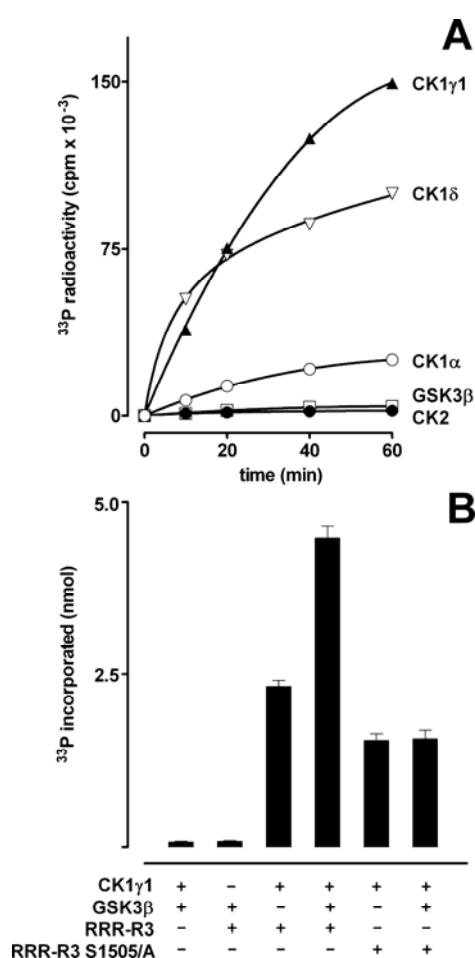


Figure 2. (on left) Phosphorylation of R3 APC peptides by various protein kinases. Cooperative phosphorylation by GSK3 is abrogated by S1505 to Ala substitution. Phosphorylation was performed in solution taking advantage of the non-immobilized peptides with the N-terminal arginyl triplet (see Materials and methods, for nomenclature, Table 1). For the time course, phosphorylation (A) conditions were those described in Materials and methods (2.5 units of each protein kinase added), and the concentration of the R3 peptide was 1 mM. Results represent the means of triplicate experiments.

In (B), experimental conditions were the same except for incubation time (2 h) and amount of protein kinases (10 units). Results are shown as the means \pm SEM of three determinations.

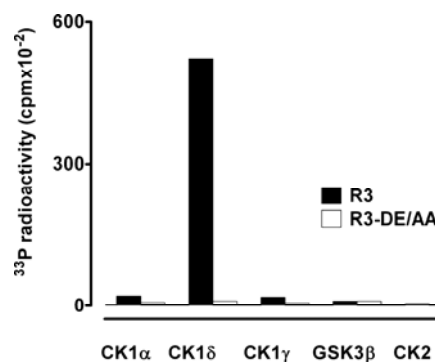


Figure 3. (above) Phosphorylation of non-primed parent R3 peptide by various protein kinases: role of D1512/E1513. Phosphorylation of 0.5 mg of the parent peptide R3 either as such (DGFSASSLSALSLEDPFIQ) or with D1512 and E1513 replaced by alanines (DGFSASSLSALSLEAPFIQ) anchored to a solid support was performed in the presence of the indicated protein kinases (equivalent in terms of units) by 60 min incubation as detailed in Materials and methods.

To identify the residues phosphorylated by CK1, the R3 peptide was synthesized immobilized to resin beads to make it amenable to automated solid-phase Edman degradation (see the Materials and methods). In this case, the N-terminal arginyl triplet was unnecessary and was omitted (peptide R3 in Table 1). The immobilized peptide was subjected to phosphorylation by the same protein kinases previously used to phosphorylate the soluble peptide. In that case, the activities

of the kinases were normalized against their specific peptide substrates (see the Materials and methods), and the same amount of each kinase, in term of units, was used in the phosphorylation

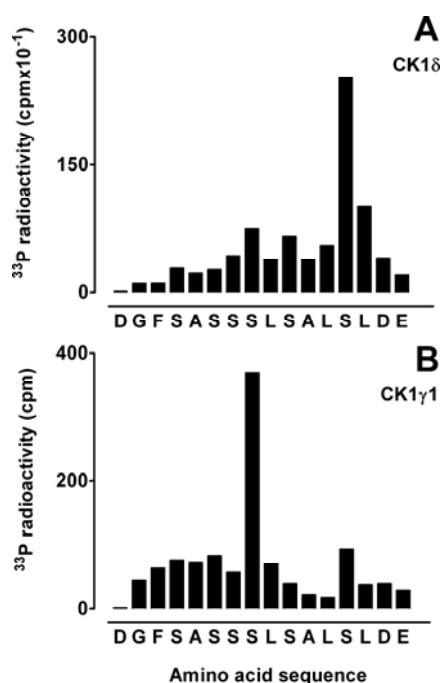


Figure 4. Localization of phosphoradiolabeled residues within R3 APC phosphorylated by either CK1 δ (A) or CK1 γ_1 (B) by solid-phase Edman sequencing. The parent unprimed peptide was phosphorylated as in Figure 2 and then subjected to solid-phase Edman sequencing as detailed in the Materials and methods. For the experiment shown in (A), the truncated CK1 δ deleted at residue 317 was used. A similar Edman profile was obtained by using full-length CK1 δ (not shown).

experiments. These were run by varying the incubation time and amount of immobilized peptide, without noting substantial differences as far as the relative susceptibility of the peptide to individual kinases was concerned. The outcome of a typical experiment is illustrated by histograms in Figure 3, showing that, at variance with the soluble peptide, the immobilized peptide is phosphorylated by the δ isoform of CK1 much more readily than by the γ_1 isoform (compare in relative terms Figure 3 with Figure 2A). Although a direct comparison between the data of Figures 2A and 3 is hampered by the impossibility to precisely quantify the immobilized peptide, these data would indicate that immobilization is detrimental to phosphorylation by CK1 γ_1 but not, or much less by, CK1 δ . Note, however, that phosphorylation by CK1 α and CK1 γ_1 is also quite significant, while phosphorylation by GSK3 and CK2, as in the case of the soluble peptide, is nearly undetectable. The latter result came as a surprise since S1510 fulfils the consensus for being a CK2 phosphoacceptor site (S¹⁵¹⁰LED, the minimum consensus being S-XX-D/E). Interestingly, as also shown in Figure 3, the two acidic residues (D1512 and E1513)

that fail to promote phosphorylation by CK2 are essential for CK1 since their replacement with alanines suppresses the phosphorylation of the R3 peptide by either the δ or the α and γ isoforms of the kinase. This finding corroborates the view that CK1 mediated phosphorylation of the APC R3 repeat is dictated by non-canonical consensus, similar to the one determining the phosphorylation of β -catenin S45 [Marin *et al.*, 2003]. These non-canonical CK1 phosphoacceptor sites in fact crucially rely on acidic residues located at a certain distance downstream from the target residue [Marin *et al.*, 2002; Marin *et al.*, 2003], instead of upstream, as in the case of canonical sites. In the case of β -catenin, moreover S45 belongs to a triplet, S⁴⁵LS, whose central hydrophobic residue was also shown to act as an important determinant since its replacement with alanine nearly suppressed phosphorylation [Marin *et al.*, 2003]. Both features are indeed displayed in the R3 peptide by S1505, whose replacement by alanine actually decreases phosphorylation by CK1 and, more importantly, abrogates the cooperative effect of adding GSK3 together with CK1 (see Figure 2B).

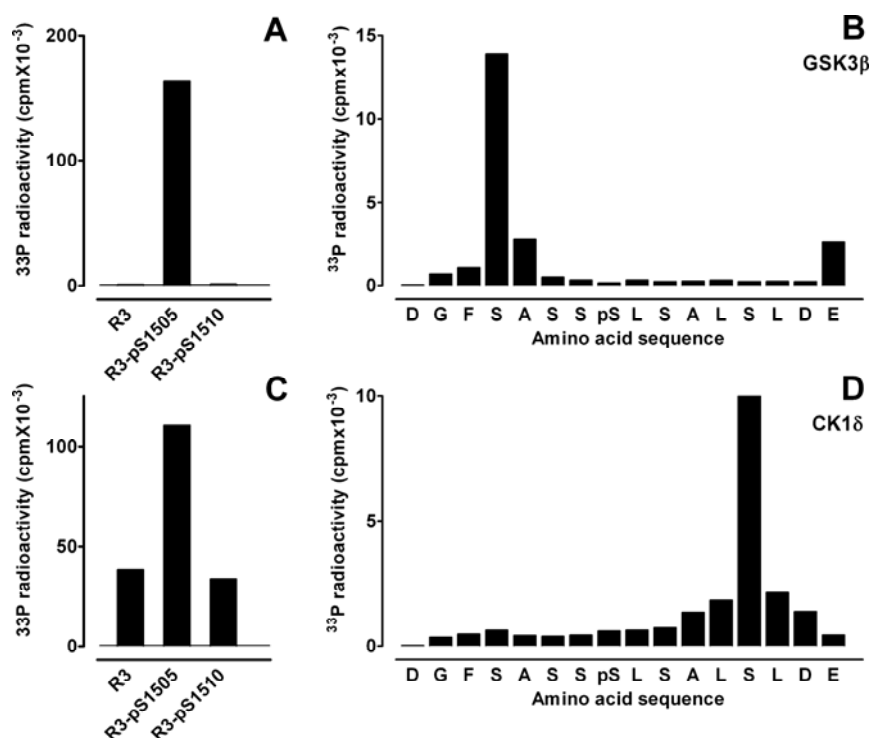


Figure 5. Phospho-S1505 but not phospho-S1510 primes S1501 phosphorylation by GSK3. In (A), phosphorylation of the immobilized phosphopeptides R3 pS1505 and R3 pS1510 by GSK3 β was performed and compared to that of the non-primed parent peptide. In (B), the phosphopeptide R3 pS1505 phosphoradiolabeled by incubation with GSK3 β (as in A) was subjected to automated Edman degradation to identify the radiolabeled residues. In (C), phosphorylation of the immobilized phosphopeptides R3 pS1505 and R3 pS1510 by CK1 δ was performed and compared to that of the non-primed parent peptide. In (D), the phosphopeptide R3 pS1505 phosphoradiolabeled by incubation with CK1 δ (as in C) was subjected to automated Edman degradation.

To identify the residue(s) phosphorylated by CK1 in the R3 peptide, its phospho-radiolabeled product was subjected to automated Edman degradation. As shown in Figure 4A, radioactive phosphate incorporated by CK1 δ is mainly recovered in S1510 and, to a lesser extent, in S1505. The opposite is observed using CK1 γ_1 , whose main target is S1505 (Figure 4B). CK1 α phosphorylates S1505 and S1510 to approximately the same extent (not shown). While the phosphorylation of S1505 was expected, as it conforms to the typical features of non-canonical CK1 sites, the phosphorylation of S1510 was not since in this case the SLS motif is partially altered (S¹⁵¹⁰LD), and the C-terminal acidic residues that are held as hallmarks of non-canonical CK1 sites are closer to the target residue than they are in NF-AT4 and in β -catenin. Note in this respect that phosphorylation of S1510, besides S1505, accounts for the failure of the S1505 to Ala mutation to suppress phosphorylation by CK1 (see Figure 2B).

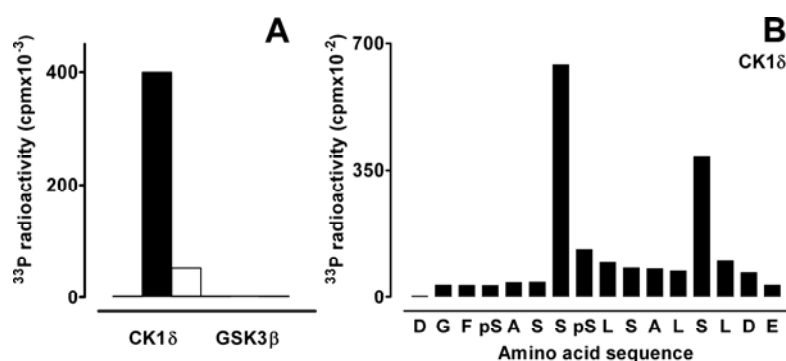


Figure 6. Bis-phosphorylated R3 pS1501-pS1505 is an excellent substrate for CK1, which specifically phosphorylates Ser1504. In (A), the phosphoradiolabeling of the bis-phosphorylated R3 pS1501-pS1505 peptide by either CK1 δ or GSK3 β is compared to that of the parent unphosphorylated peptide. In (B), the residues radiolabeled by CK1 δ in the bisphosphorylated peptide are localized by automated Edman degradation. For details, see Material and methods.

Once it was established that CK1 isoforms are variably able to phosphorylate the R3 peptide at both S1505 and S1510, we wanted to see if these phospho-residues were able to prime the intervention of GSK3. To this aim, we synthesized two phosphopeptides with either S1505 or 1510 replaced by phospho-serine, and we tested their ability to serve as substrates for GSK3 β . As shown in Figure 5A, the R3 pS1510 peptide, similar to the parent peptide R3, was unaffected by GSK3, proving that phosphorylation of S1510 is not priming the phosphorylation of any of the five seryl residues upstream. In contrast, the pS1505 peptide was readily phosphorylated. Automated Edman degradation provided the demonstration that the whole radioactivity incorporated by GSK3 is accounted for by S1501 (Figure 5B), whose phosphorylation by GSK3 is indeed expected to be primed by a phosphoresidue at position n+4 as it is phospho-S1505.

We also wanted to check if phospho-S1505 and phospho-S1510 could prime the phosphorylation of additional seryl residues by CK1. To this purpose, the phosphorylation of the two phosphopeptides R3 pS1510 and R3 pS1505 by CK1 was compared to that of the parent peptide (R3). As shown in Figure 5C, the phosphopeptide R3 pS1505 but not R3 pS1510 is phosphorylated by CK1 δ more efficiently than the parent peptide, consistent with a priming effect of phospho-S1505 but not of phospho-S1510. The radiolabeled phosphate incorporated by CK1 δ into R3 pS1505 was entirely recovered into S1510 (Figure 5D), denoting a hierarchical phosphorylation specified by a phosphoresidue at position n-5. In summary, the data on display in Figure 5 show that while primary phosphorylation of S1510 by CK1 has no priming effects, CK1 phosphorylation of S1505 primes phosphorylation of both S1510 by CK1 and, more importantly, of S1501 by GSK3.

Phospho-S1501, generated by the priming of GSK3 by phospho-S1505, should be in the proper position for the sequential priming of CK1 to phosphorylate S1504 and subsequently S1507. To validate these predictions, we first synthesized a bis-phosphorylated peptide with both S1505 and S1501 replaced by phospho-serines, and we tested it as a substrate for either GSK3 or CK1 δ . As shown in Figure 6A, the bis-phosphorylated peptide is unaffected by GSK3 while readily phosphorylated by CK1. The main phosphorylated residue was found to be S1504 with some radioactivity incorporated in S1510 as well (Figure 6B), which, however, also can be phosphorylated in the parent peptide (see Figure 4).

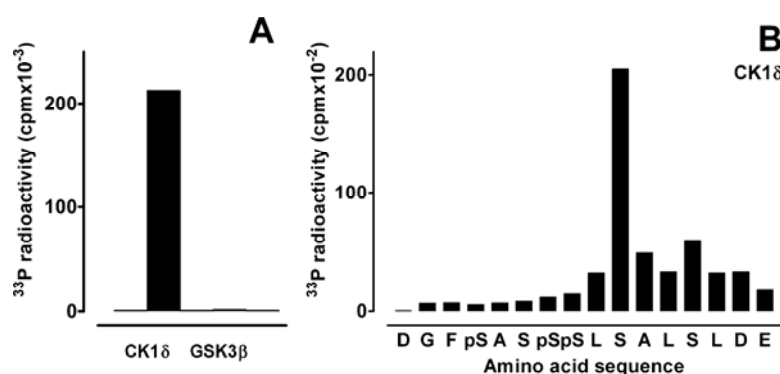


Figure 7. R3 pre-phosphorylated at serines 1501, 1504, and 1505 is further phosphorylated by CK1 at Ser1507. In (A), the phosphoradiolabeling of the tris-phosphopeptide R3 pS1501–pS1504–pS1505 by either CK1 δ or GSK3 β is shown. In (B), the residues radiolabeled by CK1 δ are localized by automated Edman degradation. For details, see Materials and methods.

Next, we synthesized the triply phosphorylated peptide with S1504, besides S1501 and S1505, replaced by phospho-serine, and we showed that again it is an excellent substrate of CK1 δ , while unaffected by GSK3 (Figure 7A), with radioactivity almost exclusively incorporated into S1507

(Figure 7B). In this series of experiments, CK1 δ could be efficiently replaced by the isoforms γ and α with substantially identical results (not shown).

In summary, at this stage, we were able to account for the phosphorylation of five out of six serine residues in the R3 peptide: S1505 and S1510 primarily phosphorylated by CK1, S1501 phosphorylated by GSK3 as a consequence of S1505 phosphorylation, and S1504 and S1507 as the result of a hierarchical process primed by GSK3 and catalyzed by CK1 isoforms. The only residue left is S1503, whose position is such to make predictable its hierarchical phosphorylation by GSK3 once S1507 has been phosphorylated by CK1. Note that once phosphorylated, S1507 also has the potential to prime the phosphorylation of S1510 by CK1, although S1510 has been shown previously to be phosphorylated by CK1 through two additional routes: non-primed phosphorylation (Figure 4A) and phosphorylation primed by phospho-S1505 (Figure 5D).

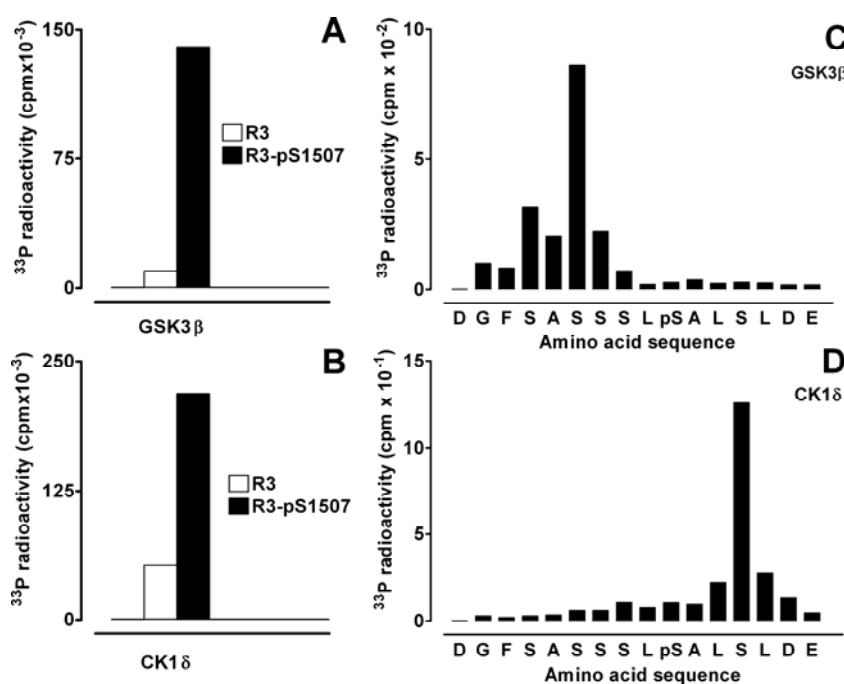


Figure 8. Phospho-S1507 primes the phosphorylation of S1510 and S1503. Phosphoradiolabeling of phosphopeptide R3 pS1507 by either GSK3 β (A) or CK1 δ (B) is compared to that of the parent peptide. In (C) and (D), the residues radiolabeled by incubation of the phosphopeptide with GSK3 β or CK1 δ , respectively, are localized by automated Edman degradation. For details, see Materials and Methods.

To validate our predictions, a phosphorylated derivative of the R3 peptide with S1507 replaced by phospho-serine was synthesized and its phosphorylation by either GSK3 or CK1 δ compared to that of the unphosphorylated peptide. As shown in Figure 8A,B, the phosphopeptide is phosphorylated more readily than the parent peptide by both kinases, consistent with a priming

effect of phospho-S1507 in both cases. As shown in Figure 8C,D, however, the residues whose phosphorylation is primed by phospho-S1507 are different depending on the phosphorylating kinase: S1503 is the main target of GSK3, while CK1 exclusively phosphorylates S1510. The data reported were obtained with CK1 δ , but the other CK1 isoforms behaved identically in this respect (not shown).

Discussion

Multiple phosphorylation of the APC protein at its third 20-mer repeat (R3) is required for high affinity association with β -catenin [Liu *et al.*, 2006], which in turn is a crucial step to accelerate the displacement of phosphorylated β -catenin from the destruction box and its commitment to ubiquitination and degradation [Rubinfeld *et al.*, 1997; Rubinfeld *et al.*, 2001] through a mechanism that still is a matter of conjecture. Interestingly, the same protein kinases, CK1 and GSK3, appear to be committed to the synergistic phosphorylation of both β -catenin and APC, although the CK1 isoforms implicated may be different: CK1 α appears to be responsible for β -catenin phosphorylation [Liu *et al.*, 2002; Matsubayashi *et al.*, 2004], whereas the isoforms responsible for APC phosphorylation *in vivo* are unknown, but *in vitro* APC can be phosphorylated by CK1 δ and by the closely related ϵ isoform [Gao *et al.*, 2002]. Likewise, by using a concentrated mixture of CK1 ϵ and GSK3 β , Ha *et al.* [Ha *et al.*, 2004] were able to incorporate up to six phosphates into a peptide reproducing the R3 APC region and to solve the structure of the complex between this phosphopeptide and the armadillo repeat region of β -catenin, disclosing the role of individual phosphoserines in tightening the interactions between the two proteins [Ha *et al.*, 2004]. By analogy with non-canonical sequences phosphorylated by CK1 in β -catenin [Marin *et al.*, 2003], these authors speculated that also in the case of R3 APC, CK1 was acting as the priming kinase by first hitting S1505 that displays the SLS motif five to ten residues upstream from acidic residues also typical of the non-canonical CK1 sites in NF-AT4 and β -catenin. Phosphorylation of S1505 would generate a consensus for subsequent phosphorylation of S1501 by GSK3, triggering a cascade of hierarchical phosphorylation steps leading to the complete phosphorylation of R3.

The data presented here, obtained by using a series of R3 APC peptides and phosphopeptides designed to dissect the individual steps of this complicated reaction orderly catalyzed by CK1 and GSK3, and schematically summarized in Figure 9, substantially confirm the mutual priming hypothesis of Ha *et al.* [Ha *et al.*, 2004]. In particular, it is clear that the original priming kinase must be CK1, which is able to phosphorylate the unphosphorylated R3 APC stretch, while GSK3

fails to do that. It is also clear that one of the residues targeted by CK1 δ (and the main one affected by CK1 γ), S1505, once phosphorylated, primes the phosphorylation of R3 APC by GSK3 at the expected S1501 residue and that now the bis-phosphorylated peptide (R3 pS1501-1505) becomes an excellent substrate for CK1, able to carry out the stepwise phosphorylation of S1504 (primed by phospho-S1501), S1507 (primed by phospho-S1504), and S1510 (primed by phospho-S1507). We also show that once phosphorylated (by CK1), S1507 not only primes the phosphorylation of S1510 (by CK1) but also that of S1504 by GSK3, thus fully accounting for the stoichiometry of six phosphates incorporated into the R3 peptide by exhaustive incubation with CK1 and GSK3 in the presence of a high ATP concentration (1 mM) [Ha *et al.*, 2004].

Another point that has been assessed by our data concerns the non-canonical mode by which CK1 recognizes unphosphorylated R3 APC: while in fact all subsequent reactions catalyzed by CK1 on variably phosphorylated R3 APC are dictated by the canonical consensus generated by a phosphorylated side chain upstream, none of the seryl residues present in unphosphorylated R3 APC display a canonical consensus, either of this type or relying on acidic side chain(s) that sometimes can efficiently surrogate the phosphorylated residue [Pinna and Ruzzene, 1996; Songyang *et al.*, 1996; Pulgar *et al.*, 1999]. Rather, S1505 typically displays the SLS motif and the presence of two acidic residues (D1512 and E1513) at positions n+7 and n+8, which are reminiscent of non-canonical sequences phosphorylated by CK1 in β -catenin [Marin *et al.*, 2003] and NF-AT4 [Marin *et al.*, 2002]. As in the cases of β -catenin and NF-AT4, moreover, these C-terminally located acidic residues act as important specificity determinants as their replacement by alanine fully abrogates phosphorylation by CK1 (see Figure 3). This also means that the whole R3 APC phosphorylation would be compromised by this substitution given the crucial priming role of phospho-S1505 for the subsequent phosphorylation of the other residues. Interestingly, the number and position of these C-terminal acidic residues are variable throughout the seven APC 20-amino acid repeats (see Figure 1), suggesting that the susceptibility to phosphorylation of individual repeats may also be quite different despite the conservation (or conservative replacement) of most of the seryl residues in them. On the other hand, it may be worth noting that our mechanistic approach clearly demonstrates the feasibility of the hierarchical phosphorylation by GSK3 of S1503 (see Figure 8), which is unique to R3, being replaced in all the other repeats by non-phosphorylatable residues. Note in this respect that R3 is the one responsible for the tightest binding of APC to β -catenin [Liu *et al.*, 2002].

An unexpected outcome of our study was the unprimed phosphorylation of S1510 by CK1 δ in the R3 parent peptide. This residue is one of those whose phosphorylation is critical for association with β -catenin [Ha *et al.*, 2004], and its hierarchical phosphorylation can be primed

by phospho-S1507 (see Figure 8B) and also by phospho-S1505 (see Figure 5D). Nevertheless, it is also the residue that is more efficiently phosphorylated by CK1 δ in unprimed R3 APC, even better than S1505 itself (see Figure 4A), although its phosphorylation, unlike that of S1505, fails to prime the phosphorylation of the R3 peptide by either GSK3 or CK1 (see Figure 5).

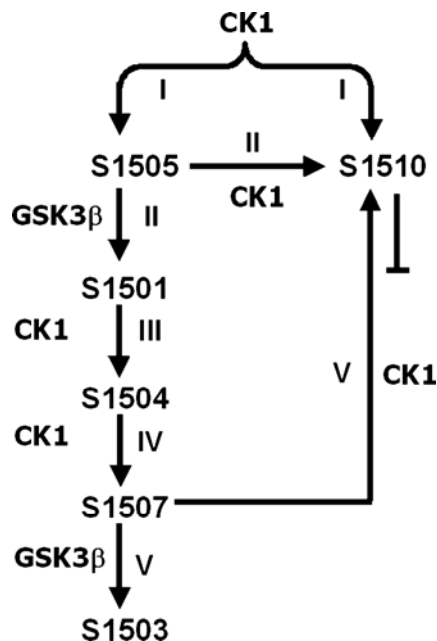


Figure 9. Schematic representation of R3 APC multistep phosphorylation by the concerted action of CK1 and GSK3. Phosphorylation is initiated by CK1, which phosphorylates the non-canonical sites S1505 and, especially in the case of the CK1 δ isoform, S1510 as well. Phospho-S1505 primes the second phosphorylation step, catalyzed by GSK3, which targets S1501. Phosphorylation of S1501 primes the third step consisting of the canonical phosphorylation of S1504 by CK1, which in turn primes the phosphorylation of S1507 by the same kinase (fourth step). Phospho-S1507 triggers the last step (fifth), leading to the phosphorylation of both S1503 and S1510 by either GSK3 or CK1, respectively. The CK1 isoforms δ , γ , and α are interchangeable at all steps, although unprimed phosphorylation of S1510 is optimally performed by CK1 δ alone (see Figure 4). S1510 phosphorylation also can be primed by phosphorylation of either S1507 or S1505. By contrast, its phosphorylation is unproductive as it does not prime further intervention of either GSK3 or CK1.

Inclusion of S1510 among non-canonical sequences phosphorylated by CK1 comes as a surprise first because it only partially fulfils the SLS motif and second because the acidic determinants that in the previously known sequences are generally located rather far away on the C-terminal side, here are very close, at positions $n+2/n+3$. This should make S1510 a good target for CK2, whose consensus is S/T-XX-E/D, but, intriguingly, CK2 is completely unable to phosphorylate it (see Figures 2 and 3). We have to assume therefore that the structural features underlying non-canonical CK1 substrate recognition need to be re-evaluated at least for the CK1 δ isoform. In the case of S1510, it is clear that the two acidic residues close to its C-terminus act as specificity determinants since their replacement with alanines abrogates its phosphorylation (see Figure 3).

It is not clear, however, as to which the other structural features that make S1510 prone to CK1 δ phosphorylation are, while unsuitable to CK2 mediated phosphorylation, also considering that many CK2 peptide substrates whose sequence is very similar to the one encompassing APC S1510 are totally unaffected by CK1. We have recently described that the efficiency in the recognition of the non-canonical motif that accounts for the S45 phosphorylation of β -catenin by CK1 α depends on the presence of the first armadillo repeat in that protein that dramatically decreases the K_m value of the reaction [Bustos *et al.*, 2006]. Since APC also contains armadillo repeats, it is likely that one or more of these repeat structures may also increase the affinity and efficiency of phosphorylation of the peptide sequences that we have described previously. Indeed, the affinity of the unprimed R3 peptide for CK1 is very low as judged from K_m values >1 mM (data not shown).

Phosphorylation of S1510 and, in general, of R3 also reveals differences in substrate specificity among different CK1 isoforms. Remarkably, phosphorylation of the R3 parent peptide that is mainly accounted for by S1510 in the case of CK1 δ , is predominantly accounted for by S1505 if the γ_1 isoform of CK1 is used (see Figure 4) and is equally distributed between S1505 and 1510 by using CK1 α (not shown). Given the crucial role of S1505 in priming all subsequent phosphorylation steps, one may argue that perhaps CK1 γ , rather than CK1 δ/ϵ , is the physiological APC kinase. On the other hand, we must take into account that if the activities of CK1 isoforms are normalized against a common canonical peptide substrate, CK1 δ and CK1 γ_1 are equally efficient to phosphorylate the soluble R3 APC peptide (see Figure 2). Indeed, the data of Gao *et al.* [Gao *et al.*, 2002] would suggest that the δ/ϵ isoforms are the main agents of APC phosphorylation. Our data would indicate that CK1 catalyzed phosphorylation of S1510, implicated in the high affinity binding of β -catenin, does not need to be primed by GSK3, which is generally held as the mediator of Wnt signaling. This may raise the question as to whether CK1 might be also directly controlled by Wnt signaling, independently of GSK3. Among CK1 isoforms, CK1 δ is the one for which more stringent evidence for a down-regulation through phosphorylation of its C-terminal domain has been reported [Graves and Roach, 1995]. It is generally held that such a phosphorylation is an autocatalytic event, but the implication of other protein kinase(s) cannot be ruled out either, considering that none of the residues potentially implicated [Graves and Roach, 1995] displays the features of a primary CK1 site.

The cooperative, mutual priming action of CK1 and GSK3 β in achieving the hyperphosphorylation of serine-/threonine-rich regions of proteins seems to be a rather widespread phenomenon. The axin scaffold holds these two kinases together in the cases of β -

catenin and APC phosphorylations. Similar physical associations may be present in other instances where these and other enzymes work in a concerted fashion.

Acknowledgements

We are grateful to Dr. M. P. Schiappelli for skilful technical assistance.

Preface to CHAPTER 7

Protein kinases are important targets in drug discovery programs because of their involvement in many important signaling pathways and cellular processes that mediate metabolism, transcription, cell-cycle progression, differentiation, cytoskeleton arrangement and cell movement, apoptosis, intercellular communication, and neuronal and immunological functions. Abnormalities in kinase activity, due to either changes in expression level or mutation in the protein sequence, lead to uncontrolled cell growth. Furthermore, kinases have been responsible in many other disease pathologies, such as immunodeficiency, inflammation, and rheumatoid arthritis. In the human genome, over 250 protein kinases map to disease loci [Eglen and Reisine, 2009]. Consequently, protein kinases have become high-profile targets for drug development aimed at treating many diseases [Bain *et al.*, 2007].

In 2008, at least 10 protein kinase inhibitors have been approved for use in the clinic and, so far, there are many more compounds in clinical trials [Johnson, 2009]. All but one (i.e. temsirolimus) of the approved drugs target the ATP-binding site on the kinase. Note that the ATP site is common to all the protein kinases, and hence, compounds targeting the ATP recognition site are, in principle, non-selective and inhibit many kinases (e.g. staurosporine). Therefore, selectivity of the therapeutically effective drugs is engineered by targeting pockets adjacent to the ATP site with groups that have chemical diversity, instead of directly interacting with the conserved phosphate transfer region. Thus, it is absolutely essential to know the structure of the target kinase.

To date, there are more than 118 protein kinase structures deposited in the protein data bank [Marsden and Knapp, 2008] that coverage most of the seven different classes of protein kinases

identified by Manning [Manning *et al.*, 2002]. Both crystallographic structures and in silico analysis of compounds bound to the ATP site have revealed, at least, five pockets that can be exploited for different chemical groups [Liao, 2007]: (i) the adenine-binding pocket that is marked by aliphatic and aromatic hydrophobic groups with the potential for two or more hydrogen bonds to the hinge region; (ii) the ribose-binding pocket that has several polar groups; (iii) the "p38" pocket above the adenine, which in p38 and other kinases (e.g. Abl) is guarded by a small residue, usually threonine, which in other kinases it is blocked by a more bulky residue (e.g. Phe80 in CDK2); (iv) the pocket below the adenine, the Lys89 pocket in CDK2 or the hydrophobic pocket in other kinases, that allows targeting by a number of different chemical groups; (v) the type II inhibitor pocket formed between the C-helix and the activation segment, which accommodates some large inhibitors that target the inactive conformation.

As with most enzymes, also kinases exist in either an active or inactive conformations, both of which have been used in strategies to produce potent and selective compounds. Changes in conformation of the activation loop, i.e., DFG loop in or out, occur either by binding of substrate or by phosphorylation within the loop itself [Eglen and Reisine, 2009]. These allosteric sites clearly represent novel targets for inhibitors. There are significant advantages in developing compounds that target the inactive form of a kinase, i.e. high specificity, because the inactive state is often unique to that protein kinase. Targeting the active conformation, on the other hand, is favourable where the diseased state has arisen from activating mutations. In patients where disease occurs through loss of regulation leading to an inappropriately active protein kinase, such as cancers caused by mutations that resulted in a constitutively active EGFR kinase domain [Johnson, 2009], targeting the active form can be advantageous. However, kinases converge to a similar conformation in the active state, hence, compounds targeting such conformation generally affect several protein kinases, resulting in less specific inhibitors. Drug resistance mutations are a potential risk for both conformational states, either active or inactive, where drug-binding regions are not directly involved in catalysis. However, the active conformation is less likely to be tolerant of mutation requiring conservation of both key residues and tertiary structure [Johnson, 2009]. Furthermore, almost always (with some exceptions, e.g. chronic myeloid leukaemia), no single mutated gene lies at the heart of cancer, but it is the cumulative mutations in a number of genes that lead to the diseased state [Johnson, 2009*].

An emerging feature in the effectiveness of a drug in vivo has been the ability of the drug to compete with cellular concentrations of ATP (typically approx. 1–10 mM) [Johnson, 2009]. As a matter of fact, one of the major drug-resistance mutations causes an increase in the affinity for

ATP. For most kinases, K_m for ATP is of the order of $10\mu\text{M}$. Indeed, the balance between ATP affinity and drug affinity determines the efficacy of the drug.

Although catalytic activity is an important component of kinase function, also spatial access to their unique substrates is a crucial factor involved in the function of these enzymes. In many cases substrates are located in different cellular compartments to the kinase. Consequently, translocation process of kinases is necessary to allow kinase–substrate interaction and represents an important regulatory mechanism by which kinases control cell activity. Different proteins are involved in the mechanisms of protein kinase translocation and compartmentalization (e.g. RACKs and AKAPs members for PKC and PKA). These proteins not only serve as shuttling or targeting proteins but are also able to put the kinases in close proximity to other proteins to generate networks of interacting proteins. In some cases, the sites of interaction of the protein kinases with these multi-tasking proteins have been identified, raising the possibility of developing new drugs that modify selective functions of the protein kinases through blocking these interactions.

CHAPTER 7

Identification of Novel Protein Kinase CK1 delta (CK1 δ) Inhibitors Through Structure-Based Virtual Screening

In eukaryotes, protein phosphorylation of serine, threonine or tyrosine residues by protein kinases plays an important role in many cellular processes. Members of the protein kinase CK1 family usually phosphorylated residues of serine that are close to other phosphoserine in a consensus motif of pS-X-X-S, and they are implicated in the regulation of a variety of physiological processes as well as in pathologies like cancer and Alzheimer's disease. Using a structure-based virtual screening (SBVS) approach we have identified two anthraquinones as novel CK1 δ inhibitors. These amino-anthraquinone analogs (derivatives 1 and 2) are among the most potent and selective CK1 δ inhibitors known today (IC_{50} = 0.3 and 0.6 μ M, respectively).

This chapter was published in:

Giorgio Cozza, Alessandra Gianoncelli, Monica Montopoli, Laura Caparrotta, Andrea Venerando, Flavio Meggio, Lorenzo A. Pinna, Giuseppe Zagotto, and Stefano Moro (2008) Identification of novel protein kinase CK1 delta (CK1 δ) inhibitors through structure-based virtual screening. *Bioorganic & Medicinal Chemistry Letters*, 18, 5672-5675

Materials and methods

Chemicals

Derivatives 1 and 3 were purchased from Janssen Chimica with a purity of 97%. Derivative 2 was purchased From Acros Organics with a purity of 96%; IC261 was purchased from Calbiochem with a purity $\geq 95\%$.

Materials

The CK1 α , CK1 $\delta^{\Delta 317}$ and CK1 γ_1 clones were obtained as described previously [Ferrarese *et al.*, 2007]. All the CK1 isoforms contained six-histidine tag in the N-terminus to facilitate the purification. CK1 α and CK1 γ_1 plasmids were used to transform *E. coli* BL21(DE3) cells whereas CK1 $\delta^{\Delta 317}$ plasmid was used to transform *E. coli* B-834. Cells were grown at 37°C to an OD₆₀₀ of 0.4–0.6 and, at this point, induced with 0.8 mM IPTG (isopropyl β -D-thiogalactoside). Induction was carried out overnight at 22°C in the case of CK1 α , while for CK1 $\delta^{\Delta 317}$ and CK1 γ_1 the temperature was maintained at 20°C. Afterward, the bacteria were pelleted, resuspended in a solution of 50 mM Tris/HCl, pH 8.0, 500 mM NaCl, 20% glycerol, 1% protease inhibitor cocktail (Sigma) and then lysed by French press. After centrifugation at 10,000g for 30 min, the supernatant was loaded onto nickel–nitriloacetic acid (Ni–NTA)–agarose columns (Qiagen) and washed with the same buffer containing 10 mM imidazole. The proteins were eluted with 50 mM Tris/HCl, pH 6.8, 50 mM NaCl, 5% glycerol and 300 mM imidazole. Native CK2 was purified from rat liver [Meggio *et al.*, 1981]; HIPK and PIM1 are kindly provided by Prof. Philip Cohen (School of Life Sciences, University of Dundee, Dundee, UK); Protein tyrosine kinases CSK, Lyn, c-Fgr, and Syk were purified from rat spleen as previously referenced [Sarno *et al.*, 1996]. PKA was a commercial product from Sigma–Aldrich Company. NPM-ALK, RET and FLT3 tyrosine kinases were provided by Dr. C. Gambacorti (National Cancer Institute, Milan, Italy). Human recombinant DYRK1a was kindly provided by Dr. W. Becker (Inst. fuer Pharmakologie und Toxikologie, Aachen, Germany).

Phosphorylation assays

CK2, CK1 α , CK1 $\delta^{\Delta 317}$ and CK1 γ_1 phosphorylation assays were carried out at 37°C in the presence of increasing amounts of each inhibitor in a final volume of 25 μ L containing 50 mM Tris-HCl, pH 7.5, 100 mM NaCl, 12 mM MgCl₂, 0.02 mM [γ -³³P]ATP (500–1,000 cpm/pmol),

unless otherwise indicated. The phosphorylatable substrate were the synthetic peptide substrate RRRADDSDDDDDD (100 μ M) and RRKHAAIGDDDDAYSITA (200 μ M) for CK2 and all CK1 isoforms, respectively. Reaction started with the addition of the kinase and was stopped after 10 min by addition of 5 μ L of 0.5 M orthophosphoric acid before spotting aliquots onto phosphocellulose filters. Filters were washed in 75 mM phosphoric acid (5–10 mL/each) four times and then once in methanol and dried before counting [Sarno *et al.*, 1996].

PIM1 activity was determined by following the same procedure by incubating the kinase in the presence of 50 mM Tris-HCl, pH 7.5, 0.1% v/v 2-mercaptoethanol, 0.1 mM EGTA, 30 μ M synthetic peptide substrate RKRRQTSMTD and 100 μ M [γ - 33 P]ATP. HIPK2 activity was determined under the same conditions used for PIM1 assays except for ATP which was 20 μ M and the use of MBP (10 μ g) as phosphorylatable substrate. PKA was assayed in the presence of 1 μ M cAMP under identical conditions by omitting NaCl and using ALRRASLGAA as synthetic peptide substrate, and tyrosine kinase activities were determined as previously described [Sarno *et al.*, 2001; Bain *et al.*, 2003; Donella-Deana *et al.*, 2005].

Kinetic determination

Initial velocities were determined at each of the substrate concentration tested. K_m values were calculated either in the absence or in the presence of increasing concentrations of inhibitor, from Lineweaver-Burk double-reciprocal plots of the data. Inhibition constants were then calculated by linear regression analysis of K_m/V_{max} versus inhibitor concentration plots. Inhibition constants were also deduced from the IC_{50}/K_i Cheng-Prusoff relationship [Cheng and Prusoff, 1973], by determining IC_{50} for each compound at 1 μ M ATP concentration, assuming a competitive mechanism of inhibition.

Cell culture, treatment, and viability assay

2008 cells derived from human ovary carcinoma cell line and its parental cisplatin-resistant variant (C13 cells) were generated by in vitro selection in the presence of increasing concentrations of cisplatin. C13 cells exhibit between 9- to 12-fold resistance to cisplatin, and the resistant phenotype is stable (i.e. it does not require the continuous presence of cisplatin to maintain the resistance). 2008 and C13 cells were routinely grown in humidified condition at 5% CO_2 and 37°C, incubated with RPMI 1640 medium, 10% FBS, 2% glutamine and 1% pen-strep. Cells were collected every 2 days with minimum amount of 0.05% trypsin–0.02% EDTA to wet

the whole culture dish surface and seeded 1×10^6 in 100 mm dish with RPMI 1640 medium, 10% FBS and 1% pen-strep. All reagents were from Cambrex, Lonza.

For cell viability assay, trypan blue dye exclusion method was used [Baran *et al.*, 2006]. Cells (5×10^5 cells/well) were grown in six-well plates with 3 ml of media in the absence or in the presence of different concentration of compound 1 and compound 2 for 24 h, 48 h, and 72 h. At the end of the experimental protocol, cells were collected with trypsin 0.02% EDTA, washed and diluted in PBS and counted using a hemacytometer in the presence of trypan blue solution at a 1:1 ratio (v/v) (Sigma–Aldrich) as described by the manufacturer. Results have been reported in fig. M1.

Compound 1	IC ₅₀ (24h) 95% CI	IC ₅₀ (48h) 95% CI	IC ₅₀ (72h) 95% CI
2008	136.7 43.93 to 225.6	14.37 3.31 to 62.41	12.80 4.27 to 38.35
C13	165.1 21.13 to 290.0	87.93 14.39 to 537.1	17.31 9.45 to 31.68

Compound 2	IC ₅₀ (24h) 95% CI	IC ₅₀ (48h) 95% CI	IC ₅₀ (72h) 95% CI
2008	152.3 106.7 to 217.0	122.4 18.02 to 331.8	60.42 16.17 to 225.8
C13	131.6 62.83 to 275.7	8.021 0.46 to 19.8	17.67 8.13 to 38.42

Figure M1. Cytotoxicity of compound 1 and 2 in human ovarian cancer cells. 2008 and C13 cells were exposed to (0.01 μ M to 1 mM) of anthraquinones derivatives for 24, 48, 72 h and cells were counted by trypan blue exclusion method. IC₅₀ values were estimated by non-linear regression analysis using GraphPad Prism software (San Diego, CA). Data are the means \pm 95% Confidence Intervals of three independent experiments.

Molecular modeling

Target Structures. The human CK1 δ catalytic subunit was built using an homology modelling approach implemented into Molecular Operating Environment (MOE) with δ isoform from *S. pombe* as template (PDB code: 2CSN e 1EH4) [Berman *et al.*, 2000]. To minimize contacts between hydrogen's, the structures were subjected to Amber99 force field minimization until the rms of conjugate gradient was $<0.05 \text{ kcal mol}^{-1} \text{ \AA}^{-1}$ keeping the all the heavy atoms fixed. To strictly validate the model generated and to calibrate our high-throughput docking protocol, a small database of known CK1 δ inhibitors was built and set of docking runs was performed [Mashhoon *et al.*, 2000; Rena *et al.*, 2004].

MMsINC database

MMsINC is a free web-oriented database of commercially available compounds for virtual screening and chemoinformatic applications. MMsINC contains over 4 million non-redundant chemical compounds in 3D format. The whole database was studied in term of uniqueness, diversity, frameworks, chemical reactivity, drug-like and lead-like properties. This study shows that there are more than 175,000 frameworks in our database. There are 3,89 millions (98%) of drug-like molecules among which more than 3,61 millions (91%) are lead-like. Moreover, 3,45 million (87%) are considered chemically stable compounds. The druglikeness and leadlikeness are estimated using Lipinski and Oprea cut-off values. The compounds are stored in a PostgreSQL database and the code to manage this database is in Java. Moreover, MMsINC is nicely integrated with PubChem and PDB databases facilitating the cross exchange of ligand information. In consequence, we have a free and easily updatable system for chemical databases management and screening sets generation. MMsINC is accessible at the following web address: <http://mms.dsfarm.unipd.it/MMsINC/>.

Optimized high-throughput docking

All MMsINC entries with a leadlikeness profile have been selected as input of our high-throughput docking protocol. Four different docking programs have been used in this step: MOE-Dock [Baran *et al.*, 2006], Glide [Schrodinger, 2001], Gold [Jones *et al.*, 1997], and FlexX [Sousa *et al.*, 2006]. Standard parameters of all four docking programs were used. For each MMsINC entry, the first best three docking poses have been kept for each docking protocol. Finally, an RMSD (root mean square deviation, the default value for this parameter is 4 Å) clustering is applied to the candidate solutions to discard redundant solutions. Clustering RMSD tool is implemented by MOE suite. Around 6 millions of plausible docking poses coming from parallel docking step have been used as starting point for the subsequent consensus scoring step.

Consensus scoring function selection

We performed consensus scoring using five scoring functions (MOE-Score, GlideScore, GoldScore, ChemScore, and Xscore) with the aim to appropriately rank all MMsINC candidate poses.

The FiTk consensus scoring function has been used to order and select the best pose candidates. This function represents the number of scoring functions for which a certain candidate pose is scored among the top k% of the database.

$$FiTk(x) = \sum_{i=1}^n f_i(x)$$

$$f_i(x) = \begin{cases} 1 & \text{if } \frac{r_i}{N-1} \in [0, \frac{k}{100}] \\ 0 & \text{if } \frac{r_i}{N-1} \in [\frac{k}{100}, 1] \end{cases}$$

We established a cut-off value for the top 5% compounds ranked by all possible combinations of docking-pose/scoring function, and prioritized the selection of those candidate poses that were positioned on the top 5% by the maximum number of scoring functions. In particular, derivatives 1 and 2 were found on the top 5% by all five scoring functions.

Results and Discussion

Very few potent and selective CK1 inhibitors have been described. Among these it is worthy to mention: the 4-[4-(2,3-dihydro-benzo[1,4]dioxin-6-yl)-5-pyridin-2-yl-1H-imidazol-2-yl] benzamide (D4476) [Rena *et al.*, 2004], the 3-[(2,4,6-trimethoxyphenyl)methylidene]-indolin-2-one (IC261) [Mashhoon *et al.*, 2000; Behrend *et al.*, 2000], and the N-(2-aminoethyl)-5-chloro-isoquinoline-8-sulfonamide (CK1-7) [Chijiwa *et al.*, 1989] with IC₅₀ of 0.3, 1.0, and 6 μM, respectively.

In recent years, we have performed an intensive screening campaign combining *in silico* and *in vitro* enzymology approaches [Moro *et al.*, 2006]. In particular, we have focused our attention on the CK1δ isoform due to its key role in the possible pathogenesis of several neurodegenerative diseases and cancer. Following some recent successful examples of new kinase inhibitors identification through structure-based virtual screening (SBVS) approaches [Moro *et al.*, 2006; Cozza *et al.*, 2006], we have performed an *in silico* study targeting the ATP-binding site of CK1 by browsing our in-house molecular database (defined as MMs-INC) which contains around 4 millions of synthetic and natural compounds. Generally speaking, SBVC approach could represent a useful strategy to prioritize the synthesis and the biological screening of novel drug candidates. In our virtual screening protocol, we have used a combination of different docking protocols in tandem with a consensus scoring strategy, as summarized in Figure 1. In particular, due to the fact that no crystal structure is available for the human CK1δ, an homology modeling approach has been carried out to obtain a suitable three-dimensional model of the CK1δ catalytic

subunit. The choice of combining different docking protocols has been dictated by the awareness that scoring is typically more important than docking in database screening, and that scoring functions performances often depend on the target active site features. However, since docking poses may significantly affect the scoring, multiple scoring functions are simultaneously used in the hit selection process, and improvements can be achieved by compensating for the deficiencies of each function. Specifically, a combination of four docking protocols (MOE-Dock, Glide, Gold, and FlexX) and five scoring functions (MOEScore, GlideScore, Gold-Score, ChemScore, and Xscore) has been used to appropriately dock and score all MMsINC entries with a leadlikeness profile. In particular, we have implemented a ‘FiTk consensus scoring function’ to appropriately rank the possible hit compounds. This function represents the number of scoring functions for which a certain candidate docking pose is scored among the top k% of the database (see Materials and methods for details).

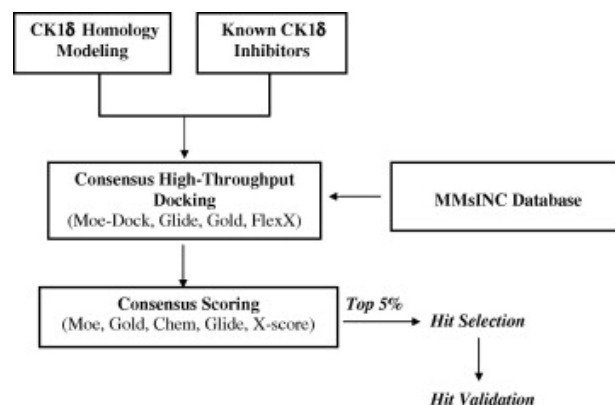


Figure 1. Flowchart of the proposed consensus high-throughput docking.

Interestingly, from our consensus SBVC protocol only few compounds (less than 150) have been scored with a full ‘FiTk consensus’. That means that these compounds appear in the top 5% of the database when ranked by every scoring function independently. After visual inspection, we have realized that two anthraquinone derivatives were among them. This finding was quite unexpected and intriguing at the same time considering that other anthraquinones were already reported to be modestly active against CK1, such as emodin [Sarno *et al.*, 2003] and 1,4-diamino-5,8-dihydroxyanthraquinone (DAA) [Meggio *et al.*, 2004]. For this reason, we decided to primarily focus our attention to these potential hit compounds. In particular, the 1,4-diamino-anthraquinone (compound 1, in Table 1) was one of the best ranked compounds of our top 5% list. Considering the encouraging virtual screening results, we have prioritized the acquisition and the biochemical characterization of derivative 1 as new potential CK1 δ inhibitor. In

particular, derivative 1 is 10-fold more potent compared with the reference CK1 δ inhibitor, 3-[(2,4,6-trimethoxyphenyl)methylidene]-indolin-2-one (IC261) [Mashhoon *et al.*, 2000; Behrend *et al.*, 2000].

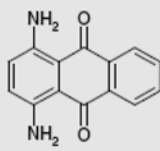
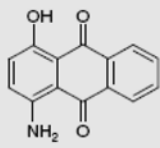
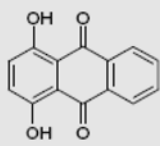
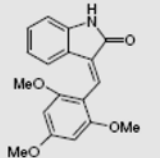
Compound	CK1 δ	CK1 γ 1	CK1 α	
1		0.33	34.0	4.0
2		0.66	26.2	4.0
3		>40	>40	>40
IC261		2.57	>40.0	1.24

Table 1. Inhibition of CK1 isoforms calculated as IC₅₀ (μ M). The values of IC₅₀ represent means of at least three independent experiments with SEM never exceeding 15%.

As shown in Figure 2, inhibition of CK1 δ by compound 1 is competitive with respect to the phosphodonor substrate ATP, and a 125 nM K_i value has been calculated from linear regression analysis of Lineweaver–Burk double reciprocal plots, which is the lowest K_i reported so far a CK1 δ inhibitor. On the other hand, according to a preliminary selectivity study (Tables 1 and 2), derivative 1 seems to be a quite specific inhibitor of CK1 δ respect the other CK1 isoforms, and also with respect to a small panel of different kinases. In particular according to our homology model, derivative 1 makes a stabilizing interaction between the amino group at the 1-position and the backbone carbonyl of Glu83 in the hinge region (Fig. 3). Moreover, one of the carbonyl groups can interact through an H-bonding with the backbone amido moiety of Leu85. These two interactions are the same generally observed in the binding of adenine moiety of ATP into the kinase active site. On the other hand, another hydrogen-bonding interaction has been detected between the amino group 4-position and the carboxylic group of Asp149. Finally, several hydrophobic interactions (Ile15, Ile23, Ala36, Leu135, Ile147) should be taken into account because they may contribute to stabilize the complex between compound 1 and CK1 δ . We can

also argue that the right balance of both polar and hydrophobic interactions and the appropriate shape complementarity with the ATP-binding cleft might be ultimately responsible for the appreciable selectivity presented by derivative 1 versus other kinases and in particular against the protein kinase CK2. In fact, the shape topology of the ATP-binding cleft of CK2 is clearly different respect CK1 (data not shown). Vice versa, more intriguing is the observation regarding the appreciable selectivity displayed by derivative 1 against the other CK1 isoforms. In fact, analyzing the sequence alignment of the corresponding kinase domains no crucial mutations are detectable and that would be able to justify the observed isoform selectivity spectrum of derivative 1. Our assumption is that in this specific case the C-terminal domain of CK1 isoforms could play an important role in the control of the inhibitor's recognition as well as in the corresponding CK1 basal kinase activity. In particular, the C-terminal domain of CK1 α and γ may have a deterrent effect on the interaction with derivative 1, reducing its inhibitory effects as collected in Table 1. This experimental evidence has been already reported also for the CK1 inhibitor, IC261 [Mashhoon *et al.*, 2000]. In fact, as suggested by a recent crystallographic information regarding the isoform CK1 γ_3 the C-terminal domain can closely approach the ATP-binding cleft directly interacting with the inhibitor (PDB code: 2CHL).

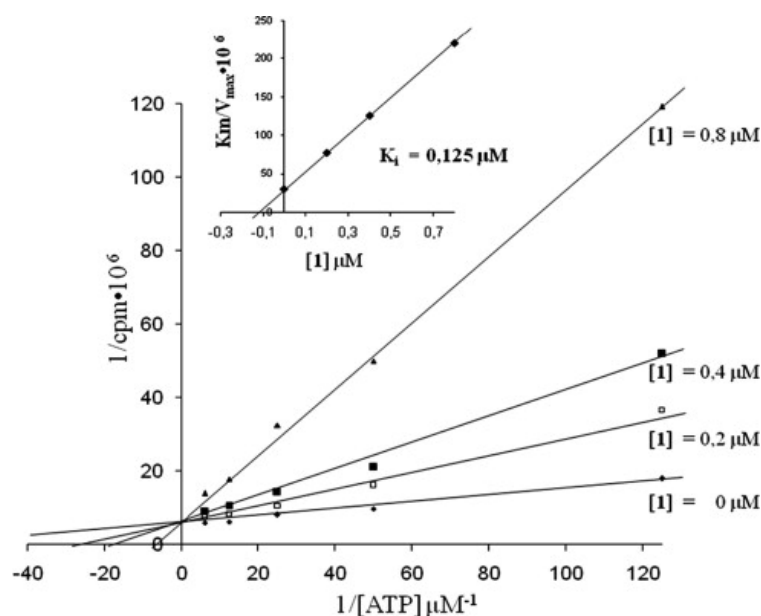


Figure 2. Kinetic analysis of compound 1/CK1 δ complexation consistent with a reversible and competitive mechanism of inhibition. CK1 δ activity was determined as described in Materials and Methods either in the absence or in the presence of the indicated compound 1 concentrations. The data represent means of triplicate experiments with SEM never exceeding 15%.

Beside derivative 1, the 1-hydroxy-4-amino-antraquinone (compound 2 in Table 1) also shows an appreciable inhibitory activity against CK1 δ ($IC_{50} = 0.6 \mu M$). To directly verify the role of the

1,4-diaminobenzene fragment, the corresponding 1,4-dihydroxy-anthraquinone was also tested as potential CK1 δ inhibitor (compound 3 in Table 1). Interestingly, compound 3 is practically inactive against the three isoforms CK1 δ , γ_1 and α supporting the critical role mediated by the aminobenzene fragment into CK1 δ recognition. Indeed, a robust and quantitative structure–activity relationship is underway in our laboratories to explore the possibility of decorating or modifying the 1,4-diamino-anthraquinone moiety increasing the pharmacodynamics of the second generation of these CK1 δ inhibitors and, at the same time, improving their pharmacokinetics profiles.

CK2	HIPK2	PIM1	DYRK1a	PKA	CSK	Lyn	Syk	Fgr	GST-ALK
18.0	3.3	24.7	3.6	>40.0	>40.0	>40.0	>40.0	24.0	>40.0

Table 2. Inhibition of a preliminary protein kinases panel by compound 1 calculated as IC₅₀ (μ M). The activity of each protein kinase was determined as described in Materials and Methods. The values of IC₅₀ represent means of at least three independent experiments with SEM never exceeding 15%.

Finally, considering the encouraging inhibitory and selectivity properties of compound 1 and 2 against isolated CK1 δ , we have also acquired a very preliminary cytotoxicity profile on human ovarian carcinoma cell line (2008) and on its cisplatin-resistant clone (C13). Results showed that after 48 h of exposure to compound 1 IC₅₀ values were 14.4 and 87.9 μ M in 2008 and C13 cells, respectively (\pm 95% confidence interval from three different experiments).

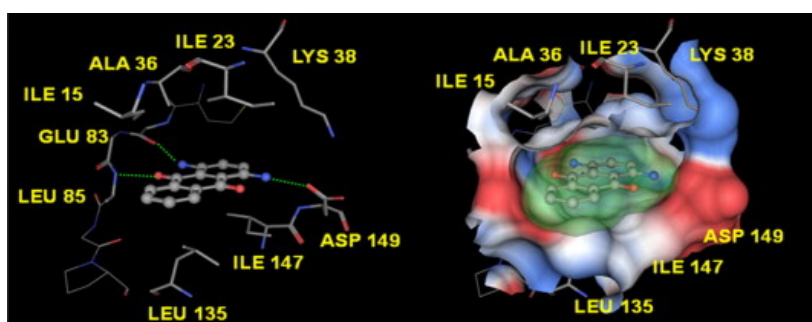


Figure 3. Molecular docking of compound 1 bound to the active site of the CK1 δ catalytic subunit. On the left, analysis of the binding mode of derivative 1 whose interactions with the most crucial amino acids are highlighted. On the right, Connolly's electrostatic charge distribution surface of ATP-binding cleft of CK1 δ (blue indicates positive surface charge and red indicates negative surface charge).

Interestingly, compound 2 was slightly more potent on the cisplatin resistant cell line (IC₅₀ 8.0 μ M) than in cisplatin sensitive cancer cells (IC₅₀ 122.4 μ M) (see also Materials and methods). Considering the wealth of kinase and non-kinase mediate biological activities of anthraquinones,

further investigations are in progress to clarify in detail the cytotoxicity pathway(s) activated and regulated in different human tumor cell lines.

Concluding, we have demonstrated the usefulness of our structure-based virtual screening (SBVS) approach to identify novel CK1 δ inhibitors. In particular, two amino-anthraquinone analogs (derivatives 1 and 2) have demonstrated being among the most potent and selective CK1 δ inhibitors known today ($IC_{50} = 0.3$ and $0.6 \mu M$, respectively). Indeed, we have conformed that anthraquinone scaffold is a versatile scaffold to design specific protein kinase inhibitors, as already reported for other classes of kinases such as for the protein kinase CK2 [Sarno *et al.*, 2002] for the Janus-activated kinase 2 (Jak2) [Muto *et al.*, 2007], for the dual-specificity tyrosine-(Y)-phosphorylation regulated kinase 1A (DYRK1A) [Sarno *et al.*, 2003; Meggio *et al.*, 2004] and the serum and glucocorticoid-inducible kinase (SGK) [Sarno *et al.*, 2003; Meggio *et al.*, 2004]. An ongoing project is now running in our laboratories to clearly understand the mechanism of action of this new class of promising CK1 δ inhibitors with the aim to design and synthesize a second generation of more potent and selective anthraquinone-driven CK1 δ inhibitors.

Acknowledgments

We are grateful to Prof. A. Donella and Dr. S. Sarno for the biochemical assay of tyrosin kinase and DYRK1a. The molecular modelling work coordinated by S.M. has been carried out with financial supports of the Italian Ministry for University and Research (MIUR), Rome, Italy and of the University of Padova, Padova, Italy. S.M. is very grateful to Chemical Computing Group for the long and fruitful collaboration. The biochemical work was financially supported by grants from AIRC (Italian Association for Cancer Research) and European Commission (Prokinaserearch LSHBCT2004-503467) to L.A.P. and F.M.

Preface to CHAPTER 8

Human T-cell leukemia virus type I (HTLV-1) is a complex retrovirus that infects an estimated 10–20 million people worldwide. HTLV-1 is the causative agent of an aggressive leukemia/lymphoma of mature CD4⁺ T-cells termed adult T-cell leukemia/lymphoma (ATLL). ATLL arises in 1–5% of HTLV-1-infected subjects after a latency period of several decades and is refractory to current therapies. Despite intensive study, the molecular determinants of ATLL are incompletely understood [Verdonck *et al.*, 2007]. HTLV-1 contains both regulatory and accessory genes in four "pX" open reading frames. Studies of the viral factors governing HTLV-1 replication and pathogenesis have been focused primarily on the transcriptional activator Tax, which plays a critical role in cell immortalization through its ability to deregulate the expression of a vast array of cellular genes and interfere with cell-cycle checkpoints [Lairmore and Franchini, 2007]. Indeed, expression of Tax in mouse thymocytes is sufficient for induction of T-cell leukemia/lymphoma [Hasegawa *et al.*, 2006]. However, the contrast between the powerful oncogenic properties of Tax and the low prevalence and long latency of ATLL in HTLV-1 infected individuals suggests the existence of mechanisms that limit the transforming/pathogenic potential of the virus and favour life-long asymptomatic persistence in the host.

Recent studies indicate that the viral accessory proteins p12, p21, p30, HBZ and p13 also contribute to HTLV-1 replication and pathogenesis [Nicot *et al.*, 2005]. pX ORF-II encodes two proteins, p13 and p30, whose roles are still being defined in the virus life cycle and in HTLV-1 virus–host cell interactions. Proviral clones of HTLV-1 with pX ORF-II mutations diminish the ability of the virus to maintain viral loads in vivo.

p13, an 87-amino acid accessory protein that is targeted to the inner membrane of mitochondria [D'Agostino *et al.*, 2005], induces mitochondrial fragmentation [Ciminale *et al.*, 1999], slows down proliferation, promotes apoptosis triggered by ceramide and FasL [Hiraragi *et al.*, 2005], and interferes with tumor growth in experimental models [Silic-Benussi *et al.*, 2004]. Although competent for replication in tissue culture, a p13-knockout virus is unable of establishing a persistent infection in a rabbit experimental model [Hiraragi *et al.*, 2006].

Functional mapping studies demonstrated that p13 includes a mitochondrial targeting signal (MTS) spanning amino acids 21–31 [Ciminale *et al.*, 1999] with four arginines. In contrast to canonical MTSs, the targeting signal of p13 is not cleaved upon import into mitochondria [Ciminale *et al.*, 1999]. The MTS of p13 (LRVWRLCTRRL) is predicted to form an α -helix, with the four arginines forming a positively charged face, thereby imparting amphipathic properties to this region [D'Agostino *et al.*, 2002]. Biophysical and biochemical analyses of a synthetic p13_[9–41] peptide confirmed that this region folds into an amphipathic α -helix upon exposure to membrane-mimetic solutions and changes mitochondrial membrane permeability to K⁺ [D'Agostino *et al.*, 2002]. Although p13 mutants carrying substitutions of the arginines with glutamines, prolines, or alanines and leucines retain mitochondrial targeting, they produce little or no mitochondrial fragmentation/swelling, indicating that the arginines of the amphipathic α -helical domain are essential for these effects [D'Agostino *et al.*, 2002].

CHAPTER 8

Section I

Modulation of Mitochondrial K⁺ Permeability and Reactive Oxygen Species Production by the p13 Protein of Human T-cell Leukemia Virus Type 1

Human T-cell leukemia virus type-1 (HTLV-1) expresses an 87-amino acid protein named p13 that is targeted to the inner mitochondrial membrane. Previous studies showed that a synthetic peptide spanning an alpha helical domain of p13 alters mitochondrial membrane permeability to cations, resulting in swelling. The present study examined the effects of full-length p13 on isolated, energized mitochondria. Results demonstrated that p13 triggers an inward K⁺ current that leads to mitochondrial swelling and confers a crescent-like morphology distinct from that caused by opening of the permeability transition pore. p13 also induces depolarization, with a matching increase in respiratory chain activity, and augments production of reactive oxygen species (ROS). These effects require an intact alpha helical domain and strictly depend on the presence of K⁺ in the assay medium. The effects of p13 on ROS are mimicked by the K⁺ ionophore valinomycin, while the protonophore FCCP decreases ROS, indicating that depolarization induced by K⁺ vs H⁺ currents has different effects on mitochondrial ROS production, possibly because of their opposite effects on matrix pH (alkalinization and acidification, respectively). The downstream consequences of p13-induced mitochondrial K⁺ permeability are likely to have an important influence on the redox state and turnover of HTLV-1-infected cells.

This section was published in:

Micol Silic-Benussi, Enrica Cannizzaro, Andrea Venerando, Ilaria Cavallari, Valeria Petronilli, Nicoletta La Rocca, Oriano Marin, Luigi Chieco-Bianchi, Fabio Di Lisa, Donna M. D'Agostino, Paolo Bernardi, and Vincenzo Ciminale (2009) Modulation of mitochondrial K(+) permeability and reactive oxygen species production by the p13 protein of human T-cell leukemia virus type 1 *Biochimica Et Biophysica Acta*, 1787, 947-954.

Materials and methods

Peptide synthesis

Full-length wild-type p13 (87-mer) and p13-AL, which contains alanines in the place of 4 arginines in the mitochondrial targeting signal/amphipathic alpha helical domain [D'Agostino *et al.*, 2002], were synthesized by a solid-phase method on a polyethylene glycol polyacrylamide (PEGA) resin functionalized with the acid labile linker 4-hydroxymethylphenoxyacetic acid (Novabiochem), using an Applied Biosystems Model 433 automated peptide synthesizer. The fluorenylmethoxycarbonyl (Fmoc) strategy [Fields and Noble, 1990] was used throughout the peptide chain assembly, with 2-(1H-benzotriazol-1-yl)-1,1,3,3-tetramethyluronium hexafluorophosphate (HBTU) and 1-hydroxybenzotriazole (HOBT) or 2-(1H-7-azabenzotriazol-1-yl)-1,1,3,3-tetramethyl uronium hexafluorophosphate methanaminium (HATU) employed as coupling reagents. The side-chain protecting groups were as follows: tert-butyl for Ser, Thr, Tyr, Asp and Glu; tert-butyloxycarbonyl for Trp; trityl for His, Cys, Asn and Gln; 2,2,4,6,7-pentamethyldihydrobenzofuran-5-sulfonyl for Arg. Acetylation steps were carried out after every coupling involving hydrophobic residues. Peptide cleavage was performed by reacting the peptidyl-resins with 95% TFA/ethanedithiol for 3 h. Crude peptides were subsequently purified by two serial chromatographic steps on preparative C8 and C18 reverse phase HPLC columns. Molecular masses of the peptides were ascertained by mass spectroscopy with direct infusion on a Waters-Micromass ZMD-4000 Mass Spectrometer. The purity of the peptides was about 95% as evaluated by analytical reversed-phase HPLC.

Assays on isolated mitochondria

Liver mitochondria isolated from albino Wistar rats weighing about 300 g were prepared by standard centrifugation techniques exactly as previously described [Costantini *et al.*, 1995]. Briefly, the liver was minced with scissors in isotonic sucrose buffer (250 mM sucrose, 10 mM Tris/HCL, 0.1 mM EGTA-Tris, pH 7.4), washed with sucrose buffer to eliminate residual blood, and then homogenized. The suspension was centrifuged at 600g for 10 min to eliminate cells and large debris. The supernatant was collected and centrifuged at 7,000g for 10 min to pellet mitochondria, which were then resuspended in the same buffer and centrifuged again at 7,000g for 10 min. The resulting washed mitochondrial pellet was resuspended in a small volume of sucrose buffer and assayed for protein content using the Biuret protein determination assay.

To assess the uptake of p13 into mitochondria, the synthetic protein (100 nM final concentration) was added to a 1 mg aliquot of mitochondria previously diluted in 2 ml KCl buffer, and incubated at 37°C for 5 min. Mitochondria were then pelleted by centrifugation at 7,000g for 10 min, washed with 2 ml KCl buffer, and centrifuged again. Resulting mitochondrial pellets were resuspended in sucrose-HEPES buffer [D'Agostino *et al.*, 2002] and incubated on ice for 2 min after addition of dimethyl sulfoxide (DMSO, 5%; serving as a control) or digitonin (0.05% or 0.5%, prepared in DMSO). The suspensions were then centrifuged at 17,500g for 10 min and resulting supernatants and pellets were solubilized and analyzed by SDS-PAGE followed by electrotransfer to PVDF membrane (HyBond P, GE Healthcare). Sodium carbonate extraction assays were carried out as described previously [D'Agostino *et al.*, 2002]. For this treatment, washed pellets of mitochondria loaded with p13 were resuspended in 100 mM sodium carbonate, pH 11.5 and incubated for 30 min on ice. The sample was then adjusted to 1.6 M sucrose, overlaid with a step gradient of 1.25 M – 250 mM sucrose, and centrifuged at 47,000 rpm for 2 h in an SW60.1 rotor (Beckman Instruments). The gradient fractions containing soluble proteins (i.e., the bottom 1.6 M sucrose layer) and membrane-inserted proteins (i.e., the 1.25 M sucrose layer plus 0.25–1.25 M sucrose interface) were precipitated using trichloroacetic acid and analyzed by SDS-PAGE followed by electrotransfer to HyBond P. Blots were probed with antibodies against p13 (rabbit anti-p13, raised against the synthetic protein), Porin (Calbiochem), and Hsp60 (Santa Cruz) followed by horseradish peroxidase-conjugated secondary antibodies (Pierce) and developed with chemiluminescence detection reagents (Pierce Supersignal Pico). Chemiluminescent signals were detected by exposure to Hyperfilm (GE Healthcare) or with a BioRad ChemiDoc XRS imager.

Mitochondrial volume changes, membrane potential, ROS production, and the threshold for opening of the permeability transition pore (PTP) were measured in a PerkinElmer 650–40 spectrofluorimeter equipped with magnetic stirring and thermostatic control. Mitochondrial volume changes were measured in “swelling assays” as the change in 90° light scattering at 540 nm [Petronilli *et al.*, 1993]. Membrane potential was assayed by measuring the change in fluorescence intensity of rhodamine 123 (Molecular Probes) added at a concentration of 300 nM [Emaus *et al.*, 1986]. The probe was excited at 503 nm, and emission was analyzed at 525 nm with the excitation and emission slits set at 2 and 5 nm, respectively. O₂ consumption was measured polarographically with a Clark oxygen electrode in a closed temperature-controlled 2 ml vessel equipped with magnetic stirring (Yellow Springs Instruments). These assays were performed at 25°C in a 2 ml final volume containing 2 mg mitochondria (measured as total protein in the Biuret assay) and KCl buffer, pH 7.4 (125 mM KCl, 10 mM Tris-MOPS, pH 7.4, 1 mM Pi-Tris, 20 μM EGTA-Tris, 5 mM glutamic acid and 2.5 mM malic acid).

Production of ROS in mitochondria was measured using Amplex UltraRed (Molecular Probes), which reacts with H₂O₂ in a 1:1 stoichiometric ratio to produce the fluorescent product Resorufin. Mitochondria (2 mg) were resuspended in KCl buffer in the presence of 5 μM Amplex UltraRed reagent and 5 mg/ml horseradish peroxidase. The probe was excited at 563 nm and its emission was measured at 587 nm over a 5 min timeframe at 37°C in the absence or presence of p13 and other treatments described in the text. The slopes (*m*) of the resulting traces were used to calculate changes in H₂O₂ production expressed as the ratio (m_2/m_1) where m_2 is the slope after the treatment and m_1 is the slope before the treatment.

The threshold for PTP opening was assessed by measuring the mitochondrial calcium retention capacity using the Ca²⁺ indicator Calcium Green-5N (Molecular Probes) as described previously [Fontaine *et al.*, 1998].

For electron microscopy isolated mitochondria were fixed overnight at 4°C in 3% glutaraldehyde prepared in 0.1 M sodium cacodylate buffer (pH 6.9), post fixed for 2 h in 1% osmium tetroxide in the same buffer and then processed according to [Rascio *et al.*, 1991]. Ultrathin sections (80 nm) were cut with an ultramicrotome (Ultracut, Reichert-Jung, Wien, Austria), stained with lead citrate and observed with a transmission electron microscope (TEM 300, Hitachi) operating at 75 kV.

Results

Fig. 1 shows the effects of full length p13 on mitochondrial light scattering, a measure of mitochondrial shape and volume. Assays performed in isotonic KCl buffer (125 mM KCl) confirmed that p13 induced a dose-dependent change of mitochondrial light scattering, and comparison with the p13_[9-41] peptide employed in previous studies indicates that full length p13 was considerably more potent (Fig. 1A; see also ref. [D'Agostino *et al.*, 2002]). To test the dependence of the effects of p13 on the K⁺ concentration, we carried out experiments in isotonic buffers containing increasing concentrations of K⁺. Fig. 1B demonstrates that the effect induced by full length p13 was strictly dependent on the KCl concentration.

Interestingly, the effects obtained with concentrations of p13 ranging from 50 nM to 400 nM were reversed after treatment with FCCP (Fig. 1C), a protonophore that collapses mitochondrial membrane potential ($\Delta\psi$). This finding is consistent with a $\Delta\psi$ -dependent uptake of K⁺ and indicates that the permeability increase induced by p13 is selective for K⁺ vs H⁺ in this concentration range. In contrast, higher p13 concentrations (0.8 and 1.6 μ M) resulted in only partial volume recovery after FCCP treatment (Fig. 1C), possibly reflecting a loss of selectivity which might have resulted in the transport of Cl⁻ as well. Importantly, no light scattering changes were induced by the p13-AL mutant (Fig. 1C, grey traces), which carries substitutions of the 4 arginine residues in the alpha helical domain with alanine and leucine and is unable to induce mitochondrial morphological changes in cells [D'Agostino *et al.*, 2002].

To interpret the effects of p13 on mitochondrial parameters it was important to verify the uptake of synthetic p13 into isolated mitochondria, and the site of its accumulation, i.e., in the outer membrane, intermembrane space, matrix, or inner membrane, as documented previously for p13 expressed in transfected HeLa cells [D'Agostino *et al.*, 2002]. For this purpose, rat liver mitochondria were incubated with p13, washed, and then incubated with DMSO (5%, serving as a control) or digitonin (0.05% or 0.5%, prepared in DMSO). Resulting supernatants and pellets were analyzed by SDS-PAGE and immunoblotting to detect p13 and Porin, a marker for the outer mitochondrial membrane, which is expected to be solubilized by 0.5% digitonin. As shown Fig. 1D, a strong p13 signal (both monomer and multimer forms) was evident in the pellet fraction of mitochondria treated with DMSO or 0.05% digitonin. This observation verified that p13 was indeed taken up by isolated rat liver mitochondria in our *in vitro* assays. Treatment with 0.5% digitonin extracted a substantial portion of Porin; in contrast, p13 was detected almost exclusively in the pellet after this extraction. This result allowed us to exclude the outer membrane as the site of p13 accumulation.

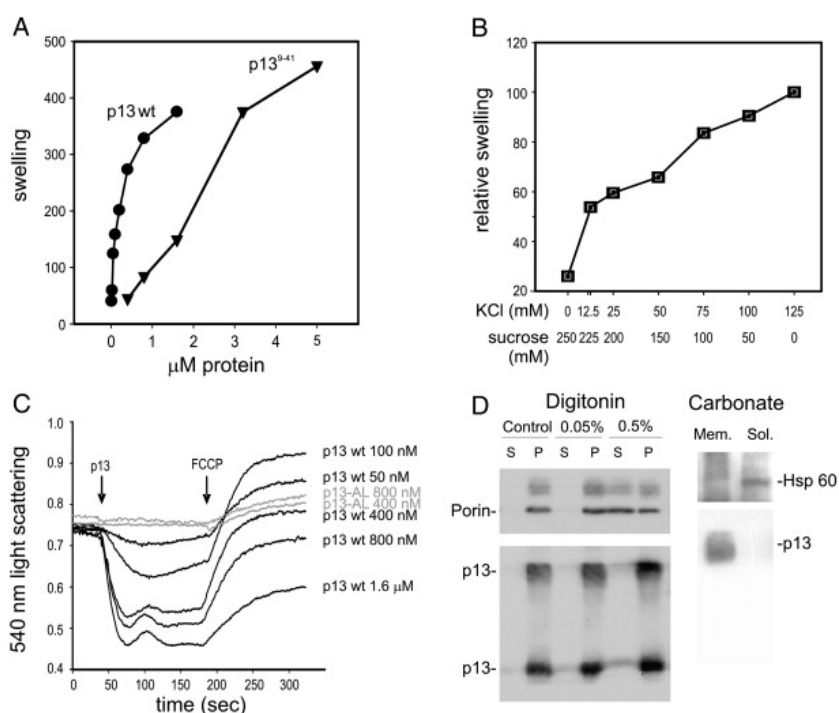


Figure 1. Effects of p13 on K^+ permeability; submitochondrial targeting of p13. Rat liver mitochondria isolated as described in the text were placed in isotonic KCl buffer and treated with synthetic p13 protein. (A) Comparison of the light scattering change induced by full-length p13 (circles) and by a peptide spanning the alpha helical region of the protein [(p13⁹⁻⁴¹), triangles]. Values on the ordinate refer to the difference in light scattering at 540 nm measured after the addition of p13. Full-length p13 was tested at 12.5, 25, 50, 100, 200, 400, 800 and 1600 nM; p13⁹⁻⁴¹ was tested at 400, 800, 1600, 3200 and 5000 nM. (B) Assays were carried out as described for panel A using 100 nM full-length p13 with the KCl and sucrose concentrations indicated on the abscissa. Values on the ordinate are scaled to a reference 100% light scattering change obtained in 125 mM KCl. (C) p13-induced changes of light scattering were reverted upon addition of 100 nM FCCP, which confirms their link to energy-dependent ion transport; in contrast, no effect on K^+ permeability was obtained with a p13 mutant carrying substitutions in the 4 critical arginine residues in the alpha helical domain of the protein (p13-AL). Results are representative of at least 3 experiments for each assay. Panel D shows results of digitonin and sodium carbonate extraction assays carried out to verify uptake of p13 into isolated mitochondria (see Materials and methods). Immunoblots were probed with antibodies against the indicated proteins and analyzed by chemiluminescent imaging (Digitonin panel) or exposure to autoradiographic film (Carbonate panel). As described in the Results, these assays indicated that p13 accumulated mainly in the inner mitochondrial membrane.

To determine whether p13 taken up by mitochondria was membrane-inserted, which would indicate its accumulation in the inner membrane rather than the matrix or intermembrane space, we subjected p13-loaded mitochondria to sodium carbonate extraction [D'Agostino *et al.*, 2002]. Resulting fractions containing membrane-integrated proteins and soluble proteins were immunoblotted to detect p13 and Hsp60 (a marker for a soluble mitochondrial protein). As shown in Fig. 1D, Hsp60 was present mainly in the soluble fraction after carbonate extraction, while p13 was detected in the membrane-associated fraction (as a multimer on this blot). Interpretation of these results together with those of the digitonin assay led us to conclude that p13 accumulated mainly in the inner mitochondrial membrane in our *in vitro* assays.

To gain insight into the basis for the light scattering changes induced by p13, we compared the ultrastructure of mitochondria subjected to treatment with p13 to that of mitochondria swollen through Ca^{2+} -mediated PTP opening. Results shown in Fig. 2 indicate that 100 nM p13 induced a shape change in mitochondria resulting in an electron-dense ring- or crescent-like morphology (Fig. 2C) that was clearly different from the large-amplitude swelling triggered by Ca^{2+} (Fig. 2B), suggesting that the two processes leading to membrane permeabilization are distinct (see Discussion). Interestingly, in analogy with results observed in the light scattering assay (Fig. 1C), treatment with 100 nM p13 followed by FCCP resulted in a recovery of the original mitochondrial ultrastructure (Fig. 2D), suggesting that the basis for the shape changes was linked to energy-dependent K^+ transport. As shown in Fig. 2E, treatment with 800 nM p13, which triggered swelling that was only partially reversed by FCCP (see Fig. 1C), resulted in a substantial proportion of mitochondria that exhibited large-amplitude swelling similar to that observed using Ca^{2+} .

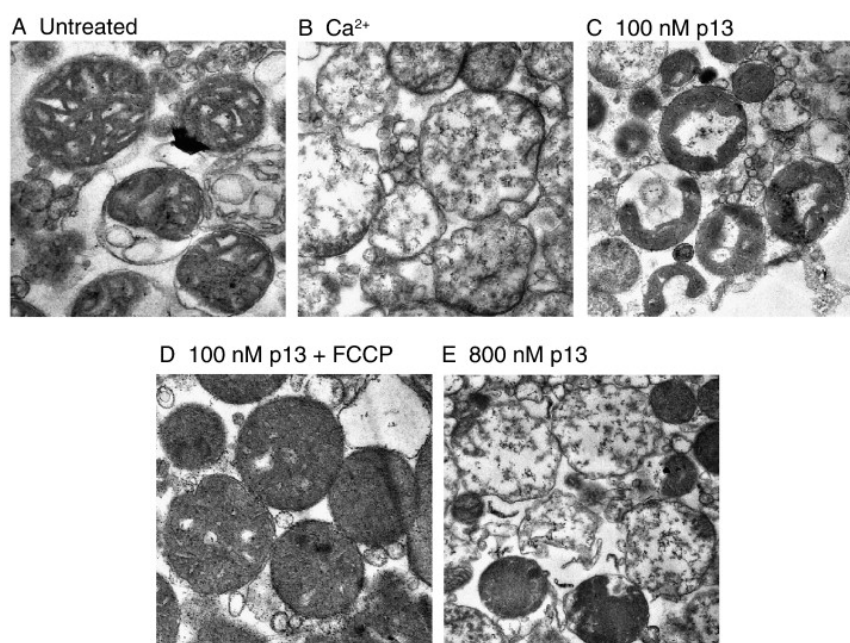


Figure 2. Effects of p13 on mitochondrial ultrastructure. Results show the ring/crescent-like morphology of mitochondria treated with 100 nM p13 (C) in comparison to large amplitude swelling induced by Ca^{2+} through PTP opening (B) or high doses of p13 (E). Effects of 100 nM p13 on ultrastructure were reverted by FCCP (D).

If the process of K^+ influx induced by p13 is electrophoretic, it should cause inner membrane depolarization. This was tested using rhodamine 123, which is taken up by energized mitochondria in a potential-dependent manner [Emaus *et al.*, 1986]. Fig. 3A shows that p13 induced depolarization, with a marginal effect seen at low concentrations (50, 100 nM) and

progressively more potent effects at higher concentrations (e.g. 1.6 μM) that nearly equaled the depolarization induced by FCCP. Interestingly, the p13-AL mutant had no effect on $\Delta\psi$ (Fig. 3A).

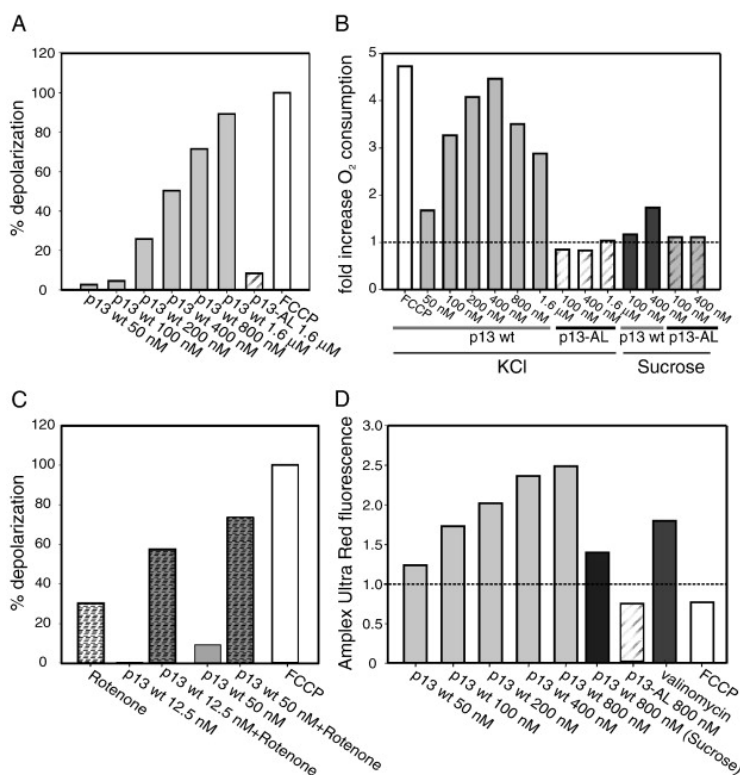


Figure 3. Effects of p13 on mitochondrial membrane potential, respiration and ROS. (A) Effects of p13 on mitochondrial membrane potential. Depolarization is reported on the y axis as the change in rhodamine 123 fluorescence expressed as the percentage of the depolarization induced by 100 nM FCCP (set as 100%). (B) Effects of p13 on mitochondrial O_2 consumption. The y axis reports the fold change in the rate of O_2 consumption compared to the basal rate recorded in the absence of p13. (C) Inhibition of the ETC by rotenone enhances the depolarizing effects of p13. Depolarization is reported on the y axis as in panel A. The additive effect of the p13-induced depolarization and ETC inhibition by 2 μM rotenone is particularly evident at low concentrations of p13 that do not induce measurable depolarization per se. (D) Effects of p13 on mitochondrial H_2O_2 , measured with the probe Amplex UltraRed. The y axis reports the ratio m_2/m_1 , where m_2 and m_1 are the slopes of the traces after and before the indicated treatment, respectively. Results are representative of at least 3 experiments for each assay.

Electron transport through the ETC is coupled to proton extrusion. Therefore, membrane depolarization is predicted to stimulate electron transport and increase O_2 consumption. Closed-chamber polarographic measurements showed that p13 induced a dose-dependent increase in O_2 consumption when added up to a concentration of 400 nM (Fig. 3B). This effect leveled off at higher p13 concentrations, suggesting that other mitochondrial alterations might ensue, e.g. release of pyridine nucleotides or cytochrome c, which may result from swelling and outer membrane rupture [Di Lisa *et al.*, 2001]. This hypothesis is consistent with the reduced selectivity of the membrane permeability changes induced by p13 at high concentrations (see results in Fig. 1C). In analogy with its lack of permeabilizing activity in other assays, the p13-AL

mutant did not affect O₂ consumption, nor did wild-type p13 when assayed in sucrose-based buffer lacking K⁺, underscoring the strict K⁺-selectivity of this effect.

We next tested whether increased proton extrusion resulting from the activation of the ETC might partially dampen p13's effects on Δψ (Fig. 3C). To this end, we exposed mitochondria to rotenone, which blocks complex I of the ETC. As expected, rotenone induced partial depolarization. Pretreatment with p13 at 12.5 nM, i.e. a concentration unable to induce measurable depolarization per se, substantially increased rotenone-induced depolarization. This effect was more pronounced at 50 nM p13, which in the presence of rotenone induced a depolarization that approached that obtained with FCCP. These data thus indicate that even low concentrations of p13 induce permeabilization to K⁺ whose consequences on membrane potential and respiration fully emerge upon inhibition of the ETC.

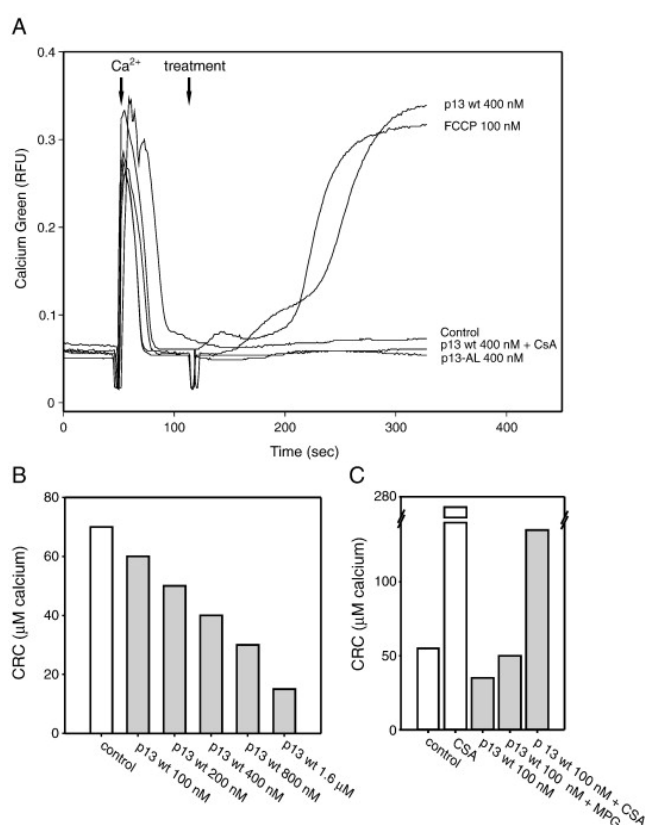


Figure 4. Effects of p13 on the opening threshold of the PTP. Effects of p13 on PTP opening were assessed by measuring the Ca²⁺ retention capacity (CRC) of isolated mitochondria (see text and ref. [Fontaine *et al.*, 1998]). The same KCl isotonic incubation medium described for other *in vitro* assays was supplemented with 1 μM Calcium Green-5N. Panel A shows a time course experiment of Ca²⁺ uptake and release following stimuli that trigger PTP opening. Panels B and C show the Ca²⁺ concentration required to trigger PTP opening following treatment with increasing doses of p13 (B) and inhibition by CsA or ROS scavengers (C). RFU, relative fluorescence units. CRC, Ca²⁺ retention capacity.

As the ETC is a major source of ROS production in mitochondria, and since the amount of ROS produced depends on the rate of electron flux and the membrane potential, we reasoned that

modulation of respiratory chain activity by p13 might be accompanied by a change in the levels of mitochondrial ROS. This possibility was tested using the H₂O₂ probe Amplex UltraRed. Fig. 3D reports the changes in probe fluorescence produced by different treatments, calculated as the ratio of the slopes after and before the treatment (see Materials and methods). Results showed that p13 induced a dose-dependent increase in ROS production (Fig. 3D). Interestingly, a similar effect was induced by the K⁺ ionophore valinomycin. In contrast, treatment with FCCP reduced H₂O₂ production, suggesting that depolarization induced by H⁺ vs K⁺ currents has opposite effects on ROS (see Discussion). Consistent with its dependence on K⁺ transport, H₂O₂ production was not observed with the p13-AL mutant (Fig. 3D).

It is known that monoamine oxidases (MAO) associated with the outer mitochondrial membrane are also an important source of ROS in mitochondria [Di Lisa *et al.*, 2007]. To specifically measure H₂O₂ originating from the ETC we inhibited MAO activity using pargyline. Although this treatment did decrease the overall fluorescence intensity, p13 was still able to increase probe's fluorescence, indicating that its effects on ROS are independent of MAO activity (data not shown).

Both mitochondrial depolarization [Bernardi, 1992] and ROS [Costantini *et al.*, 1996] are known to affect the probability of opening of the PTP, a large conductance mitochondrial channel that triggers cell death through energy shortage and release of proapoptotic factors localized in the intermembrane space [Rasola and Bernardi, 2007; Leung and Halestrap, 2008]. To test whether p13 might affect PTP opening we employed the Ca²⁺ retention capacity assay (see Materials and methods and ref. [Fontaine *et al.*, 1998]). This assay measures the sensitivity of the PTP to opening in response to Ca²⁺, which is rapidly taken up by energized mitochondria. Uptake and release of Ca²⁺ by mitochondria is measured using Calcium Green, a Ca²⁺ probe that is excluded from mitochondria and therefore fluoresces when Ca²⁺ is present outside mitochondria. Fig. 4A shows that addition of Ca²⁺ resulted in its rapid uptake by mitochondria. The mitochondria were able to retain this dose of Ca²⁺ until PTP opening was triggered by depolarization with FCCP (see trace in Fig. 4A) [Petronilli *et al.*, 1993*]. Remarkably, 400 nM p13 was also able to trigger PTP opening; in contrast, the p13-AL mutant had no effect. Further experiments carried out with serial additions of Ca²⁺ allowed us to estimate the sensitivity of the PTP based on the concentration of Ca²⁺ required to open it. Fig. 4B shows results of this analysis, expressed as the Ca²⁺ retention capacity (CRC), which demonstrated that p13 reduced the CRC of mitochondria in a dose-dependent manner, indicating that the protein may indeed affect the threshold for PTP opening. Interestingly, treatment with the ROS scavenger mercaptopropionylglycine (MPG) partly inhibited the effect of p13, suggesting that the latter is, at least in part, ROS-dependent

(Fig. 4C). Treatment of mitochondria with CsA resulted in an increase in CRC both in control and p13-treated mitochondria (Fig. 4C).

Discussion

The observations made in the present study support the working model of p13 function illustrated in Fig. 5. We have demonstrated that (i) p13 triggers an inward K^+ current into mitochondria (Fig. 1), ultrastructural changes (Fig. 2) and depolarization (Fig. 3A); (ii) depolarization induced by p13 enhances respiratory chain activity (Fig. 3B), which in turn partially dampens depolarization by increasing H^+ extrusion (Fig. 3C); (iii) these changes are accompanied by increased production of ROS (Fig. 3D) which, along with membrane depolarization, may (iv) be responsible for lowering the threshold of PTP opening (Fig. 4).

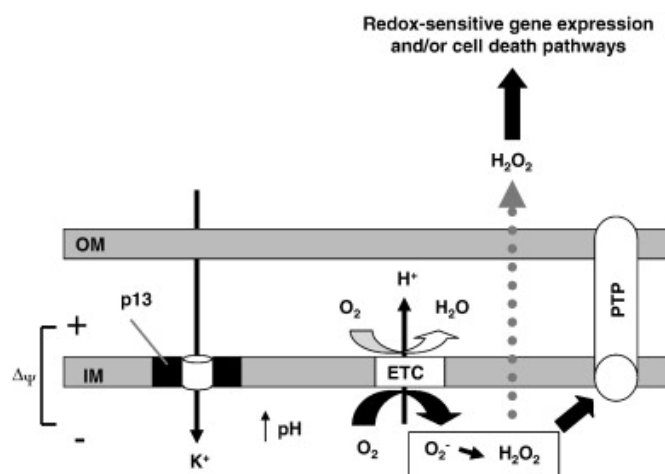


Figure 5. Working model of p13 function. p13 forms or affects a K^+ channel in the inner mitochondrial membrane (IM) leading to K^+ influx in energized mitochondria. This induces depolarization that is partly compensated by activation of the respiratory chain and consequent increased extrusion of H^+ . However, ETC activity also increases matrix pH and the chemical H^+ gradient, resulting in increased ROS production which, along with membrane depolarization, may lower the opening threshold of the PTP and trigger cell death. Increased H_2O_2 levels may also engage ROS-dependent "extramitochondrial" cell death pathways (e.g. ASK1/p38).

It remains to be determined whether p13 possesses intrinsic channel-forming activity or affects the activity of one of the described endogenous K^+ channels [Szewczyk *et al.*, 2006]. The first possibility is suggested by the previously documented ability of p13 to form multimeric structures in lipid-like environments [D'Agostino *et al.*, 2002], a property that has been described for channel-forming proteins termed viroporins that are coded by several other viruses [Gonzalez and Carrasco, 2003].

A study by Hackenbrock [Hackenbrock, 1966] demonstrated a tight link between mitochondrial ultrastructure (and light scattering properties) and the oxidative phosphorylation/electron transport state as defined by Chance and Williams [Chance and Williams, 1955]. In contrast to large amplitude osmotic swelling which leads to outer membrane rupture, cristae unfolding, marked matrix expansion and loss of mitochondrial structure and function, the ultrastructural changes accompanying shifts in metabolic state are of smaller amplitude, and readily reversible. The most dramatic “state-coupled” change was observed in the state IV to state III transition in which ETC activity is dramatically boosted by addition of ADP in the presence of substrates. In this condition, Hackenbrock observed that the matrix condensed in a peripheral eccentric or ring-like structure surrounding an “internal compartment” apparently connected to the intermembrane space [Hackenbrock, 1966]. Interestingly, these ultrastructural changes and their reversibility closely match our observations made with low (e.g. 100 nM) concentrations of p13, suggesting that the ultrastructural changes induced by p13 are likely to result from a boost in ETC activity triggered by the inward K^+ current.

The finding that p13 triggers depolarization and increases ROS balance in isolated mitochondria may appear to be in contrast with previous studies suggesting that a decreased proton electrochemical gradient due to increased electron flux should be accompanied by reduced diversion of electrons from the ETC to oxygen, which should in turn result in decreased ROS production [Brand and Esteves, 2005]. It is important to note that the data on which these conclusions are based were obtained either with the addition of protonophores or with activation of uncoupling proteins, i.e. under conditions where the depolarizing charge is carried by H^+ , which will also cause matrix acidification and substrate depletion. In our studies the depolarizing current is carried by K^+ , which causes a compensatory increase in H^+ pumping and will tend to increase matrix pH. Consistent with a key difference between depolarization by H^+ and K^+ currents, the effect of p13 on ROS production was mimicked by the K^+ -selective ionophore valinomycin, while treatment with the protonophore FCCP resulted in the expected decrease in H_2O_2 production (Fig. 3D). Our findings are also consistent with recent data of Costa *et al.* showing that opening of the mitochondrial K_{ATP} channel results in matrix alkalization and increased H_2O_2 production [Costa *et al.*, 2005].

Interestingly, mitochondrial generation of H_2O_2 was also demonstrated to occur during ceramide-induced apoptosis [Quillet-Mary *et al.*, 1997], a finding that suggests a link between the present work and previous results showing that expression of p13 in HeLa and Jurkat T-cells was associated with an increased sensitivity to apoptosis induced by ceramide [Silic-Benussi *et al.*, 2004; Hiraragi *et al.*, 2005].

As shown in Fig. 4, p13 modulates the PTP and increases its sensitivity to opening. This effect can be traced to two synergistic mechanisms, i.e. (i) ROS-mediated shifting of the PTP voltage threshold [Petronilli *et al.*, 1994], which is consistent with the recent demonstration that the pore plays a key role in the production of superoxide flashes in situ [Wang *et al.*, 2008], and (ii) lowering of the membrane potential, which would draw the resting potential nearer to the opening threshold [Scorrano *et al.*, 1997] (see [Nowikovsky *et al.*, 2009] for a recent review on the relationship between mitochondrial K⁺ channels and PTP regulation).

The ability of p13 to slow down cell growth [Silic-Benussi *et al.*, 2004] and sensitize cells to the apoptotic stimuli FasL and ceramide [Hiraragi *et al.*, 2005; Silic-Benussi *et al.*, 2004] suggests that this protein might limit the transforming potential of HTLV-1 in infected cells. This possibility is intriguing in light of the fact that Tax, the major HTLV-1-encoded oncoprotein, protects cells from apoptosis induced by mitochondria-mediated death stimuli [Saggiaro *et al.*, 2001; Trevisan *et al.*, 2004]. Therefore Tax and p13 might exert opposite effects on cell turnover, on the one hand expanding the pool of infected cells and on the other hand limiting neoplastic transformation, thus favoring viral persistence and adaptation to the host. This hypothesis is consistent with the low frequency and long clinical latency of ATLL and with results of experiments carried out in a rabbit experimental model showing that p13 is required to establish a persistent infection in vivo [Hiraragi *et al.*, 2006]. Through its stimulation of ROS, p13 could also affect redox-sensitive gene expression, the consequences of which could either favour cell survival or promote cell death.

The accumulated data describing p13's biological properties reinforce the emerging concept that manipulation of mitochondrial function is a key point of convergence in tumour virus replication strategies. Indeed, recent studies have revealed that many viruses, including all of the human tumour viruses, express mitochondrial proteins [Boya *et al.*, 2004; D'Agostino *et al.*, 2005*]. Further investigations of p13 and its interactions with mitochondria may thus provide important insights into the mechanisms of HTLV-1 replication and pathogenesis and could aid in the discovery of new targets for anti-tumour therapy.

Acknowledgments

We thank Prof. Antonio Toninello and Mario Mancon for supplying mitochondrial preparations for uptake assays. This work was supported by grants from the European Union ('The role of chronic infections in the development of cancer'; contract no. 2005-018704), Istituto Superiore di Sanità AIDS research program, the Associazione Italiana per la Ricerca sul Cancro (AIRC,

grants to V.C. and P.B.), the Ministero per l'Università e la Ricerca Scientifica, e Tecnologica Progetti di Ricerca di Interesse Nazionale, by European Commission PRO-KINASERESEARCH 503467 and the University of Padova (grant to D.M.D.). E.C. was supported by a fellowship from AIRC.

CHAPTER 8

Section II

Possible Role of Phosphorylation in the Regulation of p13 Function

This section is adapted from unpublished data of a new project in collaboration with
Vincenzo Ciminale and Roberta Biasiotto (IOV, Padua)

Materials and methods

Cell cultures

Jurkat T-cells were maintained in RPMI 1640 (Sigma) supplemented with 10% fetal calf serum (Invitrogen), penicillin/streptomycin and 2 mM L-glutamine (GIBCO).

In silico analysis of p13 amino acid sequence

The prediction of the possible kinase phosphorylating p13 was performed by PROSITE database [Bairoch *et al.*, 1997] and NetPhosK 1.0 algorithm [Blom *et al.*, 1999].

Peptide synthesis

p13_[9–22] peptides (p13wt and p13S15A) and full length p13 (87-mer) were synthesized by solid-phase methods, as described in Section I. Briefly, peptides were synthesized with an Applied Biosystems Model 433 automated peptide synthesizer using the fluoren-9-ylmethoxycarbonyl (Fmoc) chemistry and 2-(1H-benzotriazol-1-yl)-1,1,3,3-tetramethyluronium hexafluoro phosphate (HBTU)/1-hydroxybenzotriazole (HOBt) or 2-(1H-7-azabenzotriazol-1-yl)-1,1,3,3-tetramethyluronium hexafluorophosphate methanaminium (HATU) as coupling reagents. Acetylation steps were carried out after every coupling of hydrophobic residues.

The p13-derived peptides, corresponding to the 9–22 (RVWTESSFRIPSLR) N-terminal segment of p13, were synthesized on Rink-Amide resin (Novabiochem) and cleaved from the solid support by 2.5 h reaction with trifluoroacetic acid (TFA)/H₂O/thioanisole/1,2-ethanedithiol/phenol (10 mL/0.5 mL/0.5 mL/0.25 mL/750 mg). The p13_[9–22] peptides were purified by reverse phase high performance liquid chromatography (RP-HPLC) on Waters (Milford, MA) prepNova-Pak HR C18 column. Molecular masses of all peptides were confirmed by mass spectroscopy.

Cell extracts

Jurkat T-cells (ca. 50 × 10⁶) were washed in PBS, resuspended in 1 ml of TES buffer (10 mM TES, 0.5 mM EGTA, pH 7.4, 300 mM sucrose), and incubated on ice for 1 h in the presence of 10 μM cytochalasin B, in order to disrupt the cytoskeleton. Cells were homogenized with a Potter-Elvehjem homogenizer and centrifuged at 600g for 10 min at 4°C. Supernatant (S1)

was collected, while pellet was resuspended in 1 ml of TES buffer, homogenized, and centrifuged as above. The collected supernatant (S2) and supernatant S1 were centrifuged at 600g and pellet, constituted by nuclei and cell debris, was discharge. The resulting supernatants were centrifuged at 7,000g for 10 min at 4°C; the supernatants (i.e. cytosolic fractions) were collected, and the mitochondrial pellets were resuspended together in 50 µl of TES buffer. The protein concentration of both mitochondrial and cytosolic fractions was determined by Bradford Assay (Coomassie Plus Kit, Pierce). Western blotting analysis was performed using 50 and 100 µg of the preparations to assess the degree of the extraction.

Phosphorylation assay

p13_[9-22] peptides at the final concentration of 300 µM, were incubated with 21 mU of purified PKC (Calbiochem) in a 30-µl volume containing 50 mM Tris/HCl, pH 7.5, 10 mM MgCl₂, 0.6 mM CaCl₂, 0.1 mg/ml phosphatidylserine (Sigma), and 20 µM [γ -³³P]ATP (specific radioactivity 2,000 cpm/pmol). The reaction mixture was incubated for 30 min at 37°C and stopped by ice cooling and absorption on phosphocellulose p81 paper. Papers were washed three times with 75 mM phosphoric acid, dried, and counted in a scintillation counter.

Reaction conditions for peptide phosphorylation in the presence of Jurkat T-cell lysates as a source of kinases were as follows: p13_[9-22] peptides (500 µM), either wild-type or S15A, were incubated with 1 µg of Jurkat T-cell lysate (either mitochondrial or cytoplasmic fractions) in a 30-µl volume containing 50 mM Tris/HCl, pH 7.5, 10 mM MgCl₂, 0.6 mM CaCl₂, 0.1 mg/ml phosphatidylserine (Sigma), phosphatase inhibitor cocktail 1 and 2 (Sigma), and 50 µM [γ -³³P]ATP (specific radioactivity 2,000 cpm/pmol). The reaction mixture was incubated for 5 min at 37°C and stopped and counted as described above.

Reaction conditions for synthetic full-length p13 phosphorylation were identical to those used for peptides phosphorylation except for the replacement of the peptides with full length p13. The final concentration of the synthetic protein was 3.2 µM. The reaction was incubated for 10 min at 37°C and stopped by addition of 5 x Laemmli loading buffer, followed by SDS-PAGE (13,5% Bis-Tris Gel, MES-SDS running buffer added with 5 mM sodium bisulfite). Proteins were transferred to polyvinylidene fluoride (PVDF) membrane (Amersham Biosciences) and analyzed by immunoblotting and autoradiography (PerkinElmer's Cyclone Plus Storage Phosphor System).

Results

The heterogeneous effect observed in $\Delta\psi$ after treatment with p13 led us to hypothesize the existence of a regulatory mechanism of p13 function. One of the most common and useful mechanisms regulating protein function is, as already mentioned, protein phosphorylation.

A		C			
		Kinase-Specific sites (NetPhosK)			
Position	Context	Position	Context	Kinase	Score
MLIISPLPRV	WTESSFRIPS (1-20)	T-12	PRVWTESSF	PKG	0.51
LRVWRLCARR	LVPHLWGTMF (21-40)	S-14	VWTESSFRIP	PKC	0.69
GPPTSSRPTG	HLSRASDHLG (41-60)	S-15	WTESSFRIP	PKC	0.58
PHRWTRYQLS	STVPYPSTPL (61-80)	S-20	FRIPSLRVW	PKA	0.66
LPHPENL	(81-87)	T-38	HLWGTMFGP	PKC	0.63
		T-38	HLWGTMFGP	cdc2	0.56
		T-44	FGPPTSSRP	PKC	0.59
		S-46	PPTSSRPTG	cdc2	0.54
		S-56	LSRASDHLG	PKA	0.64
		T-65	PHRWTRYQL	PKA	0.64
		S-70	RYQLSSTVP	cdc2	0.57
		S-71	YQLSSTVPY	PKC	0.76
		S-71	YQLSSTVPY	cdc2	0.51
		T-72	QLSSTVPYP	PKC	0.71
		T-72	QLSSTVPYP	cdc2	0.56
		T-78	PYPSTPLL	p38MAPK	0.54
		T-78	PYPSTPLL	GSK3	0.51
		T-78	PYPSTPLL	cdk5	0.64

B	
PKC sites (PROSITE)	
Position	[ST]X[RK]
S-15	SFR
S-20	SLR
S-45	SSR

Figure 6. p13 amino acidic sequence and phosphorylation sites prediction. (A) p13 aminoacidic sequence; MTS is underlined; (B) Prediction of PKC phosphorylation sites by PROSITE, according to the consensus sequence S/T-X-R/K; (C) Prediction of kinase-specific phosphorylation sites by NetPhosK.

Therefore, we started our investigation by analysing the p13 amino acid sequence (Fig. 6A) with two freeware algorithms devised to predict potential phosphorylation sites. Firstly, the p13 sequence was analyzed by PROSITE server (www.expasy.ch), which identifies hypothetical phosphorylation sites. As shown in Fig. 6B, serines 15, 20, and 45 of p13 are predicted to be putative PKC target sites, according to the canonical PKC consensus sequence S/T-X-R/K, where S or T is the phosphorylation site, followed by a C-terminally basic residue at position n+2 (i.e. R or K). Then, p13 sequence was also analyzed by NetPhosK (www.cbs.dtu.dk/services/NetPhosK), which attributes a kinase-specific score to a given putative phosphorylation site. The score ranges from 0 to 1 accordingly to the specificity of the target site for the hypothetical kinase. NetPhosK have identified a series of kinase-specific sites within the p13 amino acid sequence, as listed in the Fig. 6C, and many of them are predicted to be PKC target sites (S14, S15, T38, T44, S71, and T72).

In accordance with the comparative analysis of the results obtained by the two different programs, we decided to focus our studies on S15 because it was identified by both predictors with a quite good score and because of its location in the proximity of the functional α -helical

domain (residues 21–30) determined previously [D'Agostino *et al.*, 2002], suggesting that S15 might be involved in the modulation of the protein function or localization. Thus, we synthesized two peptides, namely p13_[9–22] in the wild type (p13wt) and mutated form (p13S15A), this latter with S15 replaced by alanine as negative control. These peptides are suitable for phosphorylation assays with phosphocellulose papers (as described in Materials and Methods), and harbour three further possible phosphoacceptor sites (T12, S14, and S20).

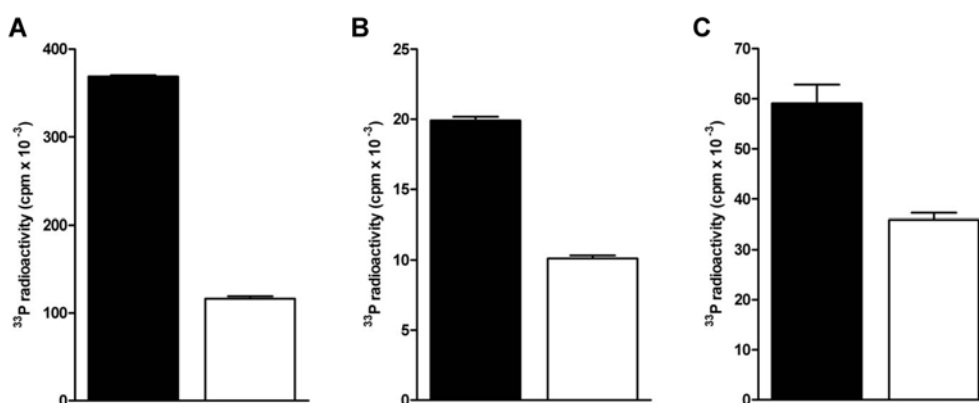


Figure 7. Phosphorylation of p13 9–22 peptides by (A) purified PKC, (B) mitochondrial, and (C) cytoplasmic fractions of Jurkat T-cells. Black bars: wild-type peptide; white bars: S15A mutant peptide.

Therefore, to assess whether S15 is PKC-specific target site, we assayed p13wt and p13S15A for their ability to undergo phosphorylation by purified PKC. As shown in Fig. 7A, wild-type peptide is readily phosphorylated by purified PKC as compared to its negative control S15A and to a specific PKC substrate, namely histone III (data not shown). Of note, the substitution of S15 with alanine causes a dramatic drop (about 70%) in the phosphorylation rate as compared to the wild-type peptide, consistent with the view that S15 is indeed the main target of PKC. Then, we also examined the phosphorylation state of the 9–22 peptides by using Jurkat T-cell lysates (both mitochondrial and cytoplasmic) as a source of kinases in order to investigate whether a cellular PKC (or eventually other cellular kinases) might be involved in S15 phosphorylation. Jurkat T-cells were chosen as a model system because *in vivo* HTLV-1 infection preferentially targets CD4⁺ T-lymphocytes. Phosphorylation of p13 peptides by cell lysates is shown in Fig. 7(B–C). As in the case of purified PKC, the wild-type peptide is markedly phosphorylated by both the extracts, as compared to the S15A mutant. Notably, the phosphate incorporation of wild-type due to the mitochondrial fraction (Figure 7B) is twice as high as that obtained with S15A peptide. A similar situation is observed by incubating the peptides with the cytoplasmic fraction (Figure 7C). Interestingly, in the case of Jurkat T-cell

extracts pretreated with a specific PKC inhibitor, chelerythrine, the phosphorylation rate of the wild-type peptide is equal of that obtained with S15A mutant (not shown). Residual phosphorylation of the S15A peptide, using both fractions, might be due to the phosphorylation of the other three possible phosphoacceptor sites within the 9–22 peptide (i.e. T12, S14, and S20). Nevertheless, the significant drop in the phosphorylation rate promoted by S15 substitution (approximately 50% and 40% with mitochondrial and cytoplasmic extracts, respectively) is consistent with the conclusion that the main phosphorylation site within the 9–22 peptide is S15.

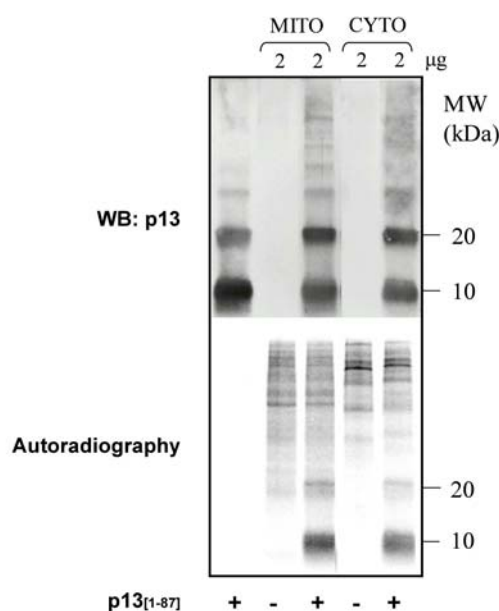


Figure 8. Phosphorylation of synthetic full-length p13 by mitochondrial and cytoplasmic lysates from Jurkat T-cells. Full-length p13 was phosphorylated by 10 min incubation with either mitochondrial or cytoplasmic fraction from Jurkat T-cells and subjected to western immunoblotting analysis with a specific antibody raised against synthetic p13. The autoradiography of the blot shows that the phosphorylation pattern correspond to mono- and dimeric form of p13.

We therefore inferred that a similar situation might also apply to the full length protein, and to address this issue we performed an *in vitro* phosphorylation assay by incubating synthetic full-length p13 in the presence of Jurkat T-cell mitochondrial and cytoplasmic lysates. In Fig. 8, phosphate incorporation is shown to occur in the correspondence of a molecular weight of 10 and 20 kD after incubation of full-length p13 with Jurkat T-cells cellular lysates, confirming the experimental observation (also shown in the western blotting with antibody against full-length p13 displayed in Fig. 8, upper panel) that p13 migrates on SDS-PAGE in two forms,

corresponding to a mono- and dimeric form. On the other hand, 2D-PAGE experiments, whose protocol includes urea denaturation, show only one band at 10 kD (not shown).

Discussion

This work has been done in collaboration with Vincenzo Ciminale and Roberta Biasiotto (IOV, Padua) aimed to disclose the regulation mechanisms of HTLV-1 and in particular of its accessory p13 protein. Data, not shown in this thesis, obtained by Biasiotto and Ciminale show that in HeLa-Tat transfected cells expressing for p13 either wild-type or its phosphoablative mutant, S15A, or the phosphomimetic form, S15D, cellular localization of p13 is different. The S15D phosphomimetic mutation, in fact, increase the mitochondrial targeting of p13, as compared to the wild-type and the S15A, but this effect is associated with an extra-mitochondrial localization both in the cytoplasm and in the nucleus, probably due to the dramatic disruption of the mitochondrial network induced predominantly by the S15D mutant. Furthermore, the phosphomimetic mutation significantly potentiates p13 effect on mitochondrial $\Delta\psi$ in living cells, inducing a marked depolarization, higher than that obtained with wild-type or S15A, even at low level of protein expression, and this depolarization occurs in a expression-dependent manner. Interestingly, at high level of expression, depolarization induced by the S15D mutant is comparable to that of wild-type, while the phosphoablative S15A form, in particular at high level, seems to inactivate p13 function.

These data confirm that p13 function might be regulated by phosphorylation at S15 and that PKC is a good candidate as p13-serine 15 specific kinase.

CONCLUSIONS

The aim of this thesis has been to gain information about structural features underlying substrate specificity of different isoforms of protein kinase CK1. As mentioned in the introduction, this issue is still a matter of debate and investigation. Thus, it is difficult to predict residues phosphorylated by CK1 in its potential substrates and evaluate the actual contribution of CK1 to available phosphoproteome data bases.

Because members of the CK1 family have been implicated in a variety of biological functions and deregulation of CK1 has been described in several diseases, the interest on this (small) independent family of Ser/Thr protein kinases has been growing in the last decades.

Our attention has been focused on three different CK1 isoforms, CK1 α , γ_1 , and δ , which are representative of the whole CK1 family. Therefore, we have cloned and expressed all these proteins in *E. coli* and purified them to homogeneity in order to obtain pure and active kinases.

The CK1 isoforms were tested for their ability to phosphorylate substrates involved in two different crucial cellular pathways: (i) recombinant p53 (residues 1–363) and a set of synthetic peptides corresponding, with suitable substitutions, to its 1–28 N-terminal segment; (ii) a series of synthetic peptides reproducing the repeat 3 (R3) region of adenomatous polyposis coli (APC) protein. Furthermore, in collaboration with Giorgio Cozza (Padua) I have been involved in a project aimed to the identification of new potent and selective inhibitors of protein kinase CK1.

Our study on the identification of possible CK1 isoform-specific phosphorylation site(s) on p53 protein suggests that indeed S20 is readily phosphorylated by the δ and ϵ and, to a lesser extent, by the α isoforms of CK1 in unprimed p53, either full length or its N-terminal peptide. S20 is in fact the only seryl residue whose replacement with alanine in the derived peptide causes a >80% drop in phosphorylation rate and whose phosphorylation in full size p53 occurs with a K_m in the sub-micromolar range, comparable to that displayed by p53 as such. Unlike the δ and α isoforms

CONCLUSIONS

of CK1, CK1 γ_1 proved unable to catalyze any appreciable phosphorylation of p53 as well as of its unprimed peptide. In contrast phosphorylation of T18 primed by previous phosphorylation of S15, is readily performed by all the three isoforms of CK1, albeit with variable efficiencies.

Phosphorylation of S20 in the p53 peptide clearly relies on the minimum consensus generated by E17, since the substitution of this residue with alanine has a detrimental effect comparable to that of substituting S20 itself. Interestingly, although a similar consensus is present upstream of S6, this residue does not appear to be affected by CK1, either in the peptide or in full size p53. Incidentally, this sheds doubt on the notion that phospho-S6 is required to prime S9 phosphorylation by CK1: it is quite clear from our experiments with recombinant p53 that S9 is robustly phosphorylated by CK1 δ in the absence of any appreciable phosphorylation of S6. Additionally, data with phosphopeptides show that the priming efficacy of phospho-S6 on S9 phosphorylation is not as pronounced as that of phospho-S15 on T18.

High affinity targeting of full size p53 critically relies on remote docking site(s) that lack in the peptide. This is demonstrated by sharply different kinetic constants calculated for CK1 δ and α phosphorylation of either the peptide or the protein at the same residues. Although the phosphorylation rate with the peptide is higher, its affinity is >3-orders of magnitude lower, consistent with the view that physiological targeting of p53 by CK1 requires high affinity interactions between a remote complementary domain, which is lost passing from full size p53 to its N-terminal segment. A similar situation has been described in the case of p53 S20 phosphorylation after HHV-6B viral infection, whose occurrence depends on the interaction of CK1 with Box IV and Box V domains of p53. These elements are also likely responsible for high affinity phosphorylation of full size p53 as compared to its N-terminal peptide. Our additional observation that such a phosphorylation is catalyzed by the α and δ/ϵ , but not by the γ isoforms of CK1 would map the complementary docking site to a region which is not conserved in the γ isoforms. From the alignment of the CK1 isoforms it appears that such a putative docking site might correspond to the K²²¹RQK²²⁴ sequence sitting in the loop next to the G-helix in CK1 δ . This basic sequence is conserved both in α (KKQK) and in ϵ (KRQK) isoforms but is deeply altered in all the γ isoforms where the first lysine is replaced by leucine and the glutamine by glutamic acid. The role of this motif as a remote docking site responsible for high affinity binding of p53 is also consistent with computer aided protein-protein docking strategy highlighting the special relevance of K221 which in the γ isoforms is replaced by a leucine. The proof of concept that such a model reflects a real situation has been provided by mutational analysis showing that replacement of K221 with leucine drastically impairs phosphorylation efficiency. Interestingly, as in the case of β -catenin S45 phosphorylation by CK1,

phosphorylation of p53 S20 appears to depend not only on remote but also on local recognizing elements since replacement of E17 with alanine is equally detrimental in the N-terminal peptide and in full-size p53 despite the ability of this latter to interact with the remote docking site present in both CK1 δ and CK1 α .

Association of β -catenin with the adenomatous polyposis coli (APC) protein, a crucial event in the Wnt pathway, requires the multiple phosphorylation of six serines (1501, 1503, 1504, 1505, 1507 and 1510) within repeat 3 (R3) region of APC. Such a phosphorylation is believed to occur by the concerted action of two protein kinases, CK1 and GSK3, but its mechanistic aspects were still a matter of debate. We used differently phosphorylated synthetic peptides derived from APC R3 region and automated Edman degradation in order to identify the residues phosphorylated by individual kinases. Our results show that the process is initiated by CK1, capable of phosphorylating S1510 and S1505, both specified by non-canonical consensus sequence. Phosphorylation of S1505 primes the subsequent phosphorylation of S1501 by GSK3. In turn phospho-S1501 triggers the hierarchical phosphorylation of S1504 and S1507 by CK1. Once phosphorylated, S1507 primes the phosphorylation of both S1510 and S1503 by CK1 and GSK3, respectively, thus completing all the 6 phosphorylation steps. Our data also show that, among CK1 isoforms, CK1 δ is more efficient than CK1 α and CK1 γ as APC R3 phosphorylating agent, and rule out the intervention of CK2 despite the presence of a potential CK2 phosphoacceptor site, S¹⁵¹⁰LDE, in the R3 repeat. S1510 is completely unaffected by CK2, while it is readily phosphorylated even in the unprimed peptide by CK1 δ but not by CK1 γ . This discloses a novel motif significantly different from the non-canonical sequences phosphorylated by CK1 in other proteins, which appears to be specifically recognized by the δ isoform of CK1.

The last chapter of this thesis deals with a study aimed at characterizing p13 protein from Human T-cell leukemia virus type 1 (HTLV-1), the etiological agent of an aggressive leukemia/lymphoma in humans. Our results, obtained with synthetic full-length p13 on isolated, energized mitochondria, demonstrate that p13 triggers an inward K⁺ current that leads to mitochondrial swelling and membrane depolarization, with both a matching increase in respiratory chain activity, and augments production of reactive oxygen species (ROS). These effects require an intact α -helical domain and strictly depend on the presence of K⁺ in the assay medium. The downstream consequences of p13-induced mitochondrial K⁺ permeability are likely to have an important influence on the redox state and turnover of HTLV-1-infected cells.

CONCLUSIONS

This work has also led to as yet unpublished data on possible role of phosphorylation in the regulation of p13 function. In particular, we have focused on S15, a putative PKC phosphorylation site located in the proximity of the functional α -helical domain.

REFERENCES

- Adorno, M., Cordenonsi, M., Montagner, M., Dupont, S., Wong, C., Hann, B., Solari, A., Bobisse, S., Rondina, M. B., Guzzardo, V., Parenti, A. R., Rosato, A., Bicciato, S., Balmain, A., Piccolo, S. (2009) A Mutant-p53/Smad complex opposes p63 to empower TGFbeta-induced metastasis, *Cell* 137, 87-98.
- Appella, E., Anderson, C. W. (2001) Post-translational modifications and activation of p53 by genotoxic stresses, *Eur. J. Biochem* 268, 2764-2772.
- Bain, J., McLauchlan, H., Elliott, M., Cohen, P. (2003) The specificities of protein kinase inhibitors: an update, *Biochem. J* 371, 199-204.
- Bain, J., Plater, L., Elliott, M., Shpiro, N., Hastie, C. J., McLauchlan, H., Klevernic, I., Arthur, J. S. C., Alessi, D. R., Cohen, P. (2007) The selectivity of protein kinase inhibitors: a further update, *Biochem. J* 408, 297-315.
- Bairoch, A., Bucher, P., Hofmann, K. (1997) The PROSITE database, its status in 1997, *Nucl. Acids Res.* 25, 217-221.
- Baran, Y., Gunduz, U., Ural, A. U. (2006) Cross-resistance to cytosine arabinoside in human acute myeloid leukemia cells selected for resistance to vincristine, *Exp. Oncol* 28, 163-165.
- Behrend, L., Milne, D., Stöter, M., Deppert, W., Campbell, L., Meek, D., Knippschild, U. (2000) IC261, a specific inhibitor of the protein kinases casein kinase 1-delta and -epsilon, triggers the mitotic checkpoint and induces p53-dependent postmitotic effects, *Oncogene* 19, 5303-5313.
- Berman, H. M., Westbrook, J., Feng, Z., Gilliland, G., Bhat, T. N., Weissig, H., Shindyalov, I. N., Bourne, P. E. (2000) The Protein Data Bank, *Nucleic Acids Res* 28, 235-242.
- Bernardi, P. (1992) Modulation of the mitochondrial cyclosporin A-sensitive permeability transition pore by the proton electrochemical gradient. Evidence that the pore can be opened by membrane depolarization, *Journal of Biological Chemistry* 267, 8834-8839.
- Blom, N., Gammeltoft, S., Brunak, S. (1999) Sequence and structure-based prediction of eukaryotic protein phosphorylation sites, *J. Mol. Biol* 294, 1351-1362.
- Blume-Jensen, P., Hunter, T. (2001) Oncogenic kinase signalling, *Nature* 411, 355-365.
- Bode, A. M., Dong, Z. (2004) Post-translational modification of p53 in tumorigenesis, *Nat. Rev. Cancer* 4, 793-805.
- Boya, P., Pauleau, A., Poncet, D., Gonzalez-Polo, R., Zamzami, N., Kroemer, G. (2004) Viral proteins targeting mitochondria: Controlling cell death, *Biochimica et Biophysica Acta - Bioenergetics* 1659, 178-189.
- Braconi Quintaje, S., Orchard, S. (2008) The annotation of both human and mouse kinomes in UniProtKB/Swiss-Prot: one small step in manual annotation, one giant leap for

REFERENCES

- full comprehension of genomes, *Mol. Cell Proteomics* 7, 1409-1419.
- Braithwaite, A. W., Del Sal, G., Lu, X. (2006) Some p53-binding proteins that can function as arbiters of life and death, *Cell Death Differ* 13, 984-993.
 - Brand, M., Esteves, T. (2005) Physiological functions of the mitochondrial uncoupling proteins UCP2 and UCP3, *Cell Metabolism* 2, 85-93.
 - Brooks, C. L., Gu, W. (2003) Ubiquitination, phosphorylation and acetylation: the molecular basis for p53 regulation, *Curr. Opin. Cell Biol* 15, 164-171.
 - Budini, M., Jacob, G., Jedlicki, A., Pérez, C., Allende, C. C., Allende, J. E. (2009) Autophosphorylation of carboxy-terminal residues inhibits the activity of protein kinase CK1alpha, *J. Cell. Biochem* 106, 399-408.
 - Burzio, V., Antonelli, M., Allende, C. C., Allende, J. E. (2002) Biochemical and cellular characteristics of the four splice variants of protein kinase CK1alpha from zebrafish (*Danio rerio*), *J. Cell. Biochem* 86, 805-814.
 - Bustos, V. H., Marin, O., Meggio, F., Cesaro, L., Allende, C. C., Allende, J. E., Pinna, L. A. (2005) Generation of protein kinase Ck1alpha mutants which discriminate between canonical and non-canonical substrates, *Biochem. J* 391, 417-424.
 - Bustos, V. H., Ferrarese, A., Venerando, A., Marin, O., Allende, J. E., Pinna, L. A. (2006) The first armadillo repeat is involved in the recognition and regulation of beta-catenin phosphorylation by protein kinase CK1, *Proc. Natl. Acad. Sci. U.S.A* 103, 19725-19730.
 - Campbell, D., Morrice, N. (2002) Identification of protein phosphorylation sites by a combination of mass spectrometry and solid phase Edman sequencing, *J Biomol Tech* 13, 119-130.
 - Carpino, L. A., Han, G. Y. (1972) 9-Fluorenylmethoxycarbonyl amino-protecting group, *The Journal of Organic Chemistry* 37, 3404-3409.
 - Cegielska, A., Gietzen, K. F., Rivers, A., Virshup, D. M. (1998) Autoinhibition of casein kinase I epsilon (CKI epsilon) is relieved by protein phosphatases and limited proteolysis, *J. Biol. Chem* 273, 1357-1364.
 - Chance, B., Williams, G. R. (1955) Respiratory enzymes in oxidative phosphorylation. III. The steady state, *J. Biol. Chem* 217, 409-427.
 - Chehab, N. H., Malikzay, A., Stavridi, E. S., Halazonetis, T. D. (1999) Phosphorylation of Ser-20 mediates stabilization of human p53 in response to DNA damage, *Proc. Natl. Acad. Sci. U.S.A* 96, 13777-13782.
 - Cheng, Y., Prusoff, W. H. (1973) Relationship between the inhibition constant (K₁) and the concentration of inhibitor which causes 50 per cent inhibition (I₅₀) of an enzymatic reaction, *Biochem. Pharmacol* 22, 3099-3108.
 - Chijiwa, T., Hagiwara, M., Hidaka, H. (1989) A newly synthesized selective casein kinase I inhibitor, N-(2-aminoethyl)-5-chloroisoquinoline-8-sulfonamide, and affinity purification of casein kinase I from bovine testis, *Journal of Biological Chemistry* 264, 4924-4927.
 - Chipuk, J. E., Green, D. R. (2003) p53's believe it or not: lessons on transcription-independent death, *J. Clin. Immunol* 23, 355-361.
 - Choi, J., Park, S. Y., Costantini, F., Jho, E., Joo, C. (2004) Adenomatous polyposis coli is down-regulated by the ubiquitin-proteasome pathway in a process facilitated by Axin, *J. Biol. Chem* 279, 49188-49198.
 - Ciminale, V., Zotti, L., D'Agostino, D., Ferro, T., Casareto, L., Franchini, G., Bernardi, P., Chieco-Bianchi, L. (1999) Mitochondrial targeting of the p13(II) protein coded by the x-II ORF of human T-cell leukemia/lymphotropic virus type I (HTLV-I), *Oncogene* 18, 4505-4514.
 - Clevers, H. (2006) Wnt/beta-catenin signaling in development and disease, *Cell* 127, 469-480.

-
- Cohen, P. (2000) The regulation of protein function by multisite phosphorylation--a 25 year update, *Trends Biochem. Sci* 25, 596-601.
 - Cohen, P. (2001) The role of protein phosphorylation in human health and disease. The Sir Hans Krebs Medal Lecture, *Eur. J. Biochem* 268, 5001-5010.
 - Cohen, P. (2002) The origins of protein phosphorylation, *Nat Cell Biol* 4, E127-E130.
 - Cordenonsi, M., Montagner, M., Adorno, M., Zacchigna, L., Martello, G., Mamidi, A., Soligo, S., Dupont, S., Piccolo, S. (2007) Integration of TGF-beta and Ras/MAPK signaling through p53 phosphorylation, *Science* 315, 840-843.
 - Costa, A., Garlid, K., West, I., Lincoln, T., Downey, J., Cohen, M., Critz, S. (2005) Protein kinase G transmits the cardioprotective signal from cytosol to mitochondria, *Circulation Research* 97, 329-336.
 - Costantini, P., Petronilli, V., Colonna, R., Bernardi, P. (1995) On the effects of paraquat on isolated mitochondria. Evidence that paraquat causes opening of the cyclosporin A-sensitive permeability transition pore synergistically with nitric oxide, *Toxicology* 99, 77-88.
 - Costantini, P., Chernyak, B., Petronilli, V., Bernardi, P. (1996) Modulation of the mitochondrial permeability transition pore by pyridine nucleotides and dithiol oxidation at two separate sites, *Journal of Biological Chemistry* 271, 6746-6751.
 - Cozza, G., Bonvini, P., Zorzi, E., Poletto, G., Pagano, M., Sarno, S., Donella-Deana, A., Zagotto, G., Rosolen, A., Pinna, L., Meggio, F., Moro, S. (2006) Identification of ellagic acid as potent inhibitor of protein kinase CK2: A successful example of a virtual screening application, *Journal of Medicinal Chemistry* 49, 2363-2366.
 - Cozza, G., Moro, S., Gotte, G. (2008) Elucidation of the ribonuclease A aggregation process mediated by 3D domain swapping: a computational approach reveals possible new multimeric structures, *Biopolymers* 89, 26-39.
 - D'Agostino, D., Ranzato, L., Arrigoni, G., Cavallari, I., Belleudi, F., Torrisi, M., Silic-Benussi, M., Ferro, T., Petronilli, V., Marin, O., Chieco-Bianchi, L., Bernardi, P., Ciminale, V. (2002) Mitochondrial alterations induced by the p13II protein of human T-cell leukemia virus type 1: Critical role of arginine residues, *Journal of Biological Chemistry* 277, 34424-34433.
 - D'Agostino, D., Silic-Benussi, M., Hilaragi, H., Lairmore, M., Ciminale, V. (2005) The human T-cell leukemia virus type 1 p13II protein: Effects on mitochondrial function and cell growth, *Cell Death and Differentiation* 12, 905-915.
 - D'Agostino *, D., Bernardi, P., Chieco-Bianchi, L., Ciminale, V. (2005) Mitochondria as functional targets of proteins coded by human tumor viruses, *Advances in cancer research* 94,87-142.
 - Di Lisa, F., Menabò, R., Canton, M., Barile, M., Bernardi, P. (2001) Opening of the Mitochondrial Permeability Transition Pore Causes Depletion of Mitochondrial and Cytosolic NAD⁺ and Is a Causative Event in the Death of Myocytes in Postischemic Reperfusion of the Heart, *Journal of Biological Chemistry* 276, 2571-2575.
 - Di Lisa, F., Canton, M., Menabò, R., Kaludercic, N., Bernardi, P. (2007) Mitochondria and cardioprotection, *Heart Failure Reviews* 12, 249-260.
 - Donella-Deana, A., Marin, O., Cesaro, L., Gunby, R. H., Ferrarese, A., Coluccia, A. M. L., Tartari, C. J., Mologni, L., Scapozza, L., Gambacorti-Passerini, C., Pinna, L. A. (2005) Unique substrate specificity of anaplastic lymphoma kinase (ALK): development of phosphoacceptor peptides for the assay of ALK activity, *Biochemistry* 44, 8533-8542.
 - Dumaz, N., Milne, D. M., Meek, D. W. (1999) Protein kinase CK1 is a p53-threonine 18 kinase which requires prior phosphorylation of serine 15, *FEBS Lett* 463, 312-316.
 - Eglén, R. M., Reisine, T. (2009) The current status of drug discovery against the human

REFERENCES

- kinome, *Assay Drug Dev Technol* 7, 22-43.
- Emaus, R., Grunwald, R., Lemasters, J. (1986) Rhodamine 123 as a probe of transmembrane potential in isolated rat-liver mitochondria: Spectral and metabolic properties, *Biochimica et Biophysica Acta - Bioenergetics* 850, 436-448.
 - Ferrarese, A., Marin, O., Bustos, V. H., Venerando, A., Antonelli, M., Allende, J. E., Pinna, L. A. (2007) Chemical dissection of the APC Repeat 3 multistep phosphorylation by the concerted action of protein kinases CK1 and GSK3, *Biochemistry* 46, 11902-11910.
 - Fields, G. B., Fields, C. G. (1991) Solvation effects in solid-phase peptide synthesis, *Journal of the American Chemical Society* 113, 4202-4207.
 - Fields, G. B., Noble, R. L. (1990) Solid phase peptide synthesis utilizing 9-fluorenylmethoxycarbonyl amino acids, *Int. J. Pept. Protein Res* 35, 161-214.
 - Flotow, H., Graves, P. R., Wang, A. Q., Fiol, C. J., Roeske, R. W., Roach, P. J. (1990) Phosphate groups as substrate determinants for casein kinase I action, *J. Biol. Chem* 265, 14264-14269.
 - Fontaine, E., Eriksson, O., Ichas, F., Bernardi, P. (1998) Regulation of the permeability transition pore in skeletal muscle mitochondria modulation by electron flow through the respiratory chain complex I, *Journal of Biological Chemistry* 273, 12662-12668.
 - Fu, Z., Chakraborti, T., Morse, S., Bennett, G. S., Shaw, G. (2001) Four casein kinase I isoforms are differentially partitioned between nucleus and cytoplasm, *Exp. Cell Res* 269, 275-286.
 - Gao, Z., Seeling, J. M., Hill, V., Yochum, A., e Virshup, D. M. (2002) Casein kinase I phosphorylates and destabilizes the beta-catenin degradation complex, *Proc. Natl. Acad. Sci. U.S.A* 99, 1182-1187.
 - Giamas, G., Stebbing, J., Vorgias, C. E., Knippschild, U. (2007) Protein kinases as targets for cancer treatment, *Pharmacogenomics* 8, 1005-1016.
 - Gietzen, K. F., Virshup, D. M. (1999) Identification of inhibitory autophosphorylation sites in casein kinase I epsilon, *J. Biol. Chem* 274, 32063-32070.
 - Gonzalez, M., Carrasco, L. (2003) Viroporins, *FEBS Letters* 552, 28-34.
 - Graves, P. R., Roach, P. J. (1995) Role of COOH-terminal phosphorylation in the regulation of casein kinase I delta, *J. Biol. Chem* 270, 21689-21694.
 - Gregorieff, A., Clevers, H. (2005) Wnt signaling in the intestinal epithelium: from endoderm to cancer, *Genes Dev* 19, 877-890.
 - Gross, S. D., Anderson, R. A. (1998) Casein kinase I: spatial organization and positioning of a multifunctional protein kinase family, *Cell. Signal* 10, 699-711.
 - Ha, N., Tonzuka, T., Stamos, J. L., Choi, H., Weis, W. I. (2004) Mechanism of phosphorylation-dependent binding of APC to beta-catenin and its role in beta-catenin degradation, *Mol. Cell* 15, 511-521.
 - Hackenbrock, C. (1966) Ultrastructural bases for metabolically linked mechanical activity in mitochondria. I. Reversible ultrastructural changes with change in metabolic steady state in isolated liver mitochondria., *Journal of Cell Biology* 30, 269-297.
 - Hämmerlein, A., Weiske, J., Huber, O. (2005) A second protein kinase CK1-mediated step negatively regulates Wnt signalling by disrupting the lymphocyte enhancer factor-1/beta-catenin complex, *Cell. Mol. Life Sci* 62, 606-618.
 - Hanks, S. K., Hunter, T. (1995) Protein kinases 6. The eukaryotic protein kinase superfamily: kinase (catalytic) domain structure and classification, *FASEB J* 9, 576-596.
 - Harris, S. L., Levine, A. J. (2005) The p53 pathway: positive and negative feedback loops, *Oncogene* 24, 2899-2908.
 - Hasegawa, H., Sawa, H., Lewis, M., Orba, Y., Sheehy, N., Yamamoto, Y., Ichinohe, T., Tsunetsugu-Yokota, Y., Katano, H., Takahashi, H., Matsuda, J., Sata, T., Kurata, T.,

-
- Nagashima, K., Hall, W. (2006) Thymus-derived leukemia-lymphoma in mice transgenic for the Tax gene of human T-lymphotropic virus type I, *Nature Medicine* 12, 466-472.
- Higashimoto, Y., Saito, S., Tong, X. H., Hong, A., Sakaguchi, K., Appella, E., Anderson, C. W. (2000) Human p53 is phosphorylated on serines 6 and 9 in response to DNA damage-inducing agents, *J. Biol. Chem* 275, 23199-23203.
 - Hiraragi, H., Michael, B., Nair, A., Silic-Benussi, M., Ciminale, V., Lairmore, M. (2005) Human T-lymphotropic virus type 1 mitochondrion-localizing protein p13 II sensitizes Jurkat T cells to Ras-mediated apoptosis, *Journal of Virology* 79, 9449-9457.
 - Hiraragi, H., Kim, S., Phipps, A., Silic-Benussi, M., Ciminale, V., Ratner, L., Green, P., Lairmore, M. (2006) Human T-lymphotropic virus type 1 mitochondrion-localizing protein p13 II is required for viral infectivity in vivo, *Journal of Virology* 80, 3469-3476.
 - Holmberg, C. I., Tran, S. E. F., Eriksson, J. E., Sistonen, L. (2002) Multisite phosphorylation provides sophisticated regulation of transcription factors, *Trends Biochem. Sci* 27, 619-627.
 - Hubbard, S. R., Wei, L., Ellis, L., Hendrickson, W. A. (1994) Crystal structure of the tyrosine kinase domain of the human insulin receptor, *Nature* 372, 746-754.
 - Hunter, T. (2009) Tyrosine phosphorylation: thirty years and counting, *Curr. Opin. Cell Biol* 21, 140-146.
 - Johnson, L. N. (2009) The regulation of protein phosphorylation, *Biochem. Soc. Trans* 37, 627-641.
 - Johnson *, L. N. (2009) Protein kinase inhibitors: contributions from structure to clinical compounds, *Q. Rev. Biophys* 42, 1-40.
 - Johnson, L. N., Lewis, R. J. (2001) Structural basis for control by phosphorylation, *Chem. Rev* 101, 2209-2242.
 - Jones, G., Willett, P., Glen, R., Leach, A., Taylor, R. (1997) Development and validation of a genetic algorithm for flexible docking, *Journal of Molecular Biology* 267, 727-748.
 - Kikuchi, A., Kishida, S., Yamamoto, H. (2006) Regulation of Wnt signaling by protein-protein interaction and post-translational modifications, *Exp. Mol. Med* 38, 1-10.
 - Kimmerlin, T., Seebach, D. (2005) '100 years of peptide synthesis': ligation methods for peptide and protein synthesis with applications to beta-peptide assemblies, *J. Pept. Res* 65, 229-260.
 - King, D. S., Fields, C. G., Fields, G. B. (1990) A cleavage method which minimizes side reactions following Fmoc solid phase peptide synthesis, *Int. J. Pept. Protein Res* 36, 255-266.
 - Knippschild, U., Milne, D. M., Campbell, L. E., DeMaggio, A. J., Christenson, E., Hoekstra, M. F., Meek, D. W. (1997) p53 is phosphorylated in vitro and in vivo by the delta and epsilon isoforms of casein kinase 1 and enhances the level of casein kinase 1 delta in response to topoisomerase-directed drugs, *Oncogene* 15, 1727-1736.
 - Knippschild, U., Gocht, A., Wolff, S., Huber, N., Löhler, J., Stöter, M. (2005) The casein kinase 1 family: participation in multiple cellular processes in eukaryotes, *Cell. Signal* 17, 675-689.
 - Knippschild *, U., Wolff, S., Giamas, G., Brockschmidt, C., Wittau, M., Würfl, P. U., Eismann, T., Stöter, M. (2005) The role of the casein kinase 1 (CK1) family in different signaling pathways linked to cancer development, *Onkologie* 28, 508-514.
 - Krauss, G. (2003) Biochemistry of signal transduction and regulation. Wiley-VCH.
 - Lacroix, M., Toillon, R., Leclercq, G. (2006) p53 and breast cancer, an update, *Endocr. Relat. Cancer* 13, 293-325.
 - Lairmore, M. D., Franchini, G. (2007) Human T-cell leukemia virus types 1 and 2. In: D.M.K.a.P.M. Howley, Editor, *Fields Virology*, Fifth Edition vol. 2, Lippincott Williams

REFERENCES

- and Wilkins, Philadelphia, 2071–2106.
- Laptenko, O., Prives, C. (2006) Transcriptional regulation by p53: one protein, many possibilities, *Cell Death Differ* 13, 951-961.
 - Lavin, M. F., Gueven, N. (2006) The complexity of p53 stabilization and activation, *Cell Death Differ* 13, 941-950.
 - Lemeer, S., Heck, A. J. R. (2009) The phosphoproteomics data explosion, *Curr Opin Chem Biol* 13, 414-420.
 - Leung, A., Halestrap, A. (2008) Recent progress in elucidating the molecular mechanism of the mitochondrial permeability transition pore, *Biochimica et Biophysica Acta - Bioenergetics* 1777, 946-952.
 - Levine, A. J., Hu, W., Feng, Z. (2006) The P53 pathway: what questions remain to be explored?, *Cell Death Differ* 13, 1027-1036.
 - Li, M., Luo, J., Brooks, C. L., Gu, W. (2002) Acetylation of p53 inhibits its ubiquitination by Mdm2, *J. Biol. Chem* 277, 50607-50611.
 - Liao, J. J. (2007) Molecular recognition of protein kinase binding pockets for design of potent and selective kinase inhibitors, *J. Med. Chem* 50, 409-424.
 - Liu, C., Li, Y., Semenov, M., Han, C., Baeg, G. H., Tan, Y., Zhang, Z., Lin, X., He, X. (2002) Control of beta-catenin phosphorylation/degradation by a dual-kinase mechanism, *Cell* 108, 837-847.
 - Liu, J., Xing, Y., Hinds, T. R., Zheng, J., Xu, W. (2006) The third 20 amino acid repeat is the tightest binding site of APC for beta-catenin, *J. Mol. Biol* 360, 133-144.
 - Longenecker, K. L., Roach, P. J., Hurley, T. D. (1996) Three-dimensional structure of mammalian casein kinase I: molecular basis for phosphate recognition, *J. Mol. Biol* 257, 618-631.
 - MacLaine, N. J., Oster, B., Bundgaard, B., Fraser, J. A., Buckner, C., Lazo, P. A., Meek, D. W., Höllsberg, P., Hupp, T. R. (2008) A central role for CK1 in catalyzing phosphorylation of the p53 transactivation domain at serine 20 after HHV-6B viral infection, *J. Biol. Chem* 283, 28563-28573.
 - Mann, M., Ong, S. E., Grønborg, M., Steen, H., Jensen, O. N., Pandey, A. (2002) Analysis of protein phosphorylation using mass spectrometry: deciphering the phosphoproteome, *Trends Biotechnol* 20, 261-268.
 - Manning, G., Whyte, D. B., Martinez, R., Hunter, T., Sudarsanam, S. (2002) The protein kinase complement of the human genome, *Science* 298, 1912-1934.
 - Manning *, G., Plowman, G. D., Hunter, T., Sudarsanam, S. (2002) Evolution of protein kinase signaling from yeast to man, *Trends Biochem. Sci* 27, 514-520.
 - Marin, O., Meggio, F., Pinna, L. A. (1994) Design and synthesis of two new peptide substrates for the specific and sensitive monitoring of casein kinases-1 and -2, *Biochem. Biophys. Res. Commun* 198, 898-905.
 - Marin, O., Burzio, V., Boschetti, M., Meggio, F., Allende, C. C., Allende, J. E., Pinna, L. A. (2002) Structural features underlying the multisite phosphorylation of the A domain of the NF-AT4 transcription factor by protein kinase CK1, *Biochemistry* 41, 618-627.
 - Marin, O., Bustos, V. H., Cesaro, L., Meggio, F., Pagano, M. A., Antonelli, M., Allende, C. C., Pinna, L. A., Allende, J. E. (2003) A noncanonical sequence phosphorylated by casein kinase 1 in beta-catenin may play a role in casein kinase 1 targeting of important signaling proteins, *Proc. Natl. Acad. Sci. U.S.A* 100, 10193-10200.
 - Marsden, B. D., Knapp, S. (2008) Doing more than just the structure-structural genomics in kinase drug discovery, *Curr Opin Chem Biol* 12, 40-45.
 - Mashhoon, N., DeMaggio, A., Tereshko, V., Bergmeier, S., Egli, M., Hoekstra, M., Kuret, J. (2000) Crystal structure of a conformation-selective casein kinase-1 inhibitor, *Journal of*

-
- Biological Chemistry* 275, 20052-20060.
- Matsubayashi, H., Sese, S., Lee, J., Shirakawa, T., Iwatsubo, T., Tomita, T., Yanagawa, S. (2004) Biochemical characterization of the Drosophila wingless signaling pathway based on RNA interference, *Mol. Cell. Biol* 24, 2012-2024.
 - Matsumoto, M., Furihata, M., Ohtsuki, Y. (2006) Posttranslational phosphorylation of mutant p53 protein in tumor development, *Med Mol Morphol* 39, 79-87.
 - McKay, R. M., Peters, J. M., Graff, J. M. (2001) The casein kinase I family in Wnt signaling, *Dev. Biol* 235, 388-396.
 - Meek, D. W. (1994) Post-translational modification of p53, *Semin. Cancer Biol* 5, 203-210.
 - Meek, D. W. (2009) Tumour suppression by p53: a role for the DNA damage response?, *Nat. Rev. Cancer* 9, 714-723.
 - Meggio, F., Deana, A. D., Pinna, L. A. (1981) Endogenous phosphate acceptor proteins for rat liver cytosolic casein kinases, *J. Biol. Chem* 256, 11958-11961.
 - Meggio, F., Pagano, M., Moro, S., Zagotto, G., Ruzzene, M., Sarno, S., Cozza, G., Bain, J., Elliott, M., Deana, A., Brunati, A., Pinna, L. (2004) Inhibition of protein kinase CK2 by condensed polyphenolic derivatives. An in vitro and in vivo study, *Biochemistry* 43, 12931-12936.
 - Merrifield, R. B. (1963) Solid Phase Peptide Synthesis. I. The Synthesis of a Tetrapeptide, *Journal of the American Chemical Society* 85, 2149-2154.
 - MOE Molecular operating environment (MOE 2008.10), C.C.G., Inc., 1255 University St., Suite 1600, Montreal, Quebec, Canada H3B 3X3
 - Moon, R. T., Bowerman, B., Boutros, M., Perrimon, N. (2002) The promise and perils of Wnt signaling through beta-catenin, *Science* 296, 1644-1646.
 - Moro, S., Varano, F., Cozza, G., Pagano, M., Zagotto, G., Chilin, A., Guiotto, A., Catarzi, D., Calotta, V., Pinna, L., Meggio, F. (2006) Pyrazoloquinazoline tricyclic system as novel scaffold to design new kinase CK2 inhibitors, *Letters in Drug Design and Discovery* 3, 281-284.
 - Muto, A., Hori, M., Sasaki, Y., Saitoh, A., Yasuda, I., Maekawa, T., Uchida, T., Asakura, K., Nakazato, T., Kaneda, T., Kizaki, M., Ikeda, Y., Yoshida, T. (2007) Emodin has a cytotoxic activity against human multiple myeloma as a Janus-activated kinase 2 inhibitor, *Molecular Cancer Therapeutics* 6, 987-994.
 - Nicot, C., Harrod, R., Ciminale, V., Franchini, G. (2005) Human T-cell leukemia/lymphoma virus type 1 nonstructural genes and their functions, *Oncogene* 24, 6026-6034.
 - Nowikovsky, K., Schweyen, R. J., Bernardi, P. (2009) Pathophysiology of mitochondrial volume homeostasis: Potassium transport and permeability transition, *Biochimica et Biophysica Acta (BBA) - Bioenergetics* 1787, 345-350.
 - Okamura, H., Garcia-Rodriguez, C., Martinson, H., Qin, J., Virshup, D. M., Rao, A. (2004) A conserved docking motif for CK1 binding controls the nuclear localization of NFAT1, *Mol. Cell. Biol* 24, 4184-4195.
 - Oleinik, N. V., Krupenko, N. I., Krupenko, S. A. (2007) Cooperation between JNK1 and JNK2 in activation of p53 apoptotic pathway, *Oncogene* 26, 7222-7230.
 - Olsen, J. V., Blagoev, B., Gnad, F., Macek, B., Kumar, C., Mortensen, P., Mann, M. (2006) Global, in vivo, and site-specific phosphorylation dynamics in signaling networks, *Cell* 127, 635-648.
 - Olsson, A., Manzl, C., Strasser, A., Villunger, A. (2007) How important are post-translational modifications in p53 for selectivity in target-gene transcription and tumour suppression?, *Cell Death Differ* 14, 1561-1575.

REFERENCES

- Patwardhan, P., Miller, W. T. (2007) Processive phosphorylation: mechanism and biological importance, *Cell. Signal* 19, 2218-2226.
- Perich, J. W., Meggio, F., Reynolds, E. C., Marin, O., Pinna, L. A. (1992) Role of phosphorylated aminoacyl residues in generating atypical consensus sequences which are recognized by casein kinase-2 but not by casein kinase-1, *Biochemistry* 31, 5893-5897.
- Peters, J. M., McKay, R. M., McKay, J. P., Graff, J. M. (1999) Casein kinase I transduces Wnt signals, *Nature* 401, 345-350.
- Petronilli, V., Cola, C., Massari, S., Colonna, R., Bernardi, P. (1993) Physiological effectors modify voltage sensing by the cyclosporin A- sensitive permeability transition pore of mitochondria, *Journal of Biological Chemistry* 268, 21939-21945.
- Petronilli *, V., Cola, C., Bernardi, P. (1993) Modulation of the mitochondrial cyclosporin A-sensitive permeability transition pore. II. The minimal requirements for pore induction underscore a key role for transmembrane electrical potential, matrix pH, and matrix Ca²⁺, *Journal of Biological Chemistry* 268, 1011-1016.
- Petronilli, V., Costantini, P., Scorrano, L., Colonna, R., Passamonti, S., Bernardi, P. (1994) The voltage sensor of the mitochondrial permeability transition pore is tuned by the oxidation-reduction state of vicinal thiols. Increase of the gating potential by oxidants and its reversal by reducing agents, *Journal of Biological Chemistry* 269, 16638-16642.
- Pinna, L. A., Ruzzene, M. (1996) How do protein kinases recognize their substrates?, *Biochim. Biophys. Acta* 1314, 191-225.
- Polakis, P. (2002) Casein kinase 1: a Wnt'er of disconnect, *Curr. Biol* 12, R499-R501.
- Poletto, G., Vilardell, J., Marin, O., Pagano, M. A., Cozza, G., Sarno, S., Falqués, A., Itarte, E., Pinna, L. A., Meggio, F. (2008) The regulatory beta subunit of protein kinase CK2 contributes to the recognition of the substrate consensus sequence. A study with an eIF2 beta-derived peptide, *Biochemistry* 47, 8317-8325.
- Price, M. A. (2006) CKI, there's more than one: casein kinase I family members in Wnt and Hedgehog signaling, *Genes Dev* 20, 399-410.
- Prives, C. (1998) Signaling to p53: breaking the MDM2-p53 circuit, *Cell* 95, 5-8.
- Pulgar, V., Marin, O., Meggio, F., Allende, C. C., Allende, J. E., Pinna, L. A. (1999) Optimal sequences for non-phosphate-directed phosphorylation by protein kinase CK1 (casein kinase-1)--a re-evaluation, *Eur. J. Biochem* 260, 520-526.
- Quillet-Mary, A., Jaffrézou, J., Mansat, V., Bordier, C., Naval, J., Laurent, G. (1997) Implication of mitochondrial hydrogen peroxide generation in ceramide- induced apoptosis, *Journal of Biological Chemistry* 272, 21388-21395.
- Rascio, N., Mariani, P., Tommasini, E., Bodner, M., Larcher, W. (1991) Photosynthetic strategies in leaves and stems of *Egeria densa*, *Planta* 185, 297-303.
- Rasola, A., Bernardi, P. (2007) The mitochondrial permeability transition pore and its involvement in cell death and in disease pathogenesis, *Apoptosis* 12, 815-833.
- Rena, G., Bain, J., Elliott, M., Cohen, P. (2004) D4476, a cell-permeant inhibitor of CK1, suppresses the site-specific phosphorylation and nuclear exclusion of FOXO1a, *EMBO Rep* 5, 60-65.
- Rivers, A., Gietzen, K. F., Vielhaber, E., Virshup, D. M. (1998) Regulation of casein kinase I epsilon and casein kinase I delta by an in vivo futile phosphorylation cycle, *J. Biol. Chem* 273, 15980-15984.
- Roach, P. J. (1991) Multisite and hierarchal protein phosphorylation, *J. Biol. Chem* 266, 14139-14142.
- Rubinfeld, B., Robbins, P., El-Gamil, M., Albert, I., Porfiri, E., Polakis, P. (1997) Stabilization of beta-catenin by genetic defects in melanoma cell lines, *Science* 275, 1790-1792.

-
- Rubinfeld, B., Tice, D. A., Polakis, P. (2001) Axin-dependent phosphorylation of the adenomatous polyposis coli protein mediated by casein kinase 1 epsilon, *J. Biol. Chem* 276, 39037-39045.
 - Ryan, K. M., Phillips, A. C., Vousden, K. H. (2001) Regulation and function of the p53 tumor suppressor protein, *Curr. Opin. Cell Biol* 13, 332-337.
 - Saggioro, D., Barp, S., Chieco-Bianchi, L. (2001) Block of a mitochondrial-mediated apoptotic pathway in tax-expressing murine fibroblasts, *Experimental Cell Research* 269, 245-255.
 - Saito, S., Goodarzi, A. A., Higashimoto, Y., Noda, Y., Lees-Miller, S. P., Appella, E., Anderson, C. W. (2002) ATM mediates phosphorylation at multiple p53 sites, including Ser(46), in response to ionizing radiation, *J. Biol. Chem* 277, 12491-12494.
 - Sakaguchi, K., Saito, S., Higashimoto, Y., Roy, S., Anderson, C. W., Appella, E. (2000) Damage-mediated phosphorylation of human p53 threonine 18 through a cascade mediated by a casein 1-like kinase. Effect on Mdm2 binding, *J. Biol. Chem* 275, 9278-9283.
 - Salvi, M., Sarno, S., Cesaro, L., Nakamura, H., Pinna, L. A. (2009) Extraordinary pleiotropy of protein kinase CK2 revealed by weblogo phosphoproteome analysis, *Biochim. Biophys. Acta* 1793, 847-859.
 - Sarno, S., Vaglio, P., Meggio, F., Issinger, O. G., Pinna, L. A. (1996) Protein kinase CK2 mutants defective in substrate recognition. Purification and kinetic analysis, *J. Biol. Chem* 271, 10595-10601.
 - Sarno, S., Reddy, H., Meggio, F., Ruzzene, M., Davies, S. P., Donella-Deana, A., Shugar, D., Pinna, L. A. (2001) Selectivity of 4,5,6,7-tetrabromobenzotriazole, an ATP site-directed inhibitor of protein kinase CK2 ('casein kinase-2'), *FEBS Lett* 496, 44-48.
 - Sarno, S., Moro, S., Meggio, F., Zagotto, G., Dal Ben, D., Ghisellini, P., Battistutta, R., Zanotti, G., Pinna, L. (2002) Toward the rational design of protein kinase casein kinase-2 inhibitors, *Pharmacology and Therapeutics* 93, 159-168.
 - Sarno, S., De Moliner, E., Ruzzene, M., Pagano, M., Battistutta, R., Bain, J., Fabbro, D., Schoepfer, J., Elliott, M., Furet, P., Meggio, F., Zanotti, G., Pinna, L. (2003) Biochemical and three-dimensional-structural study of the specific inhibition of protein kinase CK2 by [5-oxo-5,6-dihydroindolo-(1,2-a)quinazolin-7-yl]acetic acid (IQA), *Biochemical Journal* 374, 639-646.
 - Schlessinger, J. (2000) Cell signaling by receptor tyrosine kinases, *Cell* 103, 211-225.
 - Schrodinger, I., (2001) Portland, OR: Schrodinger, Inc.
 - Scorrano, L., Petronilli, V., Bernardi, P. (1997) On the voltage dependence of the mitochondrial permeability transition pore. A critical appraisal, *Journal of Biological Chemistry* 272, 12295-12299.
 - Selenko, P., Frueh, D. P., Elsaesser, S. J., Haas, W., Gygi, S. P., Wagner, G. (2008) In situ observation of protein phosphorylation by high-resolution NMR spectroscopy, *Nat. Struct. Mol. Biol* 15, 321-329.
 - Seo, J., Lee, K. (2004) Post-translational modifications and their biological functions: proteomic analysis and systematic approaches, *J. Biochem. Mol. Biol* 37, 35-44.
 - She, Q. B., Chen, N., Dong, Z. (2000) ERKs and p38 kinase phosphorylate p53 protein at serine 15 in response to UV radiation, *J. Biol. Chem* 275, 20444-20449.
 - She, Q., Ma, W., Dong, Z. (2002) Role of MAP kinases in UVB-induced phosphorylation of p53 at serine 20, *Oncogene* 21, 1580-1589.
 - Shieh, S. Y., Ikeda, M., Taya, Y., Prives, C. (1997) DNA damage-induced phosphorylation of p53 alleviates inhibition by MDM2, *Cell* 91, 325-334.
 - Shieh, S. Y., Taya, Y., Prives, C. (1999) DNA damage-inducible phosphorylation of p53 at N-terminal sites including a novel site, Ser20, requires tetramerization, *EMBO J* 18, 1815-

REFERENCES

- 1823.
- Silic-Benussi, M., Cavallari, I., Zorzan, T., Rossi, E., Hilaragi, H., Rosato, A., Horie, K., Saggiaro, D., Lairmore, M., Willems, L., Chieco-Bianchi, L., D'Agostino, D., Ciminale, V. (2004) Suppression of tumor growth and cell proliferation by p13II, a mitochondrial protein of human T cell leukemia virus type 1, *Proceedings of the National Academy of Sciences of the United States of America* 101, 6629-6634.
 - Smith, J. A., Francis, S. H., Corbin, J. D. (1993) Autophosphorylation: a salient feature of protein kinases, *Mol. Cell. Biochem* 127-128, 51-70.
 - Soderling, T. R. (1990) Protein kinases. Regulation by autoinhibitory domains, *J. Biol. Chem* 265, 1823-1826.
 - Songyang, Z., Lu, K. P., Kwon, Y. T., Tsai, L. H., Filhol, O., Cochet, C., Brickey, D. A., Soderling, T. R., Bartleson, C., Graves, D. J., DeMaggio, A. J., Hoekstra, M. F., Blenis, J., Hunter, T., Cantley, L. C. (1996) A structural basis for substrate specificities of protein Ser/Thr kinases: primary sequence preference of casein kinases I and II, NIMA, phosphorylase kinase, calmodulin-dependent kinase II, CDK5, and Erk1, *Mol. Cell. Biol* 16, 6486-6493.
 - Sousa, S., Fernandes, P., Ramos, M. (2006) Protein-ligand docking: Current status and future challenges, *Proteins: Structure, Function and Genetics* 65, 15-26.
 - Stommel, J. M., Wahl, G. M. (2004) Accelerated MDM2 auto-degradation induced by DNA-damage kinases is required for p53 activation, *EMBO J* 23, 1547-1556.
 - Szewczyk, A., Skalska, J., Głab, M., Kulawiak, B., Malińska, D., Koszela-Piotrowska, I., Kunz, W. (2006) Mitochondrial potassium channels: From pharmacology to function, *Biochimica et Biophysica Acta - Bioenergetics* 1757, 715-720.
 - Takano, A., Hoe, H., Isojima, Y., Nagai, K. (2004) Analysis of the expression, localization and activity of rat casein kinase Iepsilon-3, *Neuroreport* 15, 1461-1464.
 - Tibbetts, R. S., Brumbaugh, K. M., Williams, J. M., Sarkaria, J. N., Cliby, W. A., Shieh, S. Y., Taya, Y., Prives, C., Abraham, R. T. (1999) A role for ATR in the DNA damage-induced phosphorylation of p53, *Genes Dev* 13, 152-157.
 - Toledo, F., Wahl, G. M. (2006) Regulating the p53 pathway: in vitro hypotheses, in vivo veritas, *Nat. Rev. Cancer* 6, 909-923.
 - Trevisan, R., Daprai, L., Acquasaliente, L., Ciminale, V., Chieco-Bianchi, L., Saggiaro, D. (2004) Relevance of CREB phosphorylation in the anti-apoptotic function of human T-lymphotropic virus type 1 tax protein in serum-deprived murine fibroblasts, *Experimental Cell Research* 299, 57-67.
 - Unger, T., Juven-Gershon, T., Moallem, E., Berger, M., Vogt Sionov, R., Lozano, G., Oren, M., Haupt, Y. (1999) Critical role for Ser20 of human p53 in the negative regulation of p53 by Mdm2., *EMBO J* 18, 1805-1814.
 - Verdonck, K., González, E., Van Dooren, S., Vandamme, A., Vanham, G., Gotuzzo, E. (2007) Human T-lymphotropic virus 1: recent knowledge about an ancient infection, *Lancet Infectious Diseases* 7, 266-281.
 - Vousden, K. H., Lane, D. P. (2007) p53 in health and disease, *Nat Rev Mol Cell Biol* 8, 275-283.
 - Walsh, C. T., Garneau-Tsodikova, S., Gatto, G. J. (2005) Protein posttranslational modifications: the chemistry of proteome diversifications, *Angew. Chem. Int. Ed. Engl* 44, 7342-7372.
 - Wang, R., Lai, L., e Wang, S. (2002) Further development and validation of empirical scoring functions for structure-based binding affinity prediction, *J. Comput. Aided Mol. Des* 16, 11-26.
 - Wang, W., Fang, H., Groom, L., Cheng, A., Zhang, W., Liu, J., Wang, X., Li, K., Han, P.,

-
- Zheng, M., Yin, J., Wang, W., Mattson, M., Kao, J., Lakatta, E., Sheu, S., Ouyang, K., Chen, J., Dirksen, R., Cheng, H. (2008) Superoxide Flashes in Single Mitochondria, *Cell* 134, 279-290.
- Wei, C., Wu, Q., Vega, V. B., Chiu, K. P., Ng, P., Zhang, T., Shahab, A., Yong, H. C., Fu, Y., Weng, Z., Liu, J., Zhao, X. D., Chew, J., Lee, Y. L., Kuznetsov, V. A., Sung, W., Miller, L. D., Lim, B., Liu, E. T., Yu, Q., Ng, H., Ruan, Y. (2006) A Global Map of p53 Transcription-Factor Binding Sites in the Human Genome, *Cell* 124, 207-219.
 - Xing, Y., Clements, W. K., Kimelman, D., Xu, W. (2003) Crystal structure of a beta-catenin/axin complex suggests a mechanism for the beta-catenin destruction complex, *Genes Dev* 17, 2753-2764.
 - Xing, Y., Clements, W. K., Le Trong, I., Hinds, T. R., Stenkamp, R., Kimelman, D., Xu, W. (2004) Crystal structure of a beta-catenin/APC complex reveals a critical role for APC phosphorylation in APC function, *Mol. Cell* 15, 523-533.
 - Xu, R. M., Carmel, G., Sweet, R. M., Kuret, J., Cheng, X. (1995) Crystal structure of casein kinase-1, a phosphate-directed protein kinase, *EMBO J* 14, 1015-1023.
 - Zhai, L., Graves, P. R., Robinson, L. C., Italiano, M., Culbertson, M. R., Rowles, J., Cobb, M. H., DePaoli-Roach, A. A., Roach, P. J. (1995) Casein kinase I gamma subfamily. Molecular cloning, expression, and characterization of three mammalian isoforms and complementation of defects in the *Saccharomyces cerevisiae* YCK genes, *J. Biol. Chem* 270, 12717-12724.
 - Zolnierowicz, S., Bollen, M. (2000) Protein phosphorylation and protein phosphatases. De Panne, Belgium, September 19-24, 1999, *EMBO J* 19, 483-488.

ABBREVIATIONS

Amino Acids

Ala	Alanine	A
Arg	Arginine	R
Asn	Asparagine	N
Asp	Aspartic acid	D
Cys	Cysteine	C
Gln	Glutamine	Q
Glu	Glutamic acid	E
Gly	Glycine	G
His	Histidine	H
Ile	Isoleucine	I
Leu	Leucine	L
Lys	Lysine	K
Met	Methionine	M
Phe	Phenylalanine	F
Pro	Proline	P
Ser	Serine	S
Thr	Threonine	T
Trp	Tryptophan	W
Tyr	Tyrosine	Y
Val	Valine	V

Acronyms

2D-PAGE	Two dimensional PAGE
Å	Angstrom
Abl	Abelson tyrosine kinase
ADP	Adenosine diphosphate
AGC	cAMP-dependent protein kinase/protein kinase G/protein kinase C extended family
AKAP	A-kinase anchor proteins
APC	Adenomatous Polyposis Coli
APC-R3	Adenomatous Polyposis Coli-Repeat 3
aPK	Atypical protein kinase
ATLL	Adult T-cell leukemia/lymphoma
ATM	Ataxia telangiectasia mutated protein kinase
ATR	Ataxia telangiectasia and rad-3-related kinase
ATP	Adenosine 5'-triphosphate
ATZ	Anilinothiazolinone
BIS-TRIS	2-[Bis(2-hydroxyethyl)amino]-2-(hydroxymethyl)-1,3-propanediol
BOC	Butyloxycarbonyl
CAMK	Calcium/calmodulin-dependent protein kinase
CDC	Cell division cycle
CDK2	Cyclin-dependent kinase
c-FGR	Proto-oncogene tyrosine-protein kinase FGR
CHK	Check-point kinase
CK1	Casein Kinase 1
CK2	Casein Kinase 2
CMGC	Cyclin-dependent kinase, mitogen-activated protein kinase, glycogen synthase kinase 3, and CK2
CRC	Calcium retention capacity
CsA	Cyclosporin A
CSK	c-src tyrosine kinase
DIEA	N-ethyl-diisopropylamine

DMF	Dimethylformamide
DMSO	Dimethyl sulfoxide
DNA	Deoxyribonucleic acid
DNA-PK	DNA-dependent protein kinase
Dvl	Dishevelled
DYRK1	Dual specificity Yak1-related kinase
EDTA	Ethylenediaminetetraacetic acid
EGFR	Epidermal growth factor receptor
EGTA	Ethylene glycol tetraacetic acid
ETC	Electron transport complex
ePK	Eukaryotic protein kinase
ERK	Extracellular signal-regulated protein kinase
FasL	Fas ligand
FBS	Fetal bovine serum
FCCP	Carbonyl cyanide-p-trifluoromethoxyphenylhydrazone
FLT3	FMS-like tyrosine kinase 3
FMOC	9-Fluorenylmethoxycarbonyl
GSK3	Glycogen synthase kinase
GST	Glutathione S-transferase
GTP	Guanosine 5'-triphosphate
HATU	2-(1H-7-azabenzotriazol-1-yl)-1,1,3,3-tetramethyluronium hexafluorophosphate methanaminium
HBTU	2-(1-benzotriazol-1-yl)-1,1,3,3-tetramethyluronium hexafluorophosphate
HEPES	4-(2-hydroxyethyl)-1-piperazineethanesulfonic acid
HHV-6B	Human herpesvirus 6B
HIPK2	Homeodomain-interacting protein kinase 2
HMP	p-Hydroxymethyl phenoxymethyl polystyrene
HOBT	N-hydroxybenzotriazole
HPLC	High performance liquid chromatography
HSP60	Heat shock protein 60
HTLV-1	Human T-cell leukemia virus type 1
IC ₅₀	Half maximal inhibitory concentration
JNK	c-Jun N-terminal kinase

ABBREVIATIONS

kD	KiloDalton
K _i	Inhibition constant
K _m	Michaelis constant
IPTG	isopropyl β-D-thiogalactoside
LEF	Lymphoid enhancer-binding factor
LRP	Low-density lipoprotein receptor-related protein
LYN	Protein tyrosine kinase Lyn
MAO	Monoamine oxidase
MAP	Mitogen-activated protein kinase
MAPKAPK	MAP kinase-activated protein kinase 2
MDM	Mouse double minute
MES	2-(N-morpholino)ethanesulfonic acid
MOPS	3-(N-morpholino)propanesulfonic acid
MPG	Mercaptopropionylglycine
mRNA	Messenger ribonucleic acid
MTS	Mitochondrial targeting sequence
NF-AT	Nuclear factor of activated T-cells
Ni-NTA	Ni ²⁺ -nitriloacetate
NMP	N-methyl-2-pyrrolidone
NPM-ALK	Nucleophosmin/anaplastic lymphoma kinase tyrosine kinase
nRTK	Non-receptor tyrosine kinase
OD	Optical density
ORF	Open reading frame
PBS	Phosphate buffered saline
PDB	Protein data bank
PEGA	Polyethylenglycole
PIM1	Proto-oncogene serine/threonine-protein kinase PIM1
PKA	Protein kinase A
PKC	Protein kinase C
PTK	Protein tyrosine kinase
PTM	Posttranslational modification
PTP	Permeability transition pore
PVDF	Polyvinylidene difluoride
RACK	Receptor for activated C-kinase

RET	RET receptor tyrosine kinase
RMSD	Root mean square deviation
RNA	Ribonucleic acid
ROS	Reactive oxygen species
RP-HPLC	Reversed-phase high performance liquid chromatography
RTK	Receptor tyrosine kinase
SBVS	Structure-based virtual screening
SDS-PAGE	Sodium dodecyl sulfate polyacrylamide gel electrophoresis
SH2	Src-homology 2
SH3	Src-homology 3
SPPS	Solid-phase peptide synthesis
STE	Homologs of yeast Sterile 7, Sterile 11, Sterile 20 kinases
SYK	Spleen tyrosine kinase
TCF	T-cell factor
TES	N-Tris(hydroxymethyl)methyl-2-aminoethanesulfonic acid
TFA	trifluoroacetic acid
TGF β	Transforming growth factor beta
TK	Tyrosine kinase
TKL	Tyrosine kinase-like
TRIS	Tris (hydroxymethyl) aminomethane
WNT	Wingless and Int